NASA Contractor Report 201612

Novel Composites for Wing and Fuselage Applications

Textile Reinforced Composites and Design Guidelines

J. A. Suarez, C. Buttitta, et al.
Northrop Grumman Corporation
Advanced Technology & Development Center
Bethpage, New York

National Aeronautics and
Space Administration
Langley Research Center
Hampton, Virginia 23681-0001

FOREWORD

This Final Technical Report covers the work performed under Contract No. NAS1-18784 in Tasks 3, 4, and 5 from June 1992 through September 1994. The work was accomplished by the Advanced Technology & Development Center (ATDC) of Northrop Grumman Corporation, Bethpage, New York, and its subcontractors, ICI/Fiberite, Inc., and R. Cubed, Inc., under the sponsorship of NASA/Langley Research Center : "Novel Composites for Wing and Fuselage Applications."

The work was administered under the technical direction of Mr. H. Benson Dexter, NASA/LaRC Contracting Officer Technical Representative.

Key personnel associated with the program, and their respective areas of responsibility include:

- Northrop Grumman Corporation

J. Suarez	Program Manager
C. Buttitta	Structural Mechanics
G. Flanagan	Structural Mechanics
T. DeSilva	Structural Design
W. Egensteiner	Structural Analysis
J. Bruno	Weight Optimization
J. Mahon	Advanced Materials and Manufacturing
C. Rutkowski	Tooling
R. Collins	Quality Control
R. Fidnarick	Elements and Material Test

- ICI/Fiberite, Inc.

S. Clarke	Woven Preforms

- R. Cubed, Inc.

R. Michel	RFI Process

CONTENTS

ILLUSTRATIONS

ILLUSTRATIONS (cont'd)

TABLES

1 – INTRODUCTION & SUMMARY

1.1 TASK 3: CROSS-STIFFENED SUBCOMPONENT

Several attempts have been made to provide structural continuity through the intersection of cross-stiffened graphite composite structure. Initial attempts included bonding metal cruciforms to the graphite stiffeners at the intersection and alternately placing unidirectional tows across the intersection. Adaptations of the tow placement have been successfully tried using syntactic foam to accommodate the cross-intersection ply buildup. These methods and others have met with varying degrees of success. The primary focus of all of these innovative concepts was to improve the composite structure load-carrying capability through the cross-stiffened intersection.

It was recognized that an effective solution was necessary to further advance the utilization of advanced composite graphite-reinforced structures. Successful solution of this application would permit designs that could, until this time, be effectively achieved only with metallic designs. Efficient, supportable, and affordable graphite solutions would permit more effective composite applications for airframe components such as bulkheads, doors, window belts, and skin panels. Essentially, any cross-ribbed structure is a potential candidate.

The resulting benefits for developing such a capability are reduced weight, improved material utilization, fewer parts, and the potential for reduced costs.

With the technology development and introduction of 3-D textile weaving and braiding processes, new opportunities became available to find solutions to this problem. Weaving technology has progressed significantly for use in structural composite applications. More important, these processes offer the potential to achieve continuous through-the-intersection fiber integrity with high-strength graphite fibers.

These textile processes permitted new composite material fabrication methods to be developed. Dry unimpregnated assemblies were produced by combining/stitching various textile products, such as 2-D woven broadgoods, 3-D woven assemblies, and braided items, to form complex shapes. The resulting textile assemblies became preforms for subsequent processing.

In addition, processing methods have been developed which are compatible with textile preform assemblies. Resin Transfer Molding (RTM) and Resin Film Infusion (RFI) are two such methods currently being applied to the fabrication of airframe parts.

Northrop Grumman Corporation (NGC) was contracted by NASA to develop innovative, cost-effective, damage-tolerant design concepts for airframe structure. A major task of this program was to design and demonstrate the effectiveness of a textile cross-stiffened continuous fiber structure. This demonstration utilized advanced textile preform architectures and processing technologies to fabricate a commercial aircraft demonstration subcomponent. For the demonstration, the airframe part selected is a window belt typical of that found in a commercial aircraft. The specific reasons for this selection are: the design is generic to cross-stiffened biaxially loaded structure; it is highly loaded, carrying both fuselage bending and cabin pressure loads; it presents a fair degree of complexity; and it is a repetitive assembly along the length of an aircraft. Figure 1 depicts the area of interest, a detail of an existing metallic assembly, and an isometric of the textile subcomponent.

Unidirectional tape composites are planar materials that exhibit properties through their thickness, which are an order-of-magnitude lower than those associated with the plane in which the fibers are oriented. A cross-stiffened structure, such as a window belt, bulkhead, door, or

- CROSS-STIFFENED STRUCTURE
- BI-AXIALLY LOADED
- REPETITIVE APPLICATION

METALLIC APPLICATION

COMPOSITE PREFORM SUBCOMPONENT

R93-1172-001
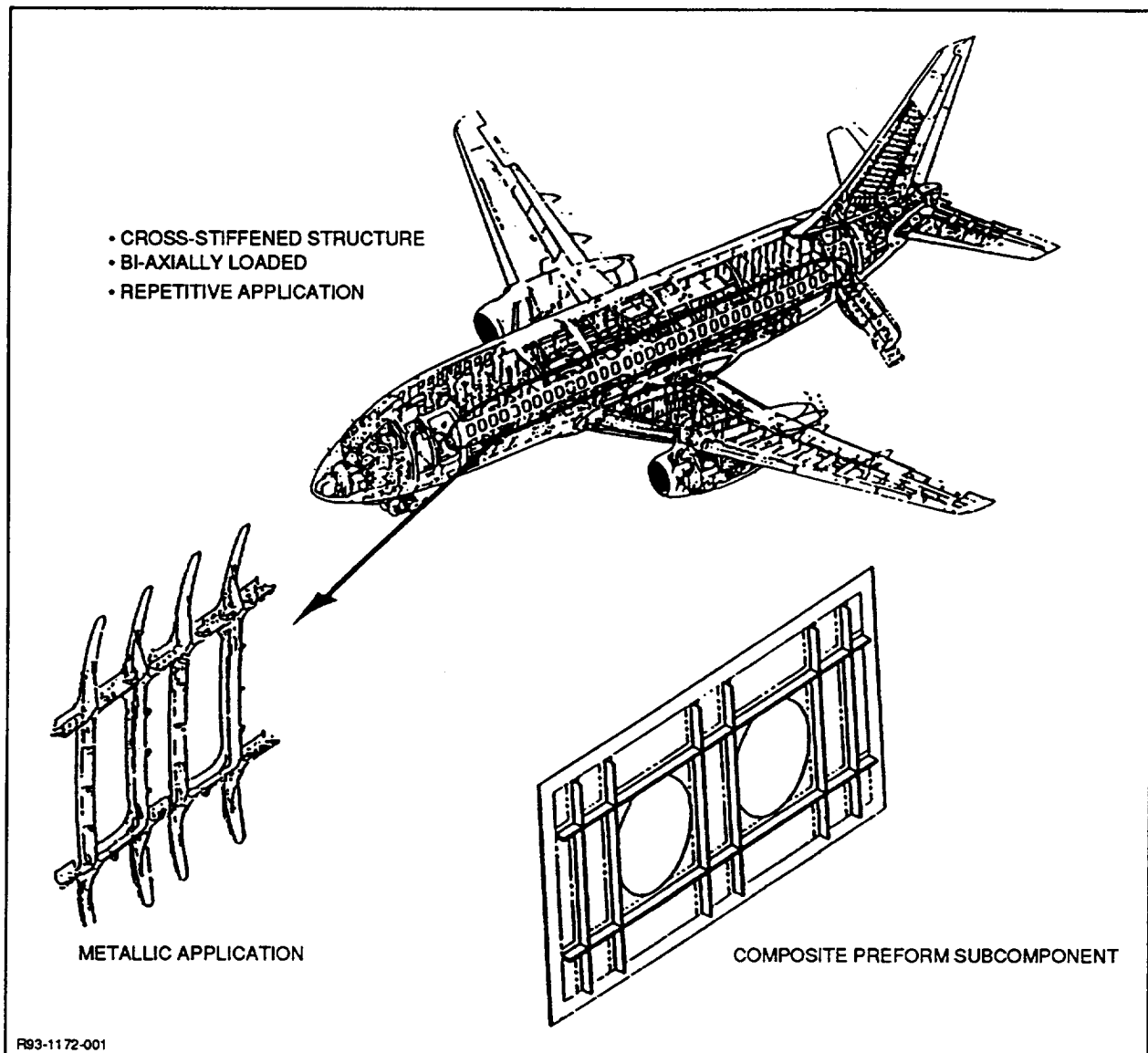
Fig. 1 Cross-stiffened Window Belt (Commercial Airframe)

skin panel, by its very nature, must employ a network of crossing stiffeners to provide axial load continuity and stabilize the skin against buckling. This is accomplished quite easily with an integrally machined isotropic metal design. At each crossing stiffener junction, the material is continuous and its properties remain unchanged. Trying to accomplish the same functions with composite stiffeners results in the primary load-carrying fibers lying in two mutually perpendicular planes that are trying to pass through each other. Since only one plane can be continuous, the development of new and innovative concepts to overcome this shortcoming has received considerable attention in this NASA contract.

Under NASA's Novel Composites for Wing and Fuselage Applications (NCWFA) Program, Contract No. NAS1-18784, NGC evaluated the structural efficiency of graphite/epoxy cross-stiffened panel elements fabricated using innovative textile preforms and cost-effective RTM and RFI processes. Two three-dimensional woven preform assembly concepts have been defined for

2

application to a representative window belt design typically found in a commercial transport airframe. The 3-D woven architecture for each of these concepts is different; one is vertically woven in the plane of the window belt geometry, and the other is loom woven in a compressed state similar to an unfolded egg crate. The feasibility of both designs has been demonstrated in the fabrication of small test element assemblies. These elements and the final window belt assemblies were structurally tested, and the results compared.

1.2 TASK 4: DESIGN GUIDELINES/ANALYSIS OF TEXTILE-REINFORCED COMPOSITES

A methodology is desired that allows a designer to select the appropriate amounts of through-thickness reinforcement needed to meet design requirements. The goal was to use a relatively simple analysis to minimize the amount of testing that must be performed, and to make test results from simple configurations applicable to more general structures. Using this methodology, it should be possible to optimize the selection of stitching materials, the weight of the yarn, and the stitching density.

The analysis approach is to treat substructure disbond as a crack propagation problem. In this approach, the stitches have little influence until a delamination begins to grow. Once the delamination reaches, or extends beyond, a stitch, the stitch serves to reduce the strain-energy-release-rate (G) at the crack tip for a given applied load. The reduced G can then be compared to the unstitched material toughness to predict the load required to extend the crack further. The current model treats the stitch as a simple spring that responds to displacements in the vertical (through-thickness) direction. In concept, this approach is similar to that proposed by other authors. (Please see Ref. 1 for example.) Test results indicate that the model should be refined to include the shearing stiffness of the stitch.

The strain-energy-release-rate calculations are performed using a code that employs interconnected, higher order plates to model built-up composite cross sections. When plates are stacked vertically, the interfacial tractions between the plates can be computed. The plate differential equations are solved in closed form. The code, called SUBLAM, was developed as part of this effort, and is described in Ref. 2 and 3. The code is limited to structures that have a constant cross section in one dimension. Because of this limitation, rows of stitches are treated as a two-dimensional sheet. The spring stiffness of a row of stitches can be estimated from the stitch material, weight, and density. One unknown in the analysis is the effective length of the spring, which depends on whether or not the stitch is bonded to the surrounding material. This issue was examined in Ref. 4. As a practical and conservative approach, we can assume that the stitch is bonded until a crack passes the stitch location. After the crack passes, it is fully debonded.

A series of tests was performed to exercise the methodology outlined above. The test incorporated an attached flange such that the sudden change in thickness initiated a delamination. Two load conditions were used (three-point and four-point bending) so that the ratio of shear load to moment load could be varied. The analysis was used to estimate the material's critical G from the unstitched specimens. With these data, a prediction was made for the load required to delaminate the stitched specimens.

Using the methodology, design charts have been created for simplified geometries. These charts give stitch force along with G_I and G_{II} as a function of the stitch spring stiffness. With the charts, it should be possible to determine the stitch spring stiffness and strength required to

3

reduce the G to a desired level. From these parameters, the actual stitching material, weight, and density can be computed. The results have been nondimensionalized for wider applicability.

1.3 TASK 5: INTEGRALLY WOVEN FUSELAGE PANEL

This task of the program extends our work on the "continuous fibers through the intersection" concept for fuselage structures, with their intersecting stringers and curved frames providing a more cost-effective, structurally efficient, and rigidized structure than otherwise possible.

Under NASA's Novel Composites for Wing and Fuselage Applications (NCWFA) Program, Contract No. NAS1-18784, Northrop Grumman with its subcontractors developed and evaluated cross-stiffened primary structure representative of fuselage designs that are typically found on commercial airframes, fabricated using innovative textile architecture, and processed via RFI. This section of the final report describes the fabrication of 60-in. x 90-in. AS4 graphite fiber cross-stiffened preforms with a 122-in. radius of curvature via 3-D weaving, an approach that allows continuous fibers through the intersection and their processing by RFI, using 3501-6 epoxy film. Element tests performed to assess the structural efficiency of the cross-stiffened designs are described, as well as the proposed test of the fuselage subcomponent by NASA. A comparison of the actual and projected acquisition costs of the cross-stiffened fuselage structure fabricated using woven and stitched preforms and processed via RFI versus the conventional tape prepreg with autoclave cure is presented.

1.4 REFERENCES

1.   Byun, Joon-Hyung, Gillespie, John W., Jr., and Chou, Tsu-Wei, "Mode I Delamination of a Three-Dimensional Fabric Composite," *J. of Composite Materials*, Vol. 24, May 1990, pp. 497-518.

2.   Flanagan, Gerry, "A Sublaminate Analysis Method for Predicting Disbond and Delamination Loads in Composite Structures," *J. of Reinforced Plastics and Composites*, Vol. 12, August 1993, pp. 876-887.

3.   Flanagan, Gerry, "A General Sublaminate Analysis Method for Determining Strain Energy Release Rates in Composites," AIAA Paper 94-1358, presented at 35th AIAA/ASME/ASCE/AHS/ASC Structures, Structural Dynamics, and Materials Conference, Hilton Head, SC, 18-20 April 1994, pp. 381-389.

4.   Flanagan, Gerry, "Development of Design Guidelines for Stitching Skins to Substructure," presented at Fourth NASA/DoD Advanced Composites Technology Conference, Salt Lake City, UT, 7-11 June 1993.

2 -- TASK 3: CROSS-STIFFENED SUBCOMPONENT

2.1 SUBCOMPONENT DESCRIPTION

The structure selected to demonstrate the effectiveness of a textile cross-stiffened continuous fiber structure is a window belt typical of that found in a commercial transport.

The textile preform window belt subcomponent design, drawing D19B1865, is shown in Fig. 2. The drawing presentation defining the composite lay-up is significantly different from one applied to a unidirectional or broadgoods composite design. For typical 2-D composite applications, fiber orientation, number of plies, and stacking sequence can be defined exactly on the engineering drawing and, in turn, fabricated as specified. On the other hand, three-dimensional woven preform assemblies cannot be defined as simply because of the diversity of weaving/knitting processes, complexity of fiber orientations, and use of yarn and variation of fiber architecture.

To enable preform fabricators to exercise creative solutions, promote freedom in design, and avoid imposing adverse restrictions to a design, drawing D19B1865 stipulates target values for fiber volume and percentage of 0°, 90°, and ±45° directional yarns and stitching yarns. This notation provides the freedom to develop a complex fiber architecture and preform assembly using the techniques and equipment familiar to each potential supplier. However, this method, if not concurrently engineered, can compromise the structural capability of the resulting assembly.

The geometrical definition -- particularly the thickness dimensions -- is called out, as are net final cure dimensions. It is desirable that the preform be within 10% of this dimension to enable tooling to be designed effectively. Preforms with lofts as high as 200% will impose restrictions on tooling designs, with the potential to increase complexity and related costs.

The design loads used to size the window belt subcomponent were obtained from Boeing Commercial Aircraft and are representative of a typical wide-body fuselage window belt region. Figure 3 displays the direction and the magnitude of the ultimate design axial loads and shears for two maximum load conditions.

The fail-safe design allowable strain (80% limit) was selected to be 2400 μin./in. for this application. This is commensurate with Boeing's fail-safe allowable strain of 2000-3000 μin./in. The resulting design ultimate strain is 4500 μin./in.

The geometrical definition was used as a guide to define the subcomponent. The actual fuselage side panel containing the widow belt has a radius of 122 in. The subcomponent was configured flat to reduce test costs. The window spacing is 22.00 in., and the longitudinal stiffener spacing, which frames the windows, is 19.00 in.

The general window component model is represented by 1066 node points (GRID) interconnected by 1004 quadrilateral bending elements (CQUAD4). This model depicts the stiffeners as a combination of bending elements which provides for the geometric distribution of the structure and also is capable of representing the structural response of the extended stiffeners. The finite-element analysis (FEA) was used to predict strains in critical areas for the subsequent component structural tests.

5

Fig. 2 Cross-stiffened, 3-D, Woven Window Belt Design, Drawing D19B1865
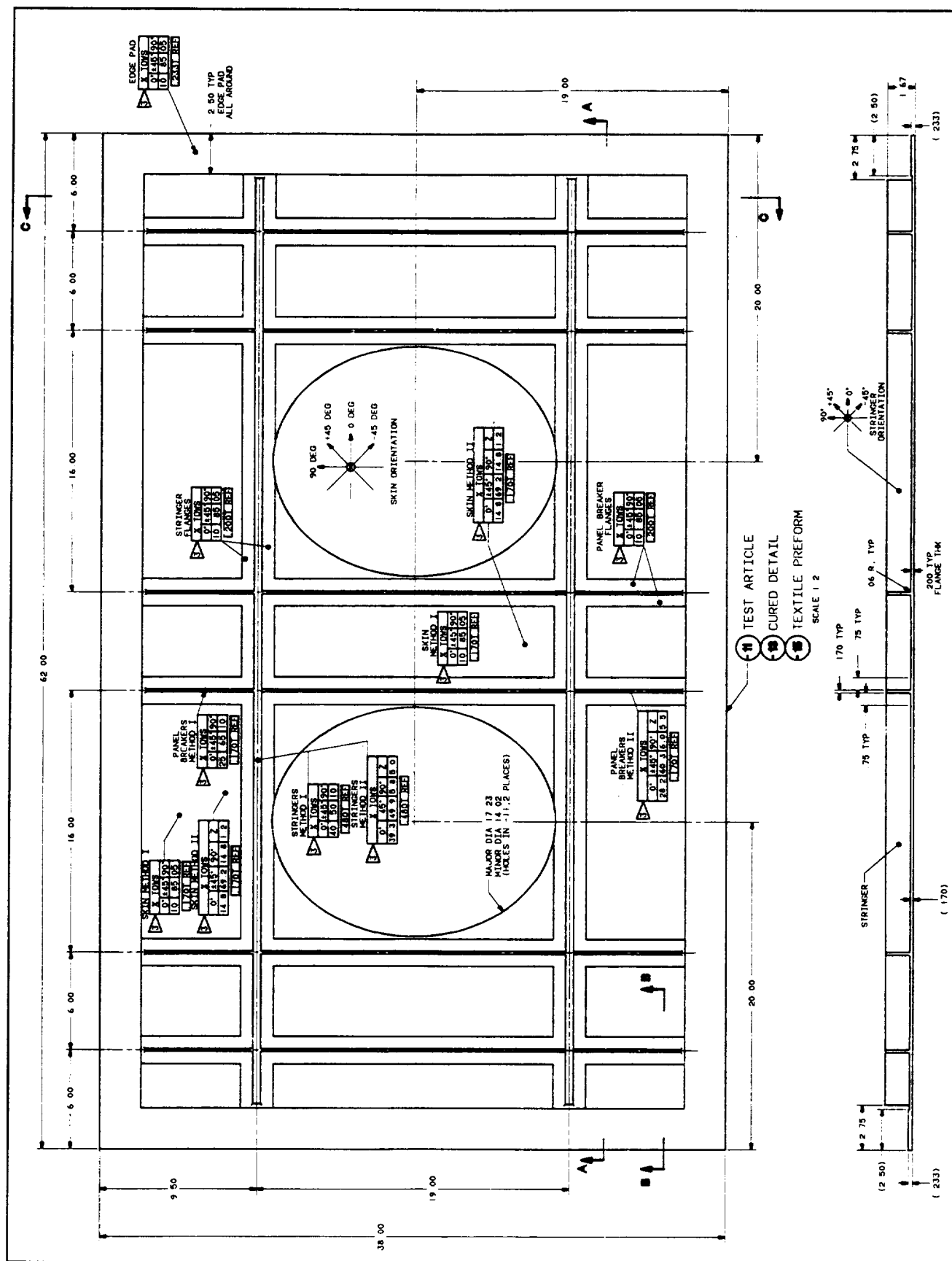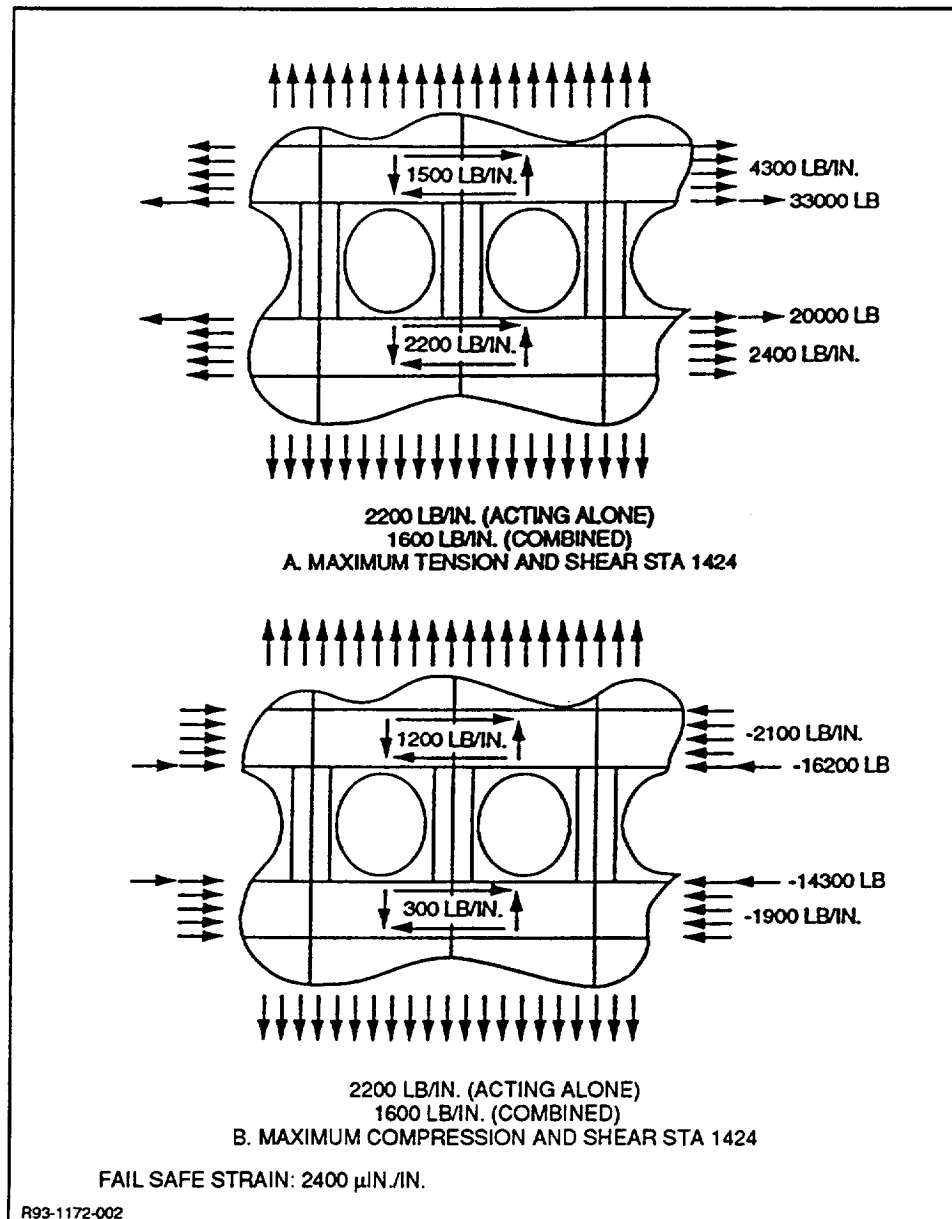
Fig. 3 Structural Design Requirements/Criteria – Maximum Load Conditions

2.2 DESIGN & ANALYSIS

2.2.1 Design

Evaluation criteria were established to compare the preform assemblies and textile processes that were proposed by suppliers. These criteria were based on parameters that would be necessary for a cross-stiffened design. The primary comparative evaluators were: the ability to provide true through-the-intersection fiber continuity; the ability to provide and control the percentage and the direction of yarn orientations; the ability to vary the thickness of the skin panel and provide different stiffener thicknesses; and the use of a process that has application for large scale-up production. Other considerations included viability of the process, cost of the final preform, and delivery schedule.

Five textile fabricators submitted proposals that described eight concepts to develop solutions for the window belt design. The designs varied and consisted of braided details, 3-D woven

7

details, stitching, and assemblies of these and 2-D components. Of the five evaluated, two were selected to produce the preform and related test elements. These two suppliers are Techniweave, Inc., of Rochester, New Hampshire, and ICI/Fiberite, of Greenville, Texas.

The two processes are significantly different. The ICI/Fiberite approach employs a conventional weaving loom with a jacquard head to fabricate the cross-stiffeners and then attach them to 2-D woven broadgoods. The Techniweave process utilizes an integral weaving technique whereby the weaving is achieved by interlacing the graphite yarns around closely spaced pins. The primary distinguishing differences is that Techniweave can weave the stiffeners integral with the skin in the plan form of the subcomponent, whereas ICI/Fiberite unfolds a loom-woven, 3-D, cross-stiffened rib structure and assembles it to the 2-D woven skin panels by using an uncatalyzed epoxy resin and stitching.

The window belt subcomponent, as shown in Fig. 4, is 38 in. x 62 in. and consists of two primary longitudinal members (0.48 in. thick), six transverse stiffeners (0.17 in. thick), and a 0.17-in. in-plane skin. The intersections of these transverse and longitudinal stiffener members have continuous fibers through the intersection to provide structural continuity at each joint. These intersecting members are attached to the skin panel with flanges to provide a load path to transfer the panel shears to the stiffeners. The entire assembly is stitched to provide stability to the dry preform and to enhance the damage tolerance of the final article. The stitching density is to be a maximum of 6% to prevent strength degradation. Two elliptical cutouts, with a major diameter of 17.25 in., replicate the windows. The provision of through-the-intersection fiber continuity is the main focus of attention.

R93-1172-003
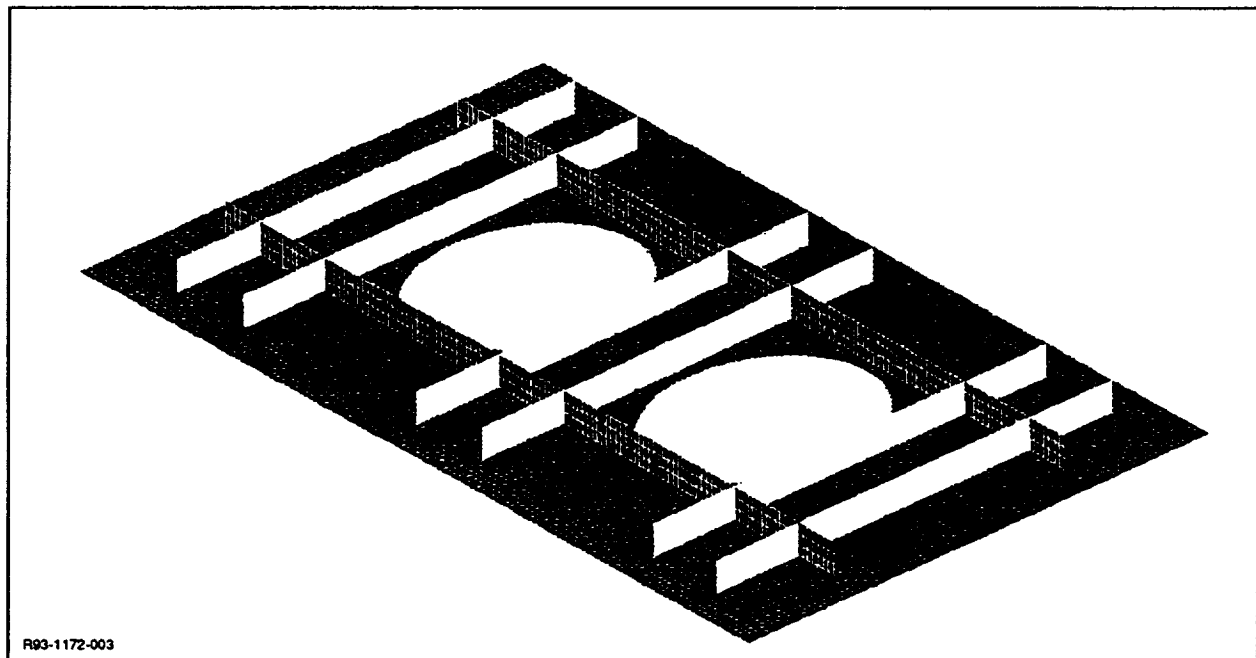
Fig. 4 Finite-Element Model

8

The textile preform window belt subcomponent drawing presentation defining the composite lay-up is significantly different from one applied to a unidirectional or broadgoods composite design. For typical 2-D composite applications, fiber orientation, number of plies, and stacking sequence can be defined exactly on the engineering drawing and, in turn, fabricated as specified. Three-dimensional woven preform assemblies, on the other hand, cannot be defined as simply, because of the diversity of weaving/stitching processes, complexity of fiber orientations, yarn tow size, and variation of fiber architecture.

The subcomponent was sized using composite laminate analysis methods with adjustments for through-the-thickness reinforcement, assuming a 60% fiber volume, 4500 μin./in. allowable ultimate strain, and IM7 graphite properties. AS4 was considered as an alternate material for the subject application.

2.2.2 Analysis

A three-dimensional NASTRAN finite-element model of the cross-stiffened Window Belt Subcomponent, Fig. 5, was constructed. The model is represented by 1066 node points (GRID) interconnected by 1004 quadrilateral bending elements (CQUAD4). This model depicts the stiffeners as a combination of bending elements which provides for the geometric distribution of the structure and also is capable of representing the structural response of the extended stiffeners.
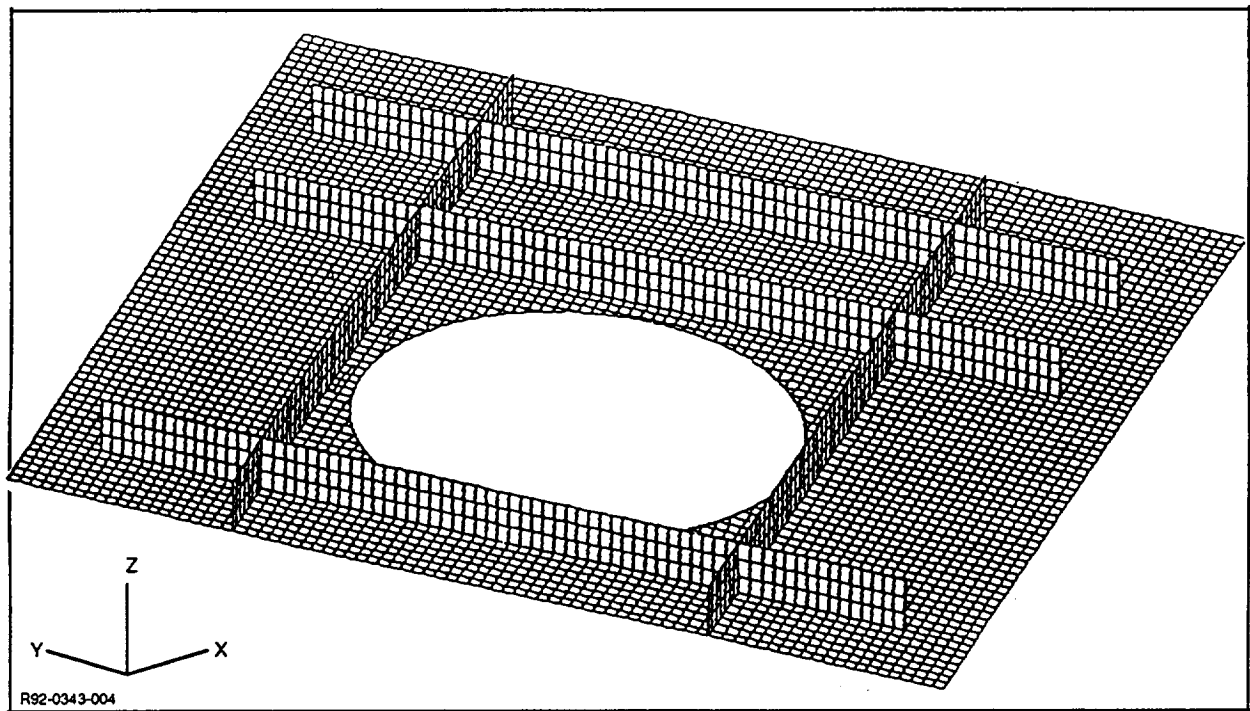
Fig. 5 Finite-Element Model Repeating Section of Window Belt

The model was later downsized to a quarter-model to reduce the solution time and to allow changes to be incorporated more rapidly. The quarter-model consisted of a single window section with three ring stiffeners and two associated longitudinal stiffeners with the adjoining skin. For the case of the subcomponent tested in picture frame shear, the model incorporated the steel load introduction rails and fasteners. Using this model, a uniform shear flow of 2200 lb/in.

9

was applied to the outer edges of the panel and reacted with appropriate asymmetric boundary conditions along the section cuts. Major and minor principal strains are plotted in Fig. 6 and 7. Maximum principal tensile strain at the edge of the unreinforced cutout is 12,000 μin./in., while the maximum principal compressive strain is 9,500 μin./in.

.0122 ■
.0113 ■
.0105 ■
.00963 ■
.00879 ■
.00794 ■
.00709 ■
.00625 ■
.00540 ■
.00455 ■
.00370 ■
.00286 ■
.00201 ■
.00116 ■
.000317 ■

R93-1172-023
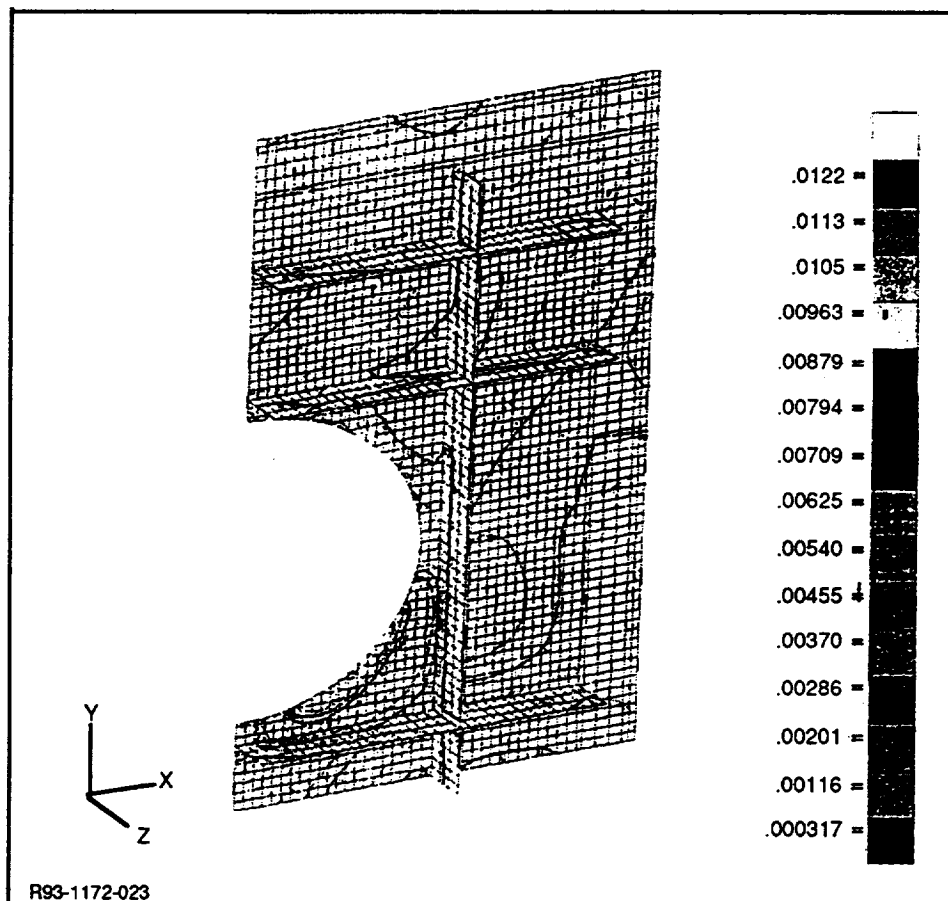
Fig. 6 Cross-stiffened Window Belt Subcomponent Principal Tension Strains

The subcomponent was sized using composite laminate analysis methods with adjustments for through-the-thickness reinforcement, assuming a 60% fiber volume, 4500 μin./in. allowable ultimate strain, and IM7 graphite properties. AS4 was considered as an alternate material for the subject application.

A 3-D NASTRAN finite-element model of a repeating section of the window belt subcomponent was constructed and is shown in Fig. 5. The section consists of a single window section with three ring stiffeners and two associated longitudinal stiffeners with the adjoining skin. A complete model of the subcomponent to be tested will consist of two such repetitive models and a boundary region component model. The latter also will be derived from a generic boundary model.

10
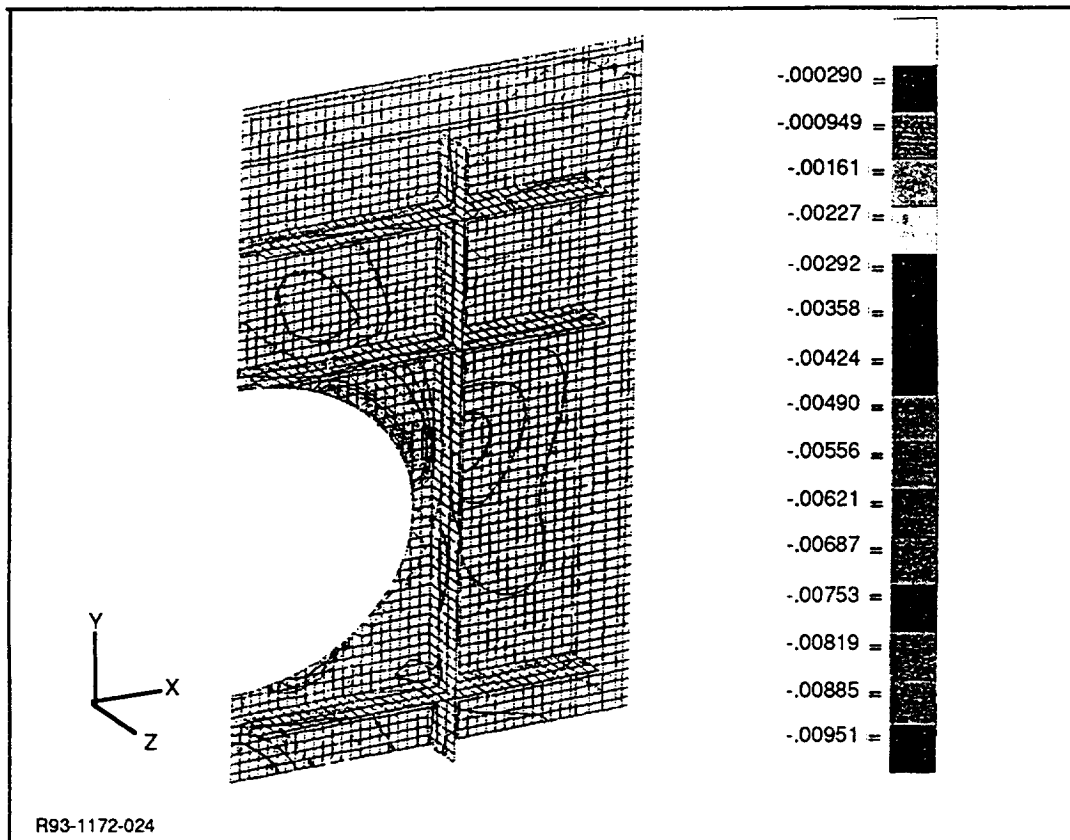
Fig. 7 Cross-stiffened Window Belt Subcomponent Principal Compression Strains

2.3 FABRICATION OF PREFORMS

2.3.1 Preform Design

The principal graphite fiber material selected for this woven and stitched preform assembly is IM7. AS4 graphite was considered as an alternate material because of its availability and widespread use. Stitching is to be performed using high-strength Toray graphite thread, or Kevlar thread as an alternate. The size of the tows and yarns was left to the suppliers and was dependent on the individual weaving processes.

The part process will be achieved using either RTM or RFI. Both processes are compatible with the preform assembly. NGC has successfully demonstrated both the RFI and the RTM methodologies in the Novel Composites for Wing and Fuselage Applications program in the manufacture of "Y" spars.

The epoxy resin materials that are being considered for RTM of the window belt article include Shell 1598/DPL 862, British Petroleum E905L two-part systems, and 3M PR500 one-part system. The resin film material being considered for RFI of the window belt is 3501-6 epoxy.

The design and manufacture of the window belt preform consisted of an innovative way of using the strengths of different preform technologies and combining them to produce a structurally sound component. The technologies that were used in the manufacture of this preform were:

- 3-D weaving
- 2-D bias weaving
- Tackifying
- Stitching.

11

Three-dimensional weaving was used in the manufacture of the window belt core. This component is the one that carries continuous fibers through the intersections of the window belt. Two-dimensional bias weaving was used in the stiffeners and the base skin plies. In the stiffeners, the use of 2-D bias weaving was necessary to introduce the bias reinforcement that 3-D weaving could not provide. Tackifying was used in the manufacture of the stiffeners and the skin. The use of a tackifier was crucial for debulking the preform to near net shape dimensions. Stitching was used in the manufacture of the stiffeners and the skin plies to mechanically integrate the bias plies to the 3-D woven core.

The design of the window belt preform was broken down into four steps: (1) design of the 0.480-in. stiffeners, (2) design of the 0.170-in. stiffeners, (3) design of the base skin of the window belt, and (4) design of the 3-D woven core that would include the 0.480-in. and 0.170-in. stiffeners. Tables 1, 2, and 3 outline the fiber architecture for the stiffeners as well as the base skin.

Table 1 Preform Fiber Orientation Percentages: Skin Thickness = 0.170 in.

	LAYER	ORIENTATION	TOW YIELD, g/m	TOW DENSITY, g/cm^3	TOWS/in.^{2}	Z ANGLE	FAW, g/m^2	PLY THICKNESS, IN.
2-D FABRIC	1	0/90	0.445	1.77	22	0	385.4	0.0158
	2	±45	0.445	1.77	24	0	420.5	0.0172
	3	±45	0.445	1.77	24	0	420.5	0.0172
	4	±45	0.445	1.77	24	0	420.5	0.0172
	5	±45	0.445	1.77	24	0	420.5	0.0172
	6	0/90	0.445	1.77	22	0	385.4	0.0158
	7	±45	0.445	1.77	24	0	420.5	0.0172
	8	±45	0.445	1.77	24	0	420.5	0.0172
	9	±45	0.445	1.77	24	0	420.5	0.0172
	10	0/90	0.445	1.77	22	0	385.4	0.0158
KEVLAR STITCHING	B*	Z	0.222	1.44	16	90	23.8	0.0020

	TOTAL THICKNESS	0.170 IN.

A* AND B* ARE TOWS THAT GO THROUGH THE THICKNESS OF THE PREFORM.
A GOES THROUGH THE THICKNESS OF THE 3-D WEAVE, &
B GOES THROUGH THE THICKNESS OF THE WHOLE PREFORM.

EST RESULTS:	V$_f$	54.40%
	%0/90°	27.87%
	%±45°	70.95%
	%Z	1.18%
MR93-1172-006		

There were two stiffeners in the window belt with the 0.480-in. thickness. These two stiffeners consisted of a 3-D woven core sandwiched between two fabric ply lay-ups. The preliminary requirements for the window belt called for these stiffeners to be 0.480 in. thick and have 40% of fibers in the 0° direction, 50% in the ±45° direction, and 10% in the 90° direction. The actual design of the preform contained 37.61% of fibers in the 0° direction, 4.74% of fibers in the Z direction, 52.07% in the ±45° direction, and 5.58% in the 90° direction. The ±45° fiber reinforcement was introduced in the form of bias fabric ply lay-ups. The fabric plies consisted of a bias fabric with IM7 material and a fiber areal weight of 420 g/m^2. There were seven plies of bias fabric laid up on each side of the 3-D woven core.

Table 2 Preform Fiber Orientation Percentages: Stiffener Thickness = 0.170 in.

	LAYER	ORIENTATION	TOW YIELD, g/m	TOW DENSITY, g/cm³	TOWS/in.²	Z ANGLE	FAW, g/m²	PLY THICKNESS, IN.
2-D FABRIC	1	±45	0.445	1.77	24	0	420.5	0.0175
	2	±45	0.445	1.77	24	0	420.5	0.0175
	3	±45	0.445	1.77	24	0	420.5	0.0175
3-D WEAVE	4	90	0.445	1.77	6	0	105.1	0.0044
	5	0	3.600	1.77	6	0	850.4	0.0355
	6	90	0.445	1.77	6	0	105.1	0.0044
	A*	Z	0.445	1.77	36	44	453.7	0.0189
2-D FABRIC	7	±45	0.445	1.77	24	0	420.5	0.0175
	8	±45	0.445	1.77	24	0	420.5	0.0175
	9	±45	0.445	1.77	24	0	420.5	0.0175
KEVLAR STITCHING	B*	Z	0.222	1.44	16	90	23.8	0.0012
						TOTAL THICKNESS		0.170 IN.

A* AND B* ARE TOWS THAT GO THROUGH THE THICKNESS OF THE PREFORM.
A GOES THROUGH THE THICKNESS OF THE 3-D WEAVE, &
B GOES THROUGH THE THICKNESS OF THE WHOLE PREFORM.

EST RESULTS:	V_f	53.30%
	%0°	20.91%
	%90°	5.17%
	%±45°	62.04%
	%Z	11.88%

MR93-1172-007

There were six stiffeners in the window belt with the 0.170-in. thickness. These stiffeners consisted of a 3-D woven core sandwiched between fabric ply lay-ups. The preliminary requirements for the window belt called for these stiffeners to be 0.170-in. thick and have 25% of fibers in the 0° direction, 65% in the ±45° direction, and 10% in the 90° direction. The actual design of the preform contained 20.91% of fibers in the 0° direction, 11.88% in the Z direction, 62.04% in the ±45° direction, and 5.17% in the 90° direction. The ±45° fiber reinforcement was introduced in the form of bias fabric ply lay-ups. The fabric plies consisted of a bias fabric with IM7 material and a fiber areal weight of 420 g/m². There were three plies of bias fabric laid up on each side of the 3-D woven core.

The base skin consisted of a fabric lay-up, and it did not contain a 3-D woven core. There were three plies of 0/90 fabric interleaved with seven layers of bias fabric. The final skin architecture consisted of 27.87% 0/90 fabric, 70.95% ±45° fabric, and 1.18% Z stitching.

The design of the 3-D woven core consisted of integrating the two 0.48-in. stiffeners with the six 0.17-in. stiffeners in a cross-stiffened arrangement. This task was carried out using ICI/Fiberite's proprietary CADET weaving program. With this software, all the tows that were part of the design of each individual stiffener were traced along their corresponding paths, as illustrated in Fig. 8. The program then turned this graphical representation of the yarn paths into weaving motions for use on the electronic jacquard weaving loom. The 3-D woven core was designed to be woven flat, like a "collapsed egg crate." After weaving, the cross-stiffened structure would be unfolded to the window belt configuration. It was necessary to weave the window belt frame as a collapsed egg crate due to the limitations of the jacquard weaving machine, which could handle only a flat configuration.

13

Table 3 Preform Fiber Orientation Percentages: Stiffener Thickness = 0.480 in.

	LAYER	ORIENTATION	TOW YIELD, g/m	TOW DENSITY, g/cm^3	TOWS/in.^{2}	Z ANGLE	FAW, g/m^2	PLY THICKNESS, IN.
2-D FABRIC	1	±45	0.445	1.77	24	0	420.5	0.0178
	2	±45	0.445	1.77	24	0	420.5	0.0178
	3	±45	0.445	1.77	24	0	420.5	0.0178
	4	±45	0.445	1.77	24	0	420.5	0.0178
	5	±45	0.445	1.77	24	0	420.5	0.0178
	6	±45	0.445	1.77	24	0	420.5	0.0178
	7	±45	0.445	1.77	24	0	420.5	0.0178
3-D WEAVE	8	90	0.445	1.77	6	0	105.1	0.0045
	9	0	3.600	1.77	6	0	850.4	0.0361
	10	90	0.445	1.77	6	0	105.1	0.0045
	11	0	3.600	1.77	6	0	850.4	0.0361
	12	90	0.445	1.77	6	0	105.1	0.0045
	13	0	3.600	1.77	6	0	850.4	0.0361
	14	90	0.445	1.77	6	0	105.1	0.0045
	15	0	3.600	1.77	6	0	850.4	0.0361
	16	90	0.445	1.77	6	0	105.1	0.0045
	17	0	3.600	1.77	6	0	850.4	0.0361
	18	90	0.445	1.77	6	0	105.1	0.0045
	A*	Z	0.445	1.77	36	44	453.7	0.0193
2-D FABRIC	19	±45	0.445	1.77	24	0	420.5	0.0178
	20	±45	0.445	1.77	24	0	420.5	0.0178
	21	±45	0.445	1.77	24	0	420.5	0.0178
	22	±45	0.445	1.77	24	0	420.5	0.0178
	23	±45	0.445	1.77	24	0	420.5	0.0178
	24	±45	0.445	1.77	24	0	420.5	0.0178
	25	±45	0.445	1.77	24	0	420.5	0.0178
KEVLAR STITCHING	B*	Z	0.222	1.44	16	90	67.2	0.0035

TOTAL THICKNESS	0.480 IN.

A* AND B* ARE TOWS THAT GO THROUGH THE THICKNESS OF THE PREFORM.
A GOES THROUGH THE THICKNESS OF THE 3-D WEAVE, &
B GOES THROUGH THE THICKNESS OF THE WHOLE PREFORM.

EST RESULTS:	V$_f$	52.40%
	%0°	37.61%
	%90°	5.58%
	%±45°	52.07%
	%Z	4.74%

MR93-1172-008

The manufacture of the preform consisted of four main tasks: (1) weaving bias fabric for stiffeners and base skin, (2) weaving of 3-D cross-stiffened frame, (3) assembly of the preform, and (4) stitching.

Weaving of Bias Fabric -- Weaving of the bias plies was done by using ICI/Fiberite's PX weaving equipment. This weaving machine is capable of weaving a continuous length material with fiber orientations at ±45°. Once the bias fabric was woven, it was sprayed with a tackifier. About 3% by volume of tackifier was deposited on the plies of fabric. The tackifier consisted of an uncatalyzed epoxy resin (a mixture of Shell Epon 836 and Epon 1001F). This tackifier was chosen because it would dissolve in the resin system during infiltration of the preform. The main role of the tackifier was to allow debulking during lay-up.

14
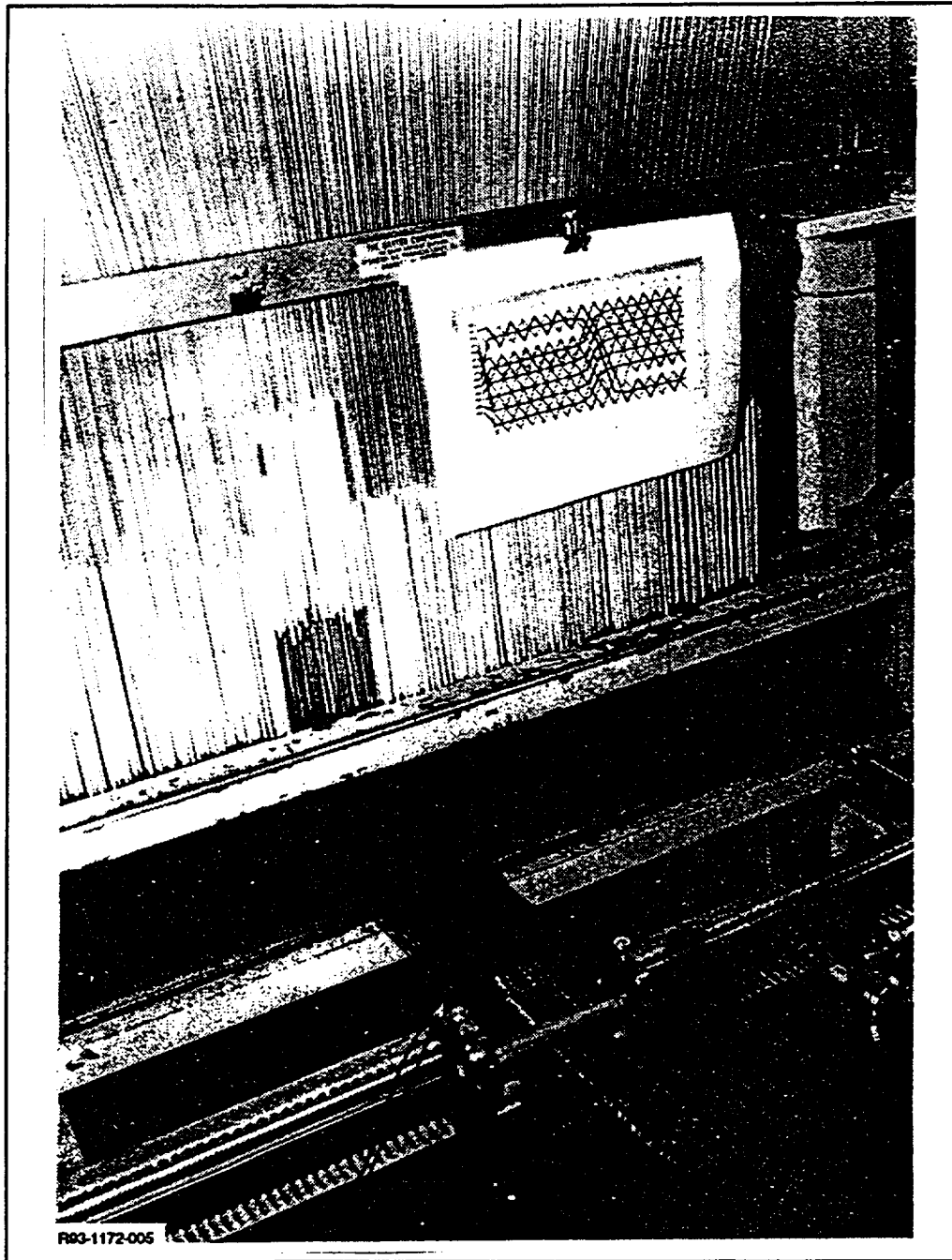
Fig. 8 Weaving of IM7 Graphite Crossing Stiffeners

__Weaving of 3-D Cross-Stiffened Window Belt__ -- Weaving the window belt in a collapsed configuration presented the greatest challenge during fabrication of the window belt preform. Because all of the intersections were continuous, it was necessary to carry very close tolerances during the weaving operation to ensure that the intersections occurred at the right place. Every weaving motion had to be carried out with extreme care to ensure that no level of bulk was woven into the part. The use of tracer threads became an essential part of the control operation; each stiffener was woven with a glass tracer every linear inch. As each inch was woven, careful measurements of each stiffener were made, and this information was fed back to the weaving program either to validate the take-up rate or to modify it accordingly.

15

Assembly of the Preform -- The assembly of the preform was done with the aid of a preforming tool that consisted of aluminum blocks to position the stiffeners in their desired locations. The use of the tackifier became a crucial element in aiding the debulking of the preform while working with the forming tools. The application of heat was necessary to soften the tackifier. The rectangular tools were then pressed into location, forcing the preform into the desired locations. When the preform cooled down, the preforming tools were removed and the preform was set up for stitching.

Stitching -- This was carried out immediately after the preform was removed from the preforming tool in order to minimize the bulking back of the preform. Kevlar 29 1,600-denier sewing thread was used for stitching of the preform. Stitching was done every 3/8-in. row spacing and 1/4-in. stitch length. Stitching was crucial in integrating the laid-up plies with the woven core. Once stitching was completed, the preform was a self-supporting piece that could withstand further handling during infiltration. Figure 9 shows stiffener side close-ups of the ICI/Fiberite cross-stiffened preform.
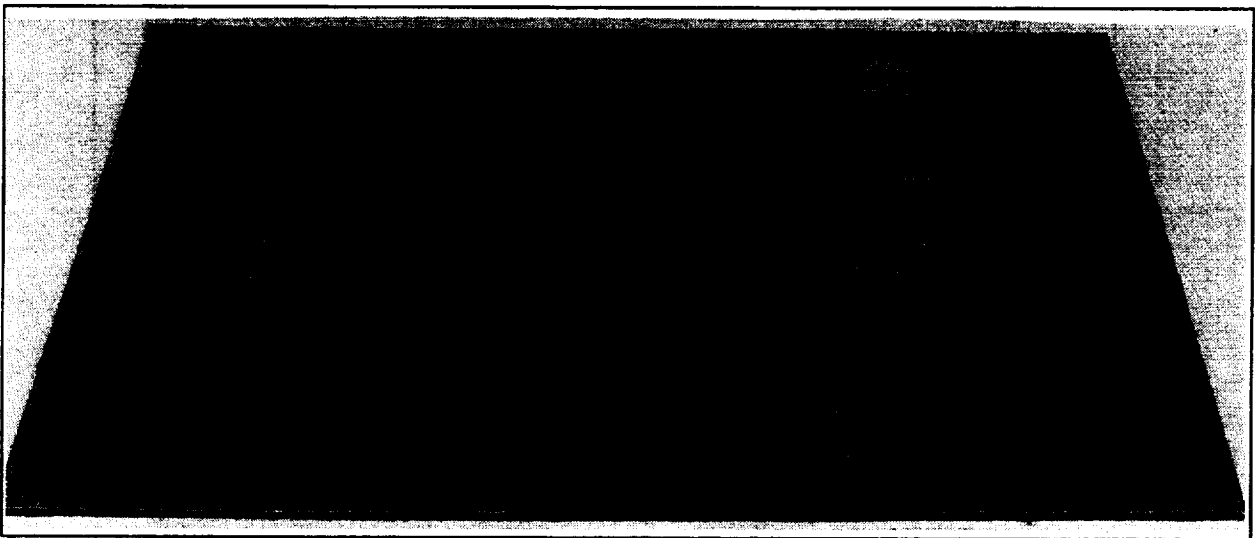
R93-1172-009

Fig. 9 ICI/Fiberite IM7 Graphite Cross-stiffened Preform

2.3.2 Preform Manufacturing

The Techniweave fabricated preform is an assembly consisting of a large 3-D integrally woven detail and several 2-D woven broadgood ply details. Figure 10 is a schematic representation of this final product. The 3-D detail as shown is the predominant feature that integrates the panel skin and stiffeners, and provides the continuity of fibers through the intersection. The 2-D bias broadgood plies are stitched to the stiffeners and skin panel to complete the assembly.

16

STRIP PLIES
2-D WOVEN FABRIC
AS4

ASSEMBLY STITCHING
T900 FIBER

3-D INTEGRALLY
WOVEN DETAIL
AS4 FIBER 0° & Z
T900 FIBER 90°
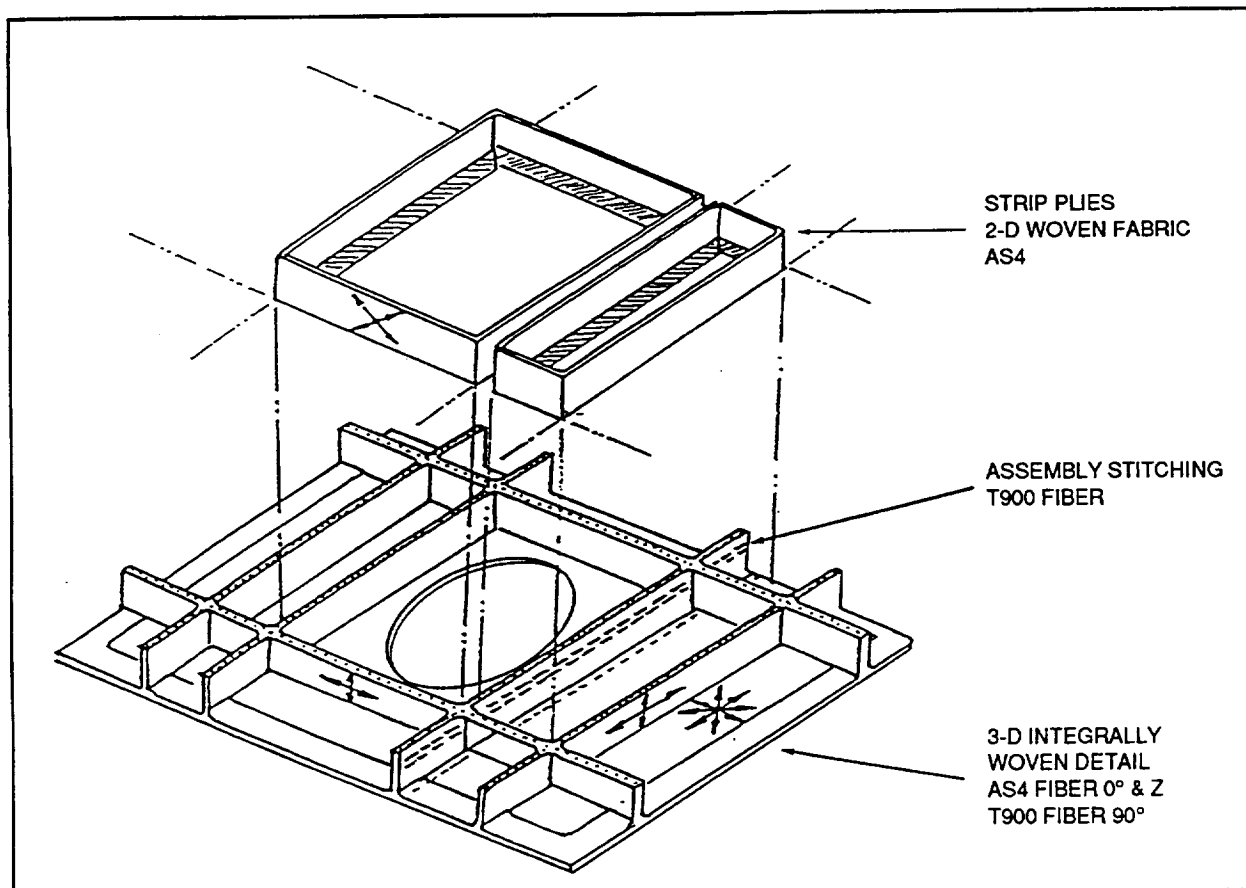
R92-0343-005

Fig. 10 Preform Assembly, Techniweave, Inc., Method

The 3-D weaving process employed to fabricate the core detail is unique. It is a method that has been demonstrated in various thick preform assemblies made by Techniweave and others. More recently, Techniweave has developed fabrication technology for application to thin wall sections, such as defined for the window belt design. Currently, it is a manual process where the weaving is done in layers following predescribed paths. Registration of successive layers is assured through the use of tooling to define through-the-thickness yarn sites. Figures 11, 12, and 13 show vertical yarn stitch sites for a 7-in. x 7-in. test element and two skin surface weave layer definitions: 0° and 45°.

Weaving starts from the surface panel and continues vertically to build up the skin thickness and stiffener heights. The yarns are interwoven through the predescribed paths, as shown in the layer diagrams, in the required orientations: 0°, ±45°, and 90°. Since this is a planar process, the bias weave is easily accommodated in the skin panel, but it cannot be incorporated into the stiffeners. The applied stiffener yarns consist of the 0° orientations that are continuous through the intersection and the "Z" weaving yarns woven through the thickness, as shown in Fig. 14.

Upon completion of this initial weaving phase, the vertical yarn sites are consecutively stitched. These yarns provide the 90° orientation in the stiffeners and the stitching in the skin panel area. The preform is completed by stitching the bias 2-D details to the main core piece.

The completed preform will have a 120-180% loft, or 1.2-1.8 times the drawing net final thickness. Debulking will be done to compress the preform using a combination of stitching and a low-temperature melting point uncatalyzed epoxy resin binder.

Techniweave is currently in the process of installing a machine to automate the 3-D weaving process; it is scheduled to be on-line in the near future.

17

BASE PLATE   VERTICAL STITCH SITES
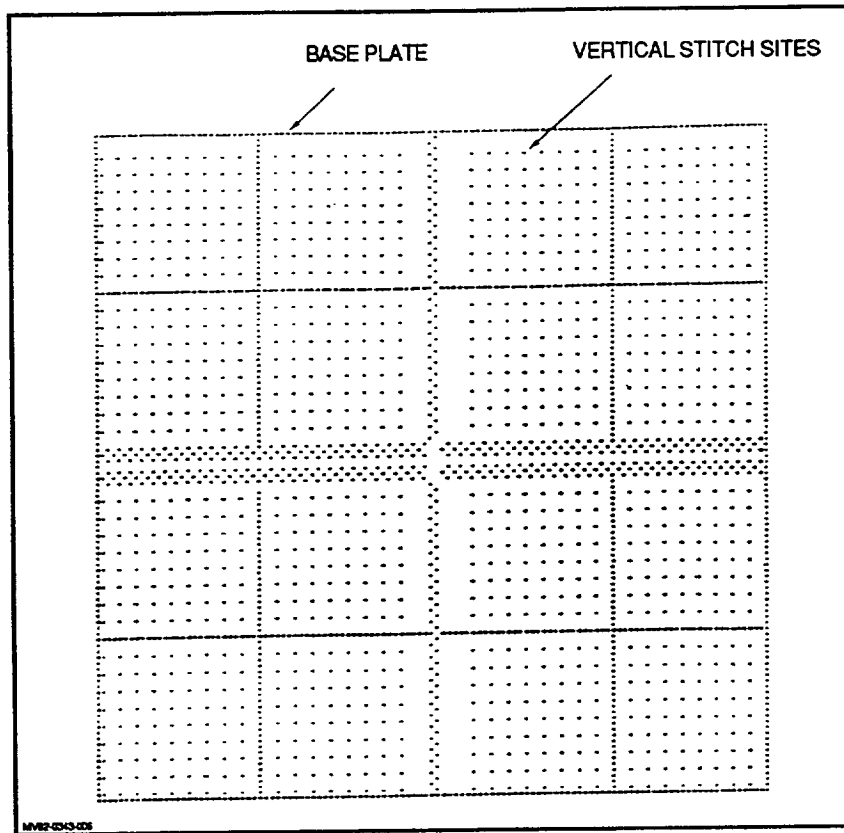
Fig. 11 Seven-by-seven Test Element Pin Pattern

WA #0899

$$\frac{PLY\ C}{PLY\ D}$$

AS4-3K CONTINUOUS YARN
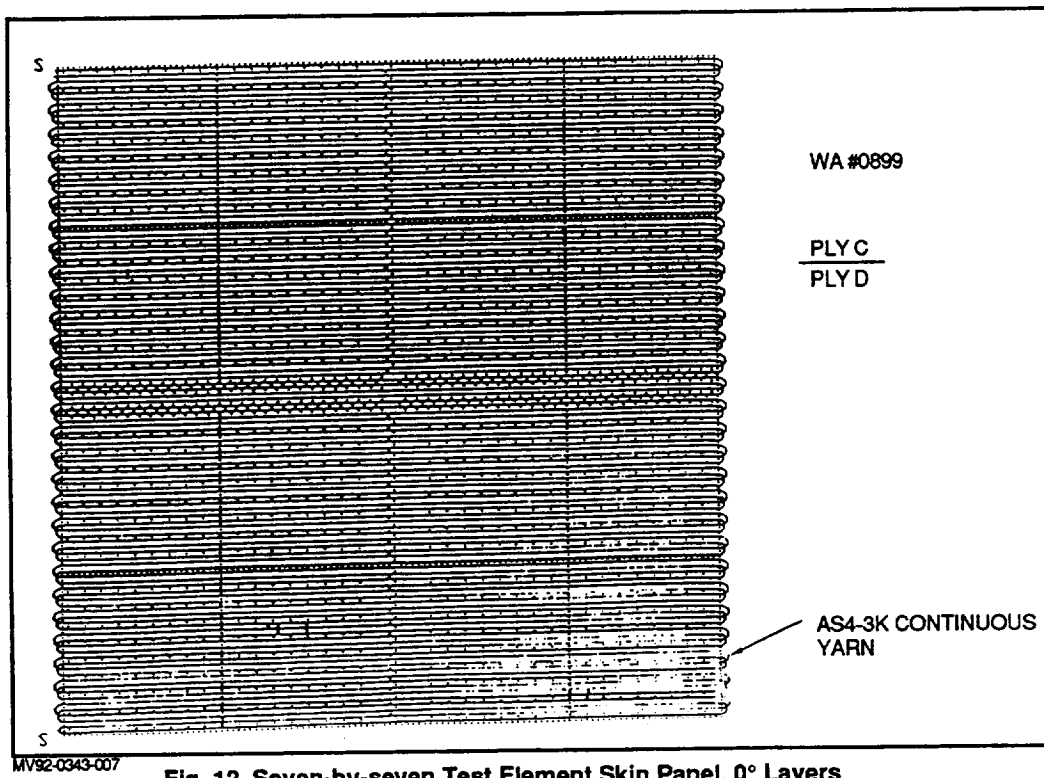
Fig. 12 Seven-by-seven Test Element Skin Panel, 0° Layers

18

AS4-3K CONTINUOUS YARN
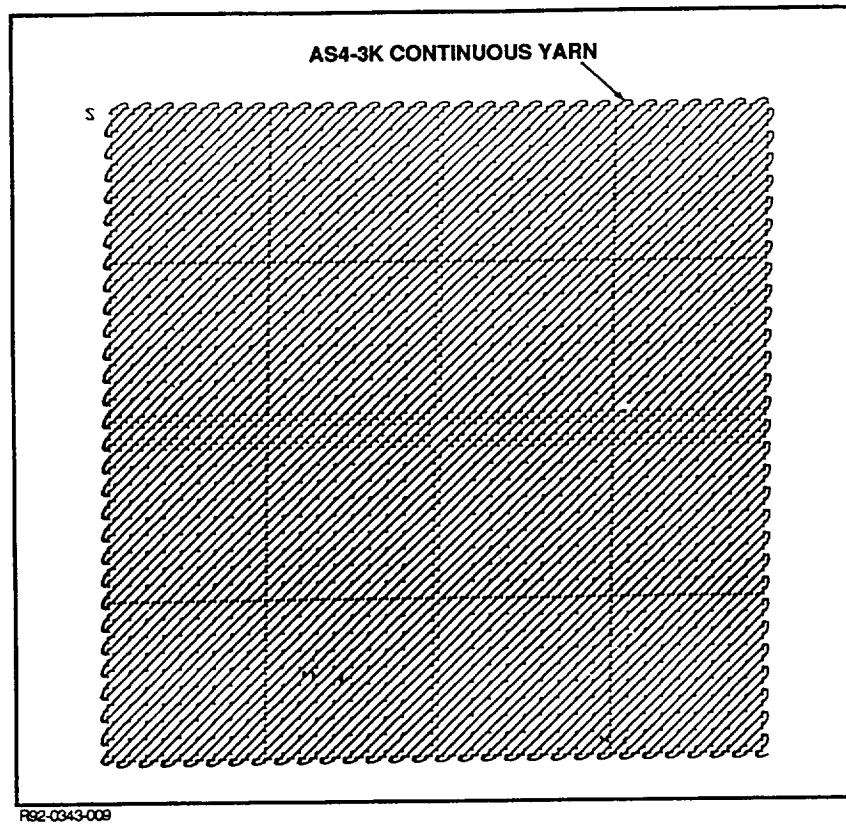
Fig. 13 Seven-by-seven Test Element Skin Panel, 45° Bias Layers

0° YARNS

90° STITCH YARNS

"Z" WEAVER YARNS
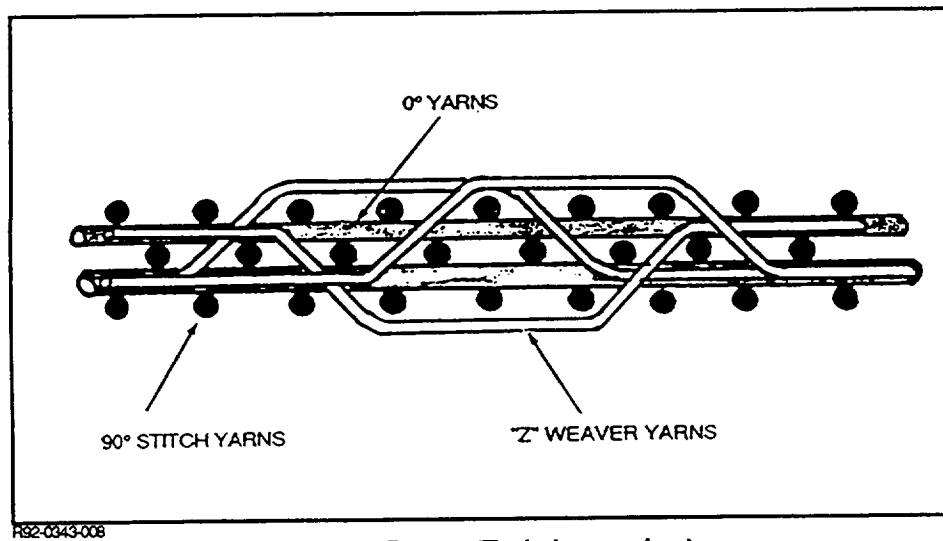
Fig. 14 Weaving Pattern (Techniweave, Inc.)

The translation of the original design into a preform required some compromise in fiber volume, stacking, and percentage of fiber orientations. Table 4 shows the initial target fiber orientation percentages from the engineering drawing (D19B1865) and the resulting preform compromise from Techniweave. Techniweave will use AS4-3K yarn for the stiffener 0° orientations and panel 0°, 90°, and ±45° orientations. The "Z" direction weaver yarns will be T300-1K. The stiffener 90° orientation and all stitching will be achieved using Toray T900 high-strength graphite yarn. The 2-D material will be AS4-5H. The basic design concept for the stiffeners is shown in Fig. 15, 16, and 17.

Table 4 Preform Fiber Orientation Percentages, Fiber Volume, & Material

APPLICATION & ORIENTATION	NORTHROP GRUMMAN D19B1865 TARGET VALUES	TECHNIWEAVE METHOD	ICI/FIBERITE METHOD
PANEL			
0 DEG	10%	12% AS4-3K	9%
±45 DEG	85%	82% AS4-3K	82%
90 DEG	5%	6% AS4-3K	9%
Z	NA	N/A	NA
FIBER VOLUME	58%	57%	58%
HORIZONTAL STIFFENER			
0 DEG	40%	38% AS4-3K	28% IM7-12K
Z	NA	3% T300-1K	8% IM7-12K
±45 DEG	50%	46% AS4-5H	54% IM7-5H
90 DEG	10%	10% T900-3K	10% IM7-12K
FIBER VOLUME	58%	57%	52%
VERTICAL STIFFENER			
0 DEG	25%	28% AS4-3K	15% IM7-12K
Z	NA	6% T300-1K	5% IM7-12K
±45 DEG	65%	56% AS4-54	72% IM7-5H
90 DEG	10%	9% T900-3K	8% IM7-12K
FIBER VOLUME	58%	54%	56%
ASSEMBLY			
STITCHING	LESS THAN 6%	2% T900-3K	2% KEVLAR

R92-0343-010

CORE WEAVE OF 0° & 90°

BIAS PLIES ARE ATTACHED BY STITCHING THROUGH THE RIB & THE PANEL

90° FROM THE CORE PENETRATE & TACK INTO THE SKIN PANEL
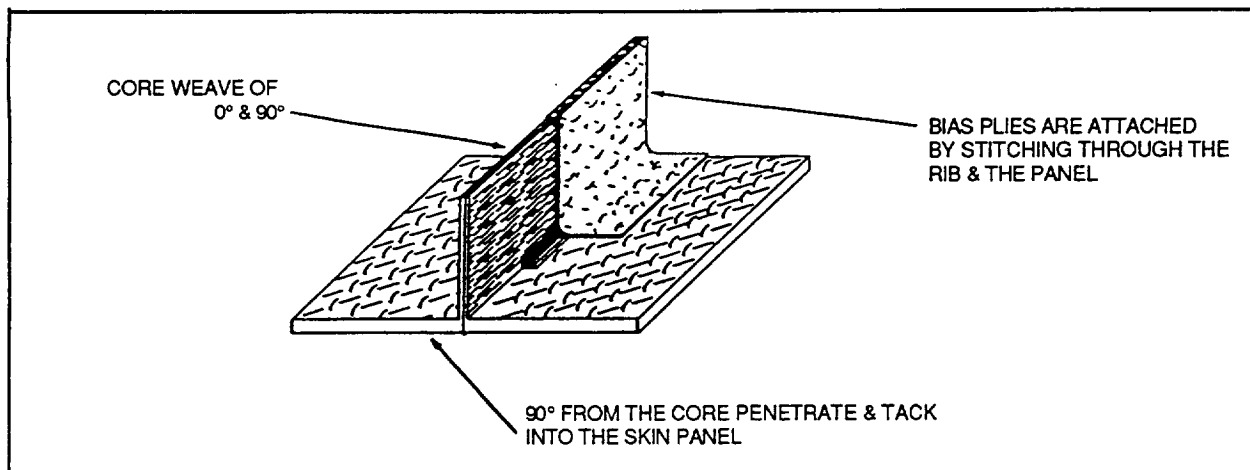
R92-0343-011

Fig. 15 0.170 Stiffener Construction

CORE HAS 0°, 90°, & 45°

BIAS PLIES ARE ATTACHED BY STITCHING THROUGH THE RIB & THE PANEL

90° FROM THE CORE PENETRATE & TACK INTO THE SKIN PANEL
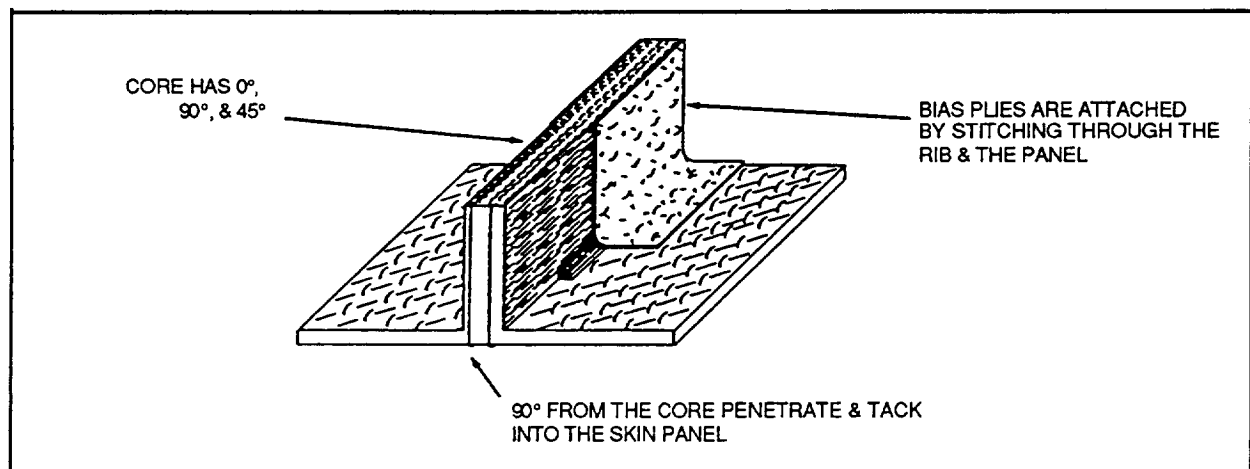
R92-0343-012

Fig. 16 0.48 Stiffener Construction

ALL OF THE 0° DIRECTION REINFORCEMENTS IN THE RIBS ARE CONTINUOUS THROUGH THE INTERSECTIONS
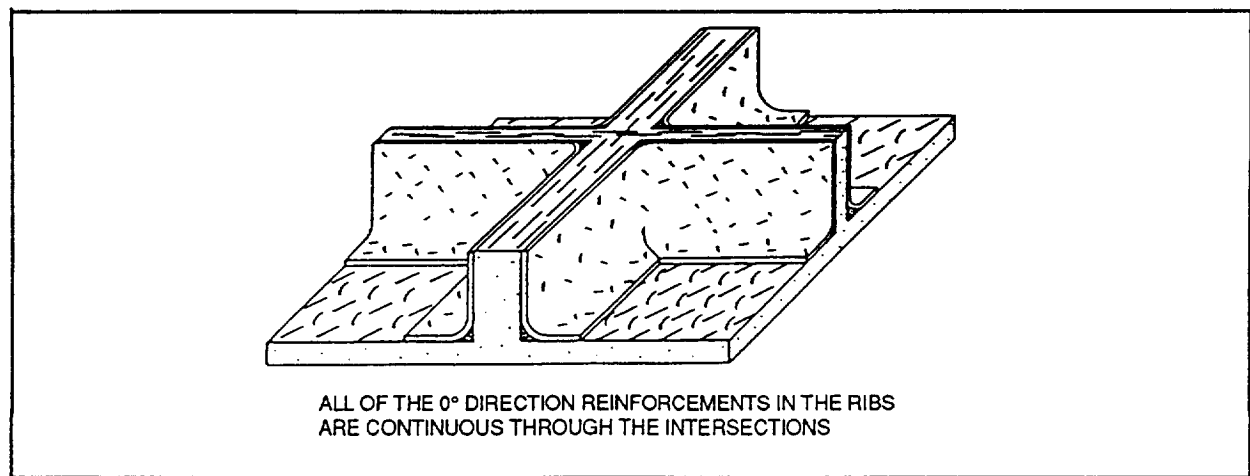
R92-0343-013

Fig. 17 Typical Rib Intersection

21

There are several unique aspects of this process that are beneficial to fabricating preforms. Among these are the ability to weave the preform in the drawing orientation without requiring an unfolding operation, the ability to weave the skin and intersecting stiffeners as one core detail, the potential for automation and scale-up, and the ability to weave in-plane holes into the preform.

The ICI/Fiberite approach to the window belt design is conceptually shown in the schematic of the test element in Fig. 18. It consists of a 3-D woven core and several 2-D woven details that are assembled and debulked to form the preform. The core is produced on an ICI-built loom capable of weaving thicknesses up to 3.5 in. and outfitted with a Staubli electronic jacquard head.
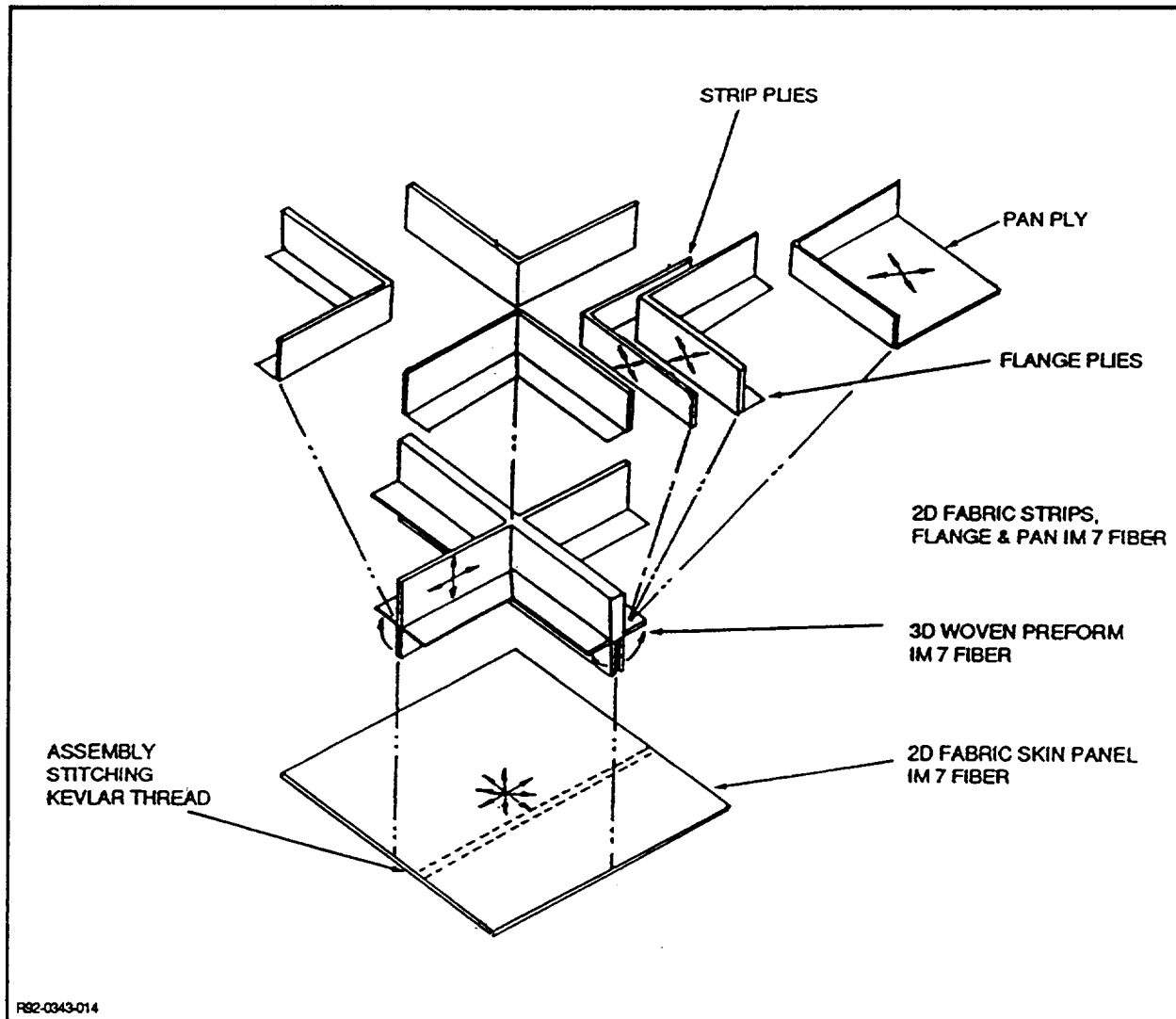
Fig. 18 Test Element Preform Assembly, ICI Method

The 3-D core is the principal feature of the design and provides the through-the-intersection fiber continuity. Figure 19 shows the woven preform prior to being expanded and erected vertically. Essentially, it resembles a collapsed egg crate. The preform exits the loom in the longitudinal direction parallel to the 0° fiber orientation direction.

22

Fig. 19 Unexpanded, As-woven, Core Detail by ICl/Fiberite
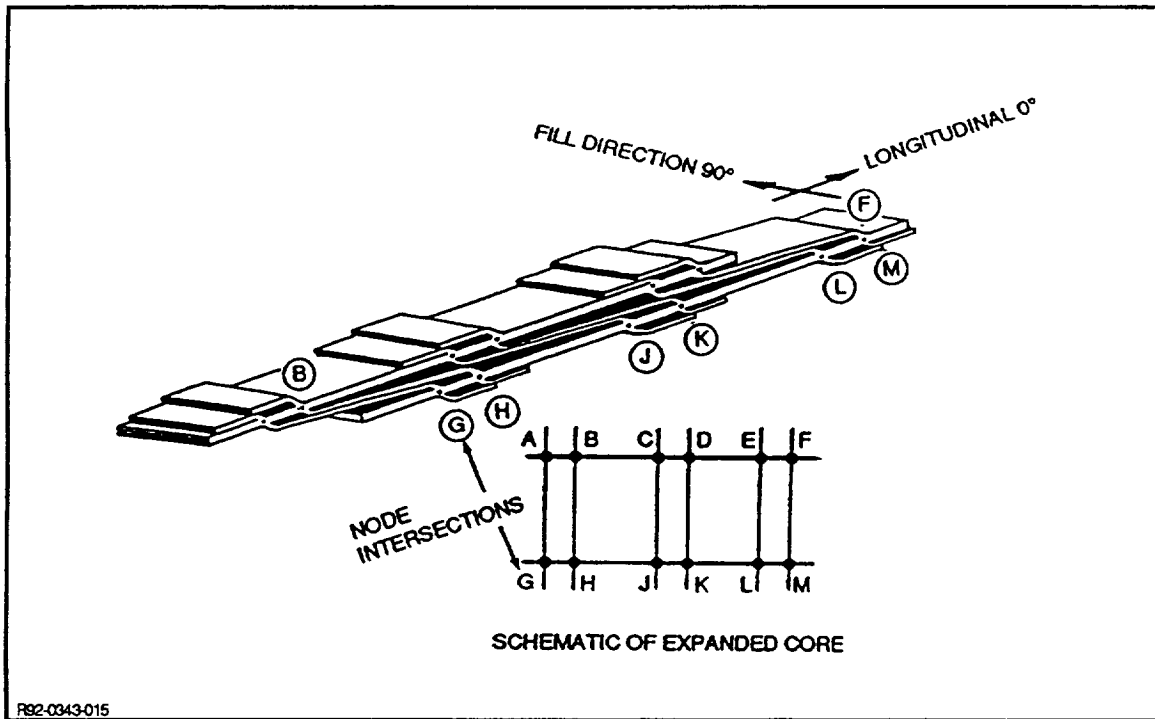
A schematic representation of the 3-D fiber architecture is shown in Fig. 20. The preform consists of three principal fiber orientations: 0°, depicted by the solid horizontal lines; "Z" direction, represented by the angular translational lines; and the 90 fill yarns shown by the circles. The through-the-intersection fiber continuity is shown and is achieved by rotating the 0.17 stiffener legs 90°.

Fig. 20 Fiber Architecture 3-D Woven Core Preform, ICI Method

23
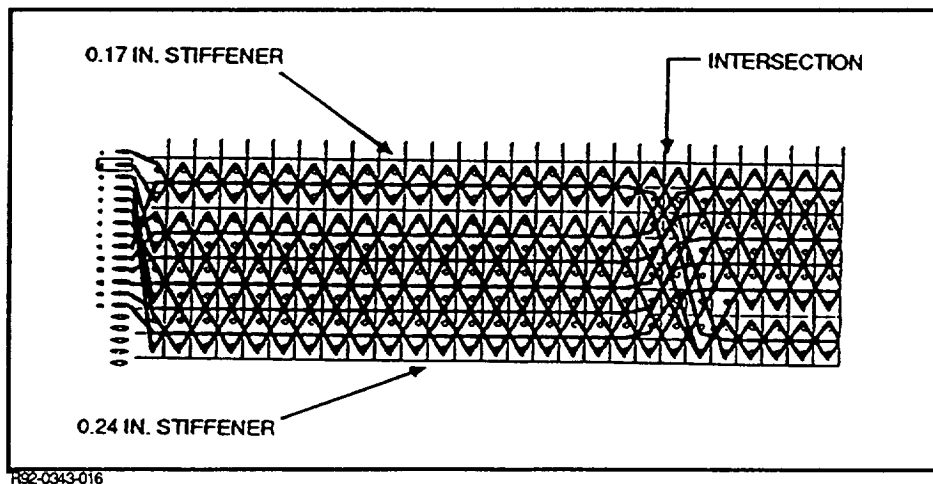
Producing this preform is a compromise of the initial target drawing (D19B1856) fiber volumes and percentages, as shown in Table 4. For this process, "Z" yarns are introduced and are required to interlock the longitudinal and fill yarns together, thus giving a structural rigidity to the preform. These "Z" yarns replace some of the longitudinal 0°, as they do in the Techniweave process. The angular paths are expected to reduce the stiffener axial load capability. This will be verified during the testing phase. Also, the angular path of the "Z" yarns is related to the thickness of the assembly. The longitudinal stiffener (0.24-in.-thick) angle is 44°, and the vertical stiffener (0.17-in.-thick) angle is 20° The severity of the angle is expected to be directly related to the stiffness and axial load capability.

The 2-D broadgood materials that make up the remainder of the preform definition are assembled to the 3-D core to form the skin panel, stiffener buildups, and flanges. For this application, these plies take the form of strips, sheets, and pans. Figures 21 and 22 show the completed preform cross-sectional assembly of the longitudinal and vertical stiffeners. Figure 23 shows the plan view of the assembled stiffener intersection.

ICI debulks the completed preform to as close to net shape as possible, using a tackifier or binder resin. An uncatalyzed epoxy resin, 8% volume, is sprayed on the woven details prior to the preform assembly to provide a tackiness to hold the net dimensional compressed shape and to add rigidity to the preform. This tackifier is a Shell product, a combination of Epon 836 and 1001F, and has a low melting point, 130°F. This compressed preform is stitched using a Kevlar thread at a 1/4-in. stitch pitch in 3/8-in. spaced rows. The stitching provides additional rigidity to the preform and aids in holding the net dimensional shape. Stitching is a requirement to enhance the damage tolerance of the assembled 2-D material. For this application, the stitching volume percent is less than 2.

A 14-in. x 14-in. cross-stiffened preform test element was fabricated by ICI. This cross-stiffened element represents a stiffener intersection of the window belt and was used to demonstrate the preform fabrication methodology. Similar test elements will be used during subsequent tests to demonstrate RTM and RFI processibility and structural performance.

This preform will utilize IM7 graphite for the preform yarn and 2-D woven broadgoods as the basic construction material. The 3-D core woven detail will be fabricated using 12K yarn for all of the orientation, 0°, 90°, and "Z" angular directions.

A second cross-stiffened preform was fabricated by Fiber Innovations, Inc., (FII) using AS4 graphite. Three-dimensional weaving was used in the fabrication of the crossing stiffeners but, instead of 2-D bias fabric, ±45/0° triaxial braiding was used to introduce the bias reinforcement that 3-D weaving cannot provide. ±45/0° triaxial braiding also was used for the skin edge reinforcement. Figures 24, 25, and 26 show stiffener side, skin side, and close-up of the FII cross-stiffened preform, respectively.

Resin film infusion (RFI) was done with the parts upside down. The vacuum ports of the bag were taped to prevent the bag from sagging. After the initial infusion, the parts were heated right side up for any additional bleeding or flattening of the wrinkles beneath the stiffeners. The temperature was kept in the range of 150-200°F. The maximum time at temperature was 2 hr.

3501-6 epoxy resin in bulk form was obtained from Hercules, Inc. Chunks of resin were broken from a 70-lb block and several smaller blocks. The resin was heated on a flat aluminum plate with a release ply and an edge dam to contain the resin and define the size of the cast. This was heated to 150°F, and the resin was spread as evenly as possible. The resin was rolled up and stored after cooling to a solid film.

LEGEND
FLANGE PLIES
STRIP PLIES
3-D WOVEN CORE
PAN PLIES
SKIN PLIES

0.170 IN.
0.061 IN.
1.500 IN.
0.750 IN.
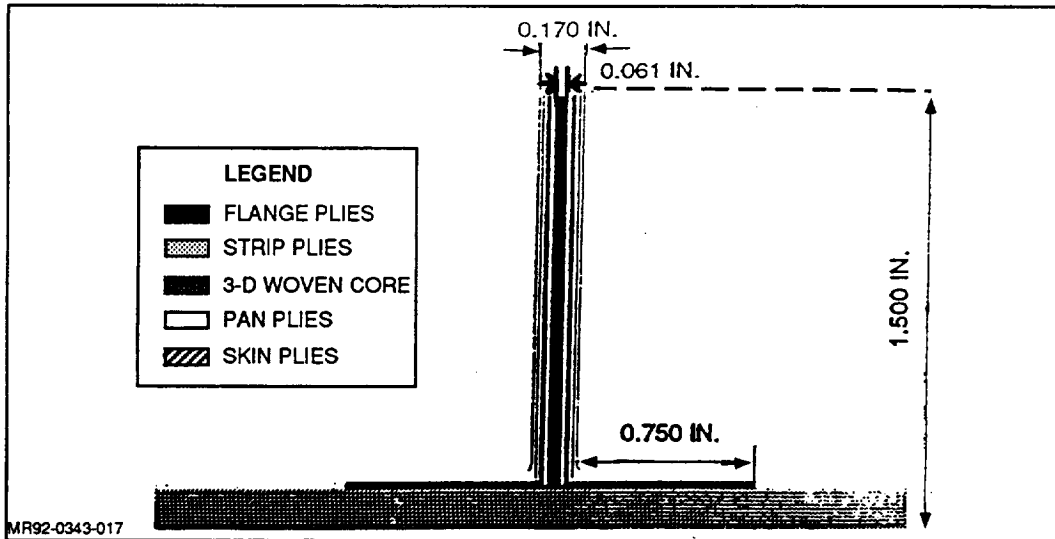
MR92-0343-017

Fig. 21 0.17-in-thick Stiffener; Ply Lay-up (ICI)

0.480 IN.
0.240 IN.

LEGEND
FLANGE PLIES
STRIP PLIES
3-D WOVEN CORE
PAN PLIES
SKIN PLIES

1.500 IN.
0.750 IN.
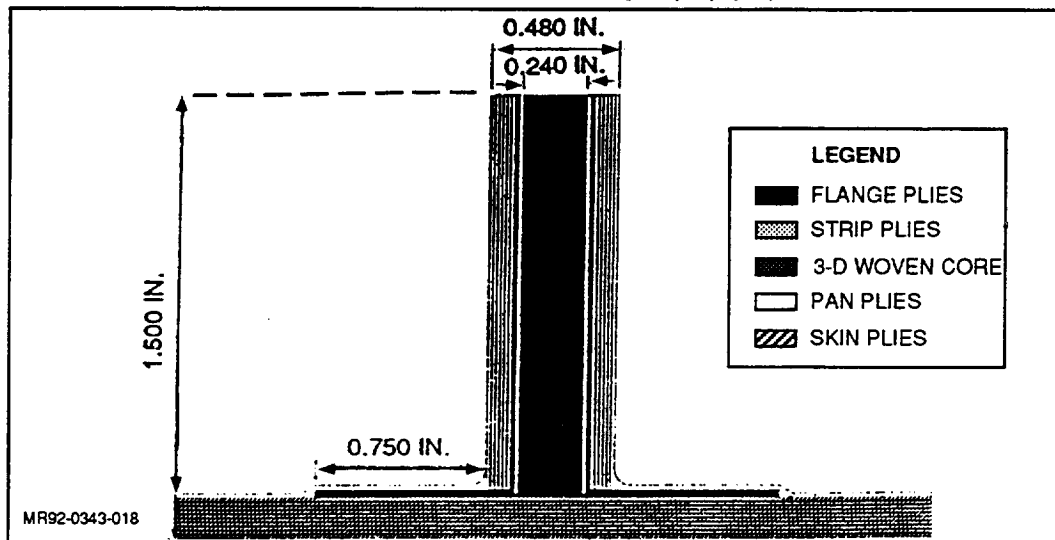
MR92-0343-018

Fig. 22 0.48-in.-thick Stiffener; Ply Lay-up (ICI)

0.480 IN.
0.240 IN.

LEGEND
FLANGE PLIES
STRIP PLIES
3-D WOVEN CORE
PAN PLIES
SKIN PLIES

0.170 IN.
0.061 IN.
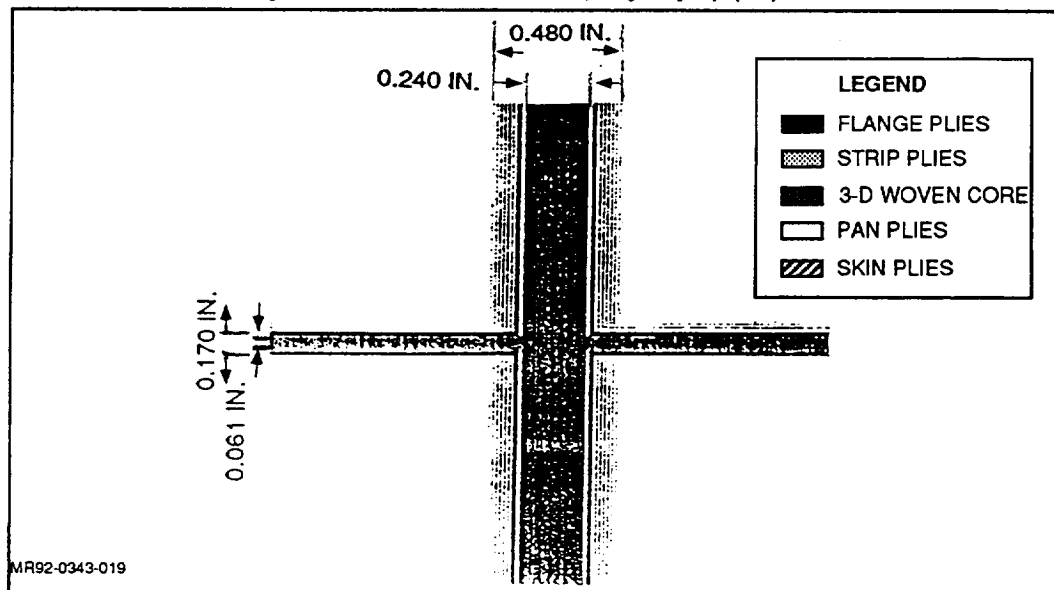
MR92-0343-019

Fig. 23 Intersection; Ply Lay-up (ICI)
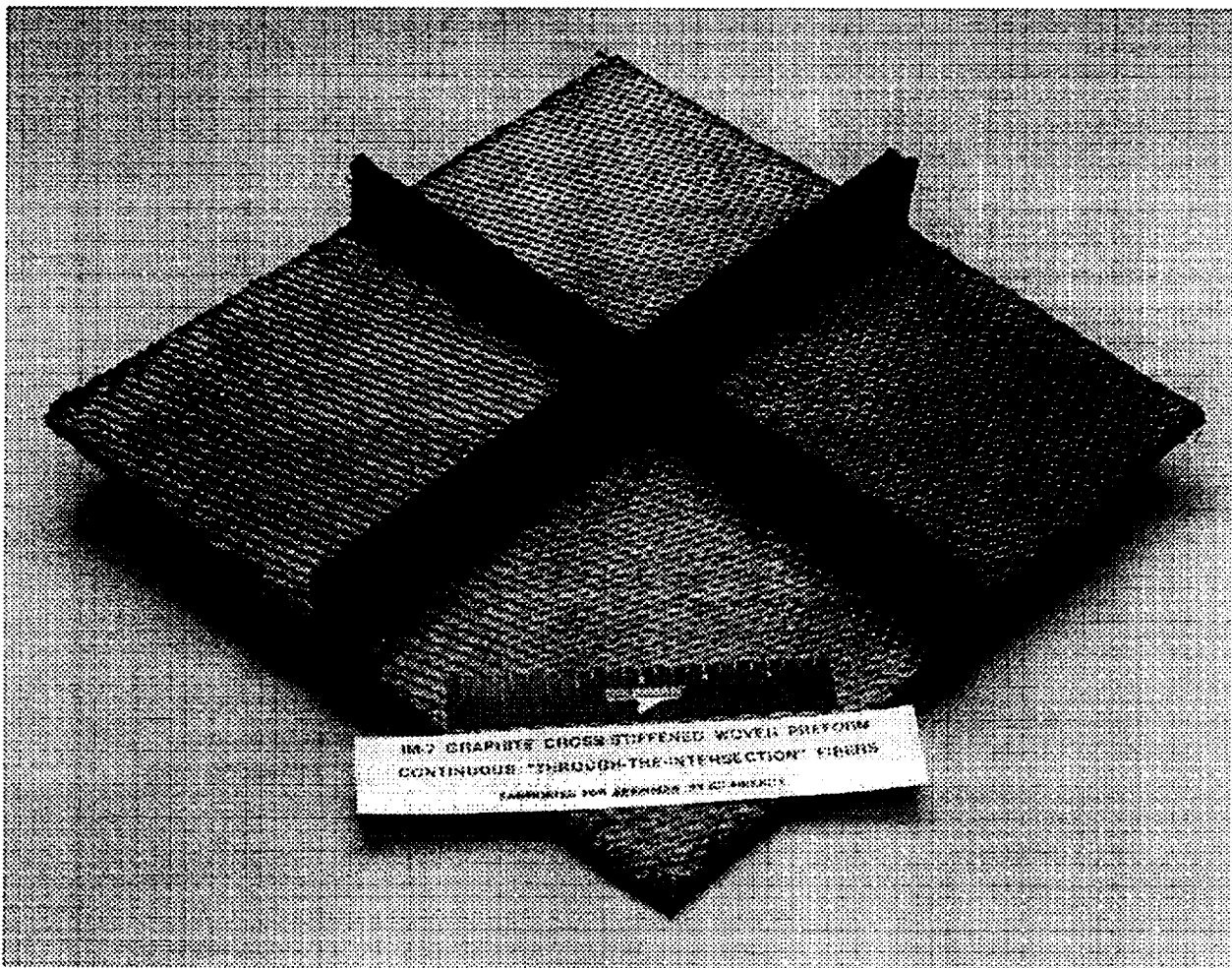
R92-0343-020

Fig. 24 14-in. x 14-in., Woven, Cross-stiffened Test Element (ICI/Fiberite)

The infusion began with a single sheet of resin weighing 20 lb. This was an initial 48% resin content. We expected to bleed down to 36% resin content. The bagging scheme was a film of pin pricks over the tooling, two layers of bleeder to absorb the resin, and then two films of pin pricks to prevent plugging of vacuum ports. The first infusion went for 2 hr before bleed started to show through along the top edge of the stiffeners. The infusion was stopped because of the amount of time at temperature. The part had a very heavy resin film remaining on the bottom. The resin content was still 44%.

26
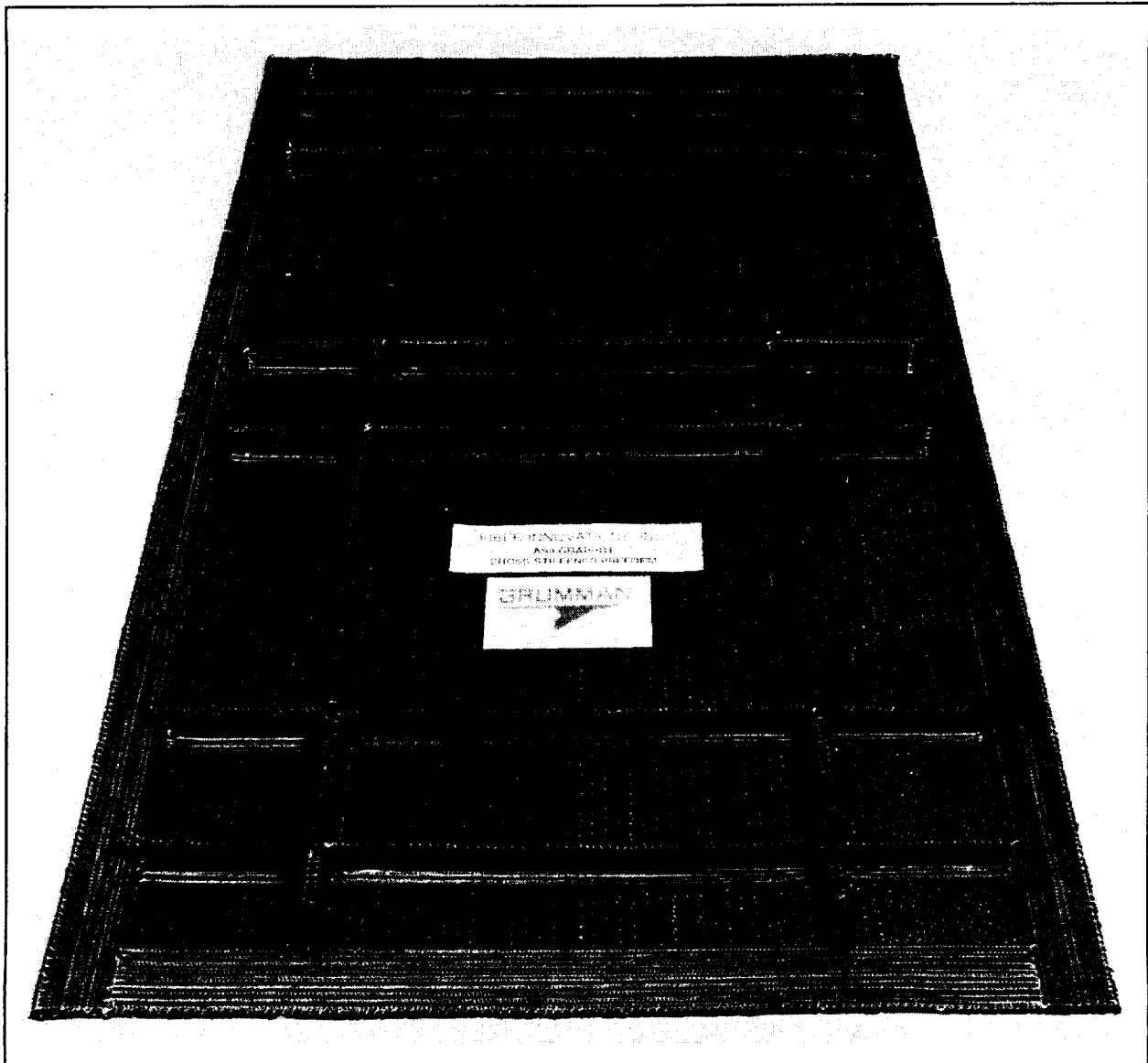
R93-1172-012

Fig. 25 Fiber Innovations AS4 Graphite Cross-stiffened Preform

It was decided to try a second bleeder infusion. One layer of bleeder went under the window belt with a separator layer of TFP between. The bleeder went on the bottom because of concern that the resin had advanced enough so that bleeding through the thickness of the panel was questionable. The bleeder also went across the top to draw resin out of the stiffeners, which were too thick. Pin pricks did not go under the bleeder but did go on top to prevent plugging of the vacuum ports. The part was pressurized to 30 psi to drive off excess resin. This bleed infusion did drive the resin content down to 33.8%, which was within the processing parameters.

27
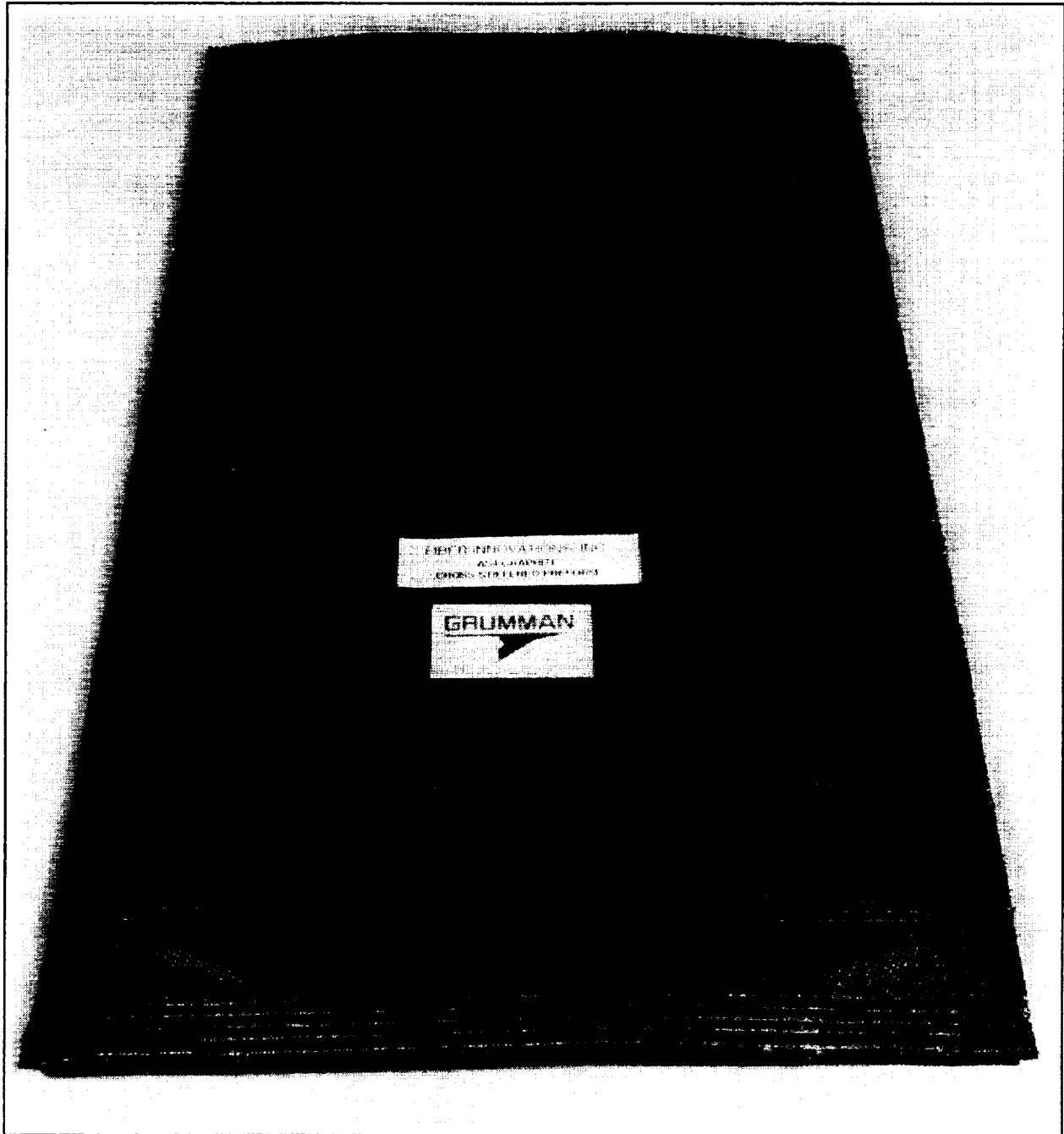
Fig. 26 AS4 Graphite Cross-stiffened Preform Back Face

To eliminate wrinkling, the part with the infusion tooling -- together with a simple vacuum bag to hold everything in place -- was heated to 150°F to soften the resin. An aluminum plate went over the stiffeners, and 200 lb was loaded on top. The part was held this way for 30 min. This process was repeated a second time, with 600 lb to finally smooth out the wrinkles.

28

The Fiberite window belt went through the same process as the Fiber Innovations, Inc., (FII) window belt except that the starting resin content was much lower, 12.5 lb or 36.5%. This proved to be too little; the stiffeners did not wet out. More resin was added (1.5 lb total) in strips along the 0.480 stiffeners. This resin was absorbed into the stiffeners on the second infusion.

2.4 FABRICATION OF SUBCOMPONENT

The tooling concept employed for the RTM process was a bolted multi-piece steel mold that provided a compression/wedge action. An assembly of the subcomponent tool is shown in Fig. 27. Although a press is preferred for tool closure, a bolted strong back design was selected due to the size limitations of the current prototype RTM lab facility press, 30 in. x 30 in. The wedge action provides the side pressure on the preform as the mating tool is closed to complete the debulking to the final part dimensions and to attain the required fiber volume. Inserts within the tool are free and permitted to float.

Other tooling concepts considered include aluminum mandrels/steel base plate, an aluminum-filled epoxy casting system, and rubber intensifiers. These concepts were discarded in favor of the steel wedge design based on positive past experience.

The injection design used multiple ports, one at each center support post, with four vent exits. Also included in the design is a resin reservoir on the two long sides which provides resin reserve to back-fill the preform during cooling.

Resin flow was initially determined by using a glass broadgoods replica preform in the tooling prove-out phase. The tool was evacuated, and the resin introduced at 50 psi and 180°F. Upon resin introduction, the exit ports were opened and flow regulated to ensure complete filling. Sequencing and utilization of the exit ports were determined. This trial method provided confidence in the process prior to curing the graphite preform.

The tooling concept employed for curing the subcomponent consists of multiple aluminum and aluminum-faced rubber details that provide compression/wedge action. The assembly of the tool is shown in Fig. 28. The rubber details had built-in 1/8-in. aluminum facesheets to provide better surface flatness. A strip of aluminum (2 1/2-in.-wide) went around the edge pad to provide a surface free of mark-off, except at the corners. The spacer bars were made of composite instead of aluminum so that there would be no thermal mismatch.

The window belt infusion tooling is shown schematically in Fig. 29. Flat 1/8-in. aluminum plates with evenly spaced holes covered the web between stiffeners. A mitered strip of aluminum (2 1/2-in.-wide) with spaced holes covered the edge pad, and 2 x 3/4 x 1/8 mitered aluminum angles tooled the stiffeners. A 1/2-in. thick interlocking spacer bar system with evenly spaced holes was used to bleed the stiffeners and define thickness. Figure 30 shows the preform in the infusion tool.

The cure began with 20-30 in. Hg vacuum drawn on the part. The part was then moved into the autoclave and 15 psi applied. The heat-up ramp rate was slow because of the mass involved, approximately 1°F/min. to 225°F. The part was dwelled for 45 min. at 225°F. Pressure was increased to 30 psi, while the vacuum was vented. With vacuum vented, the pressure was raised

Fig. 27 Tooling Design Concept, Window Belt Subcomponent, Drawing D19B1865-11BOF

-101 Al   -103 RUBBER
-105 Al   -107 RUBBER
-109 Al   -111 RUBBER
          -113 RUBBER

MV93-1172-026
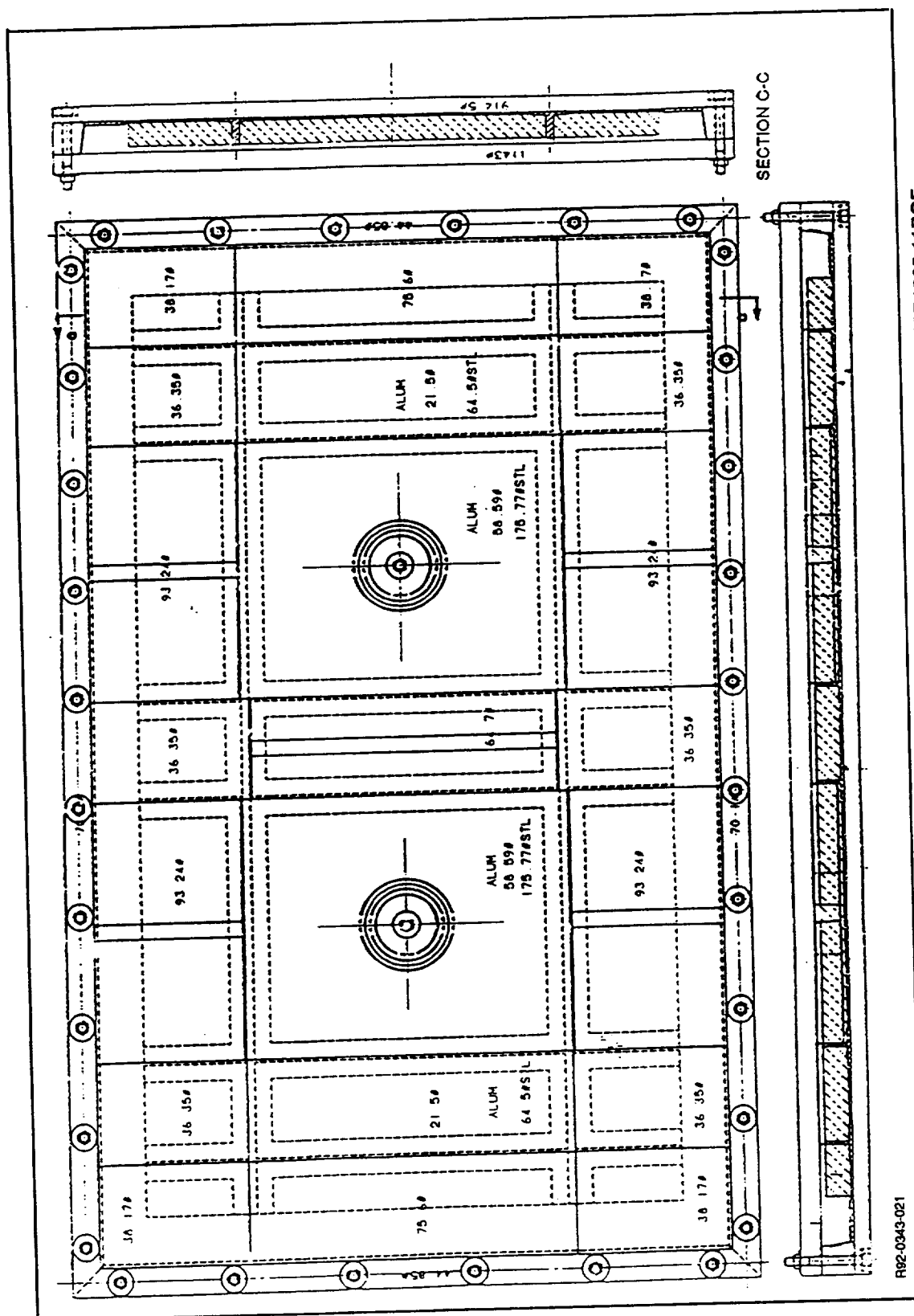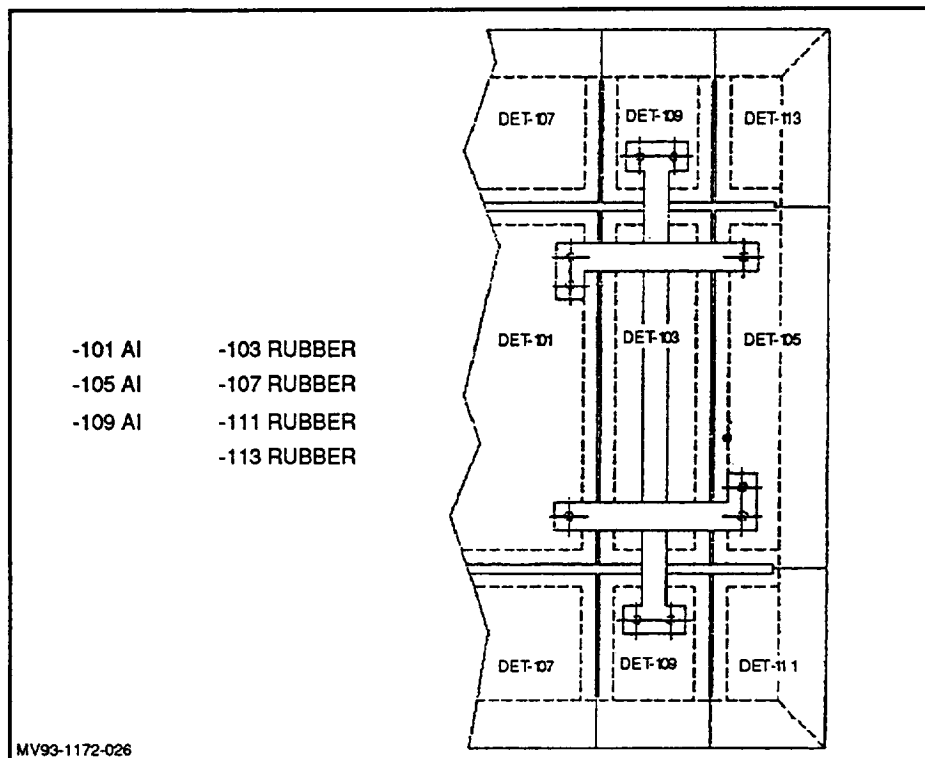
Fig. 28 Cure Tool Assembly for Window Belt

SPACER BAR

SPACER BAR

2 x 3/4 x 1/8 ANGLE

1/8 FLAT PLATE

MV93-1172-026
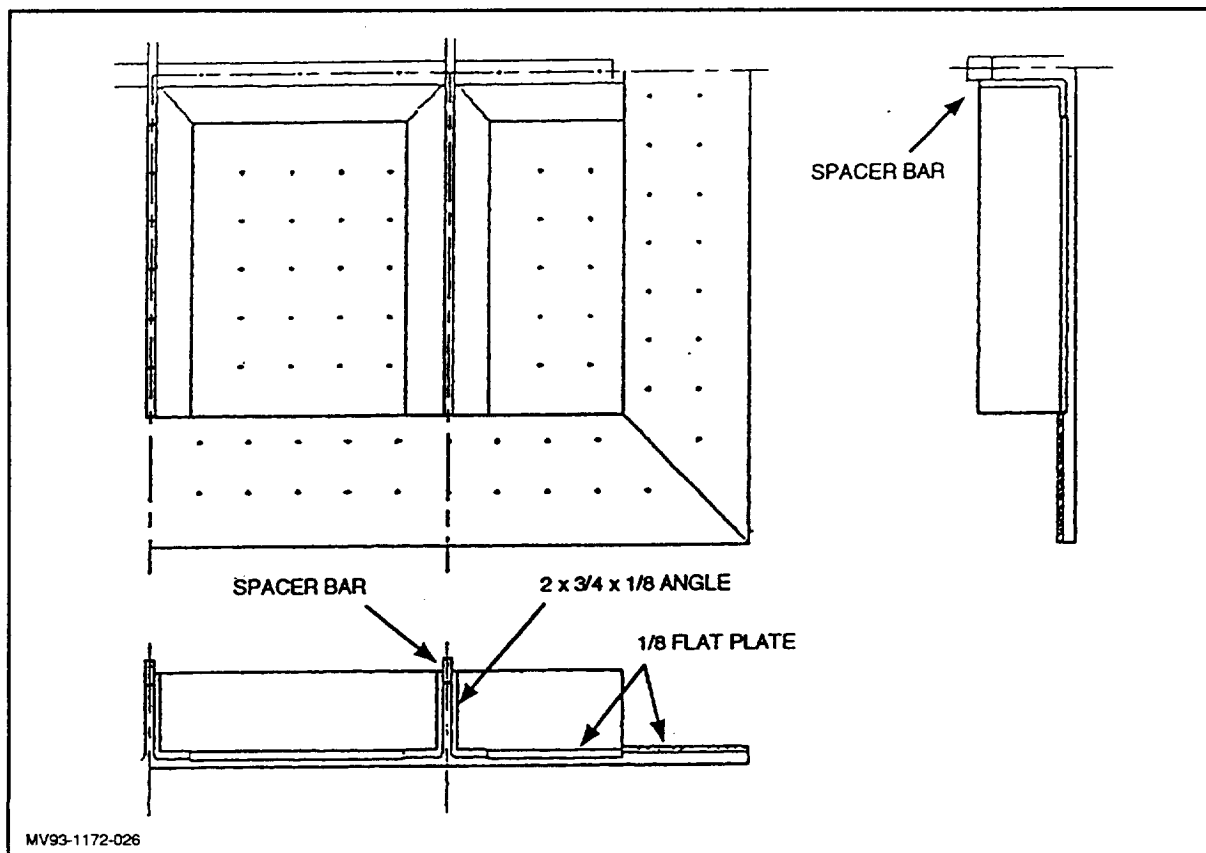
Fig. 29 Window Belt Infusion Tooling

31
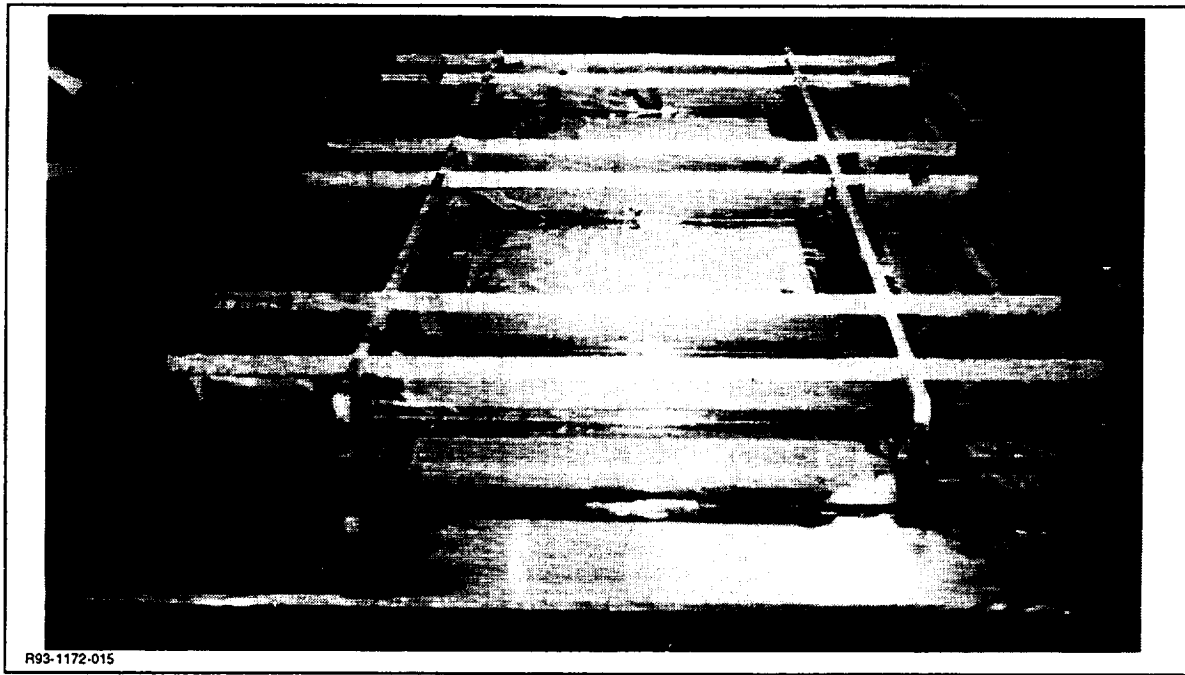
Fig. 30 Infusion Tool With TFP & Spacer Bars

to 100 psi. Heating continued at 1°F/min. to 350°F. The second hold was for a minimum of 120 min. The part was then cooled to 150°F before releasing pressure and removing the part. After inspection, the parts went through a freestanding post-cure of 4 hr at 350°F. This was to achieve the maximum Tg of the material. The final infused panel is shown in Fig. 31.
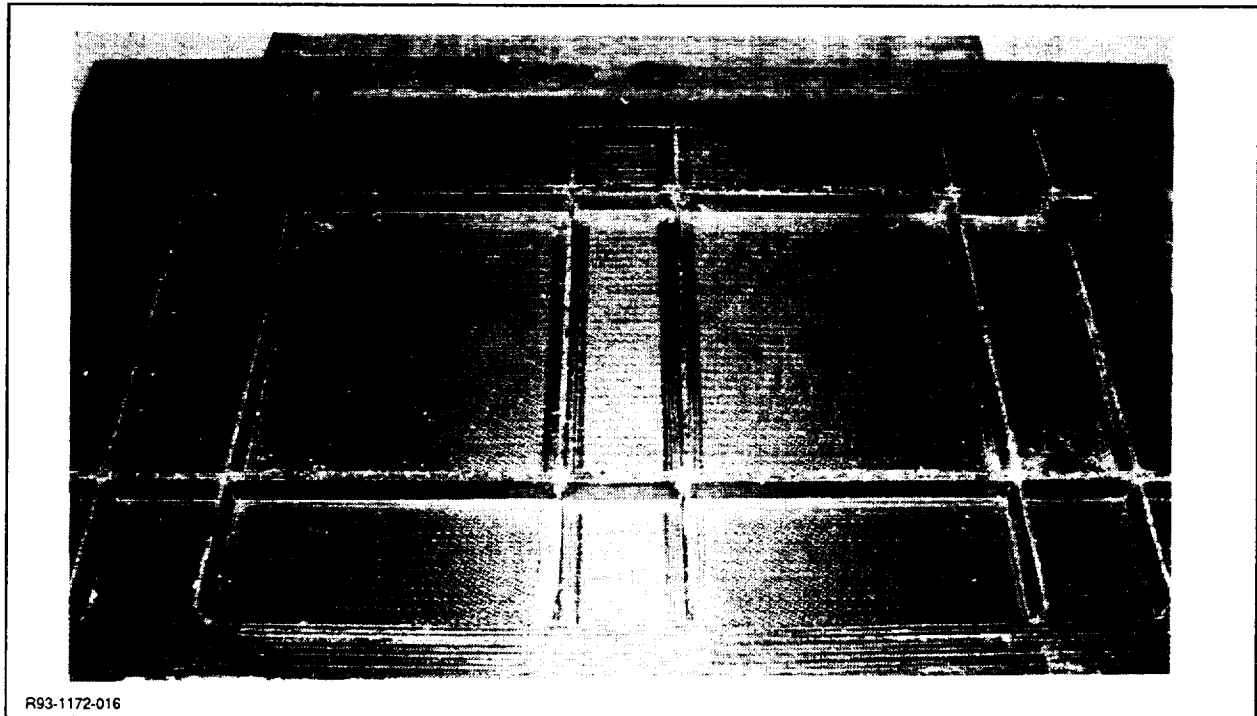
Fig. 31 Cross-stiffened Preform After Infusion With 3501-6 Epoxy Resin (38 in. x 62 in.)

32

The Fiberite window belt was closest to the final dimensional tolerances and was cured first. As with the earlier preforms, the panel was covered in TFP. This was to be both a release and a breather path for trapped volatiles under the tooling. Tape went around all the edges and was used to seal all corners and intersections. The part was already at 32.8% resin, and a minimum of bleed was desired.

The tooling fit easily between the stiffeners because the tooling had been sized down for thermal expansion. A set of composite interlocking spacer bars went on top of the stiffeners and between the aluminum and rubber details. This was to help define the intersections, thickness, and straightness of the stiffeners. Tie bars were then bolted across the aluminum details to align these together. Next, 2-in.-wide tape was wrapped around the perimeter of the part to act as a further barrier against bleed. Figure 32 shows the cured subcomponent with the window cutouts.

The bagging and cure process for the FII window belt was the same, except for perforations in the tape across the top of the stiffener. The holes were to allow some bleed because the stiffeners were too thick. Two layers of bleeder went across the spacer bars to absorb the resin bleed. In addition, a 0.020-in. layer of resin was applied to the base to bring the thickness into tolerance.

The tooling was much more difficult to install. We had been unable to bleed the thicker stiffeners of the FII window belt to the same thickness as the Fiberite part. The part had to be heated to get the tools to press into place.

R93-1172-017
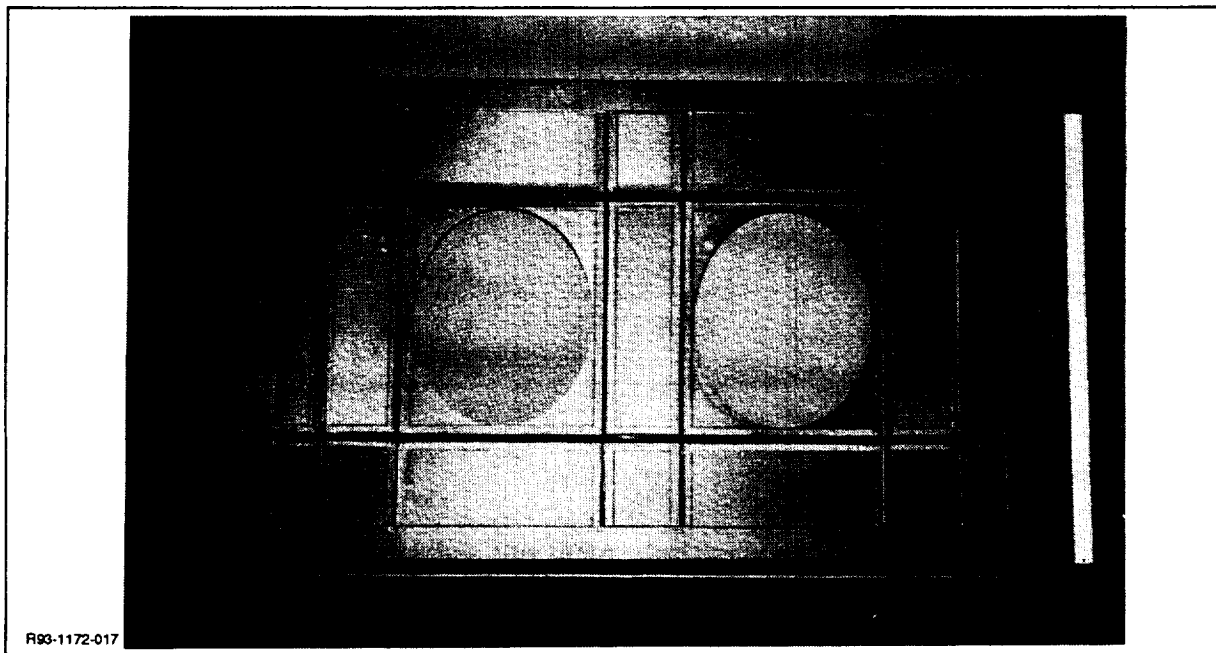
Fig. 32 Cured IM7/3501-6 Graphite/Epoxy Cross-stiffened Panel With Window Cutouts (38 In. x 62 In.)

2.5 NON-DESTRUCTIVE INSPECTION

Dimensionally, the ICI/Fiberite part was within tolerance; visually, the stiffeners were straight and intersections square. The edges were trimmed and squared by hand. The elliptical

holes were CNC machined with a high-speed air tool and a 1/4-in. diamond router. The holes were located as dimensioned on the drawing, and the centers were within 0.010 in. of an edge.

Dimensionally, the FII part was out of tolerance on the stiffener thickness and in a few places in the distance between stiffeners. This was to be expected because the FII stiffeners had been thick on the preforms as well, and did not compact down to the proper thickness. This had a direct effect on the straightness of the stiffeners. Because the stiffeners were too thick, the tooling pushed them out of line to seat properly. As a result, the stiffeners were not as straight as the ICI/Fiberite stiffeners. If the FII window belt had been sized correctly, it would have cured-out dimensionally as well as the Fiberite window belt. Table 5 shows a comparison of dimensions and weights from dry to cured for the two subcomponents.

Table 5 Comparison of Dimensions from Dry to Cured for ICI/Fiberite & FII Subcomponents
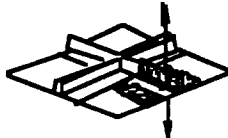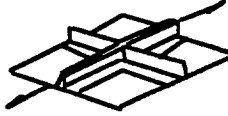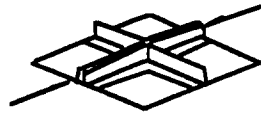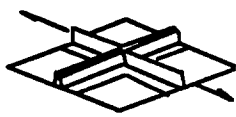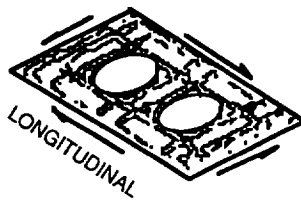
	ICI/FIBERITE WINDOW BELT	FIBER INNOVATIONS (FII) WINDOW BELT
DRY		
0.170 STIFFENER	0.227	0.284
0.480 STIFFENER	0.541	0.634
0.170 SKIN	0.250	0.153
WEIGHT, LB	21.5	21.5
BEFORE CURE		
0.170 STIFFENER	0.187	0.227
0.480 STIFFENER	0.510	0.544
0.170 SKIN	0.186	0.159
0.200 SKIN/FLANGE	N/A	N/A
WEIGHT, LB	33	33
% RESIN BY WT	32.8%	38.5%
AFTER CURE		
0.170 STIFFENER	0.171	0.202
0.480 STIFFENER	0.465	0.509
0.170 SKIN	N/A	N/A
0.200 SKIN/FLANGE	0.207	0.202
WEIGHT, LB	32	33
% RESIN BY WT	32.8%	34.8%

MR93-1172-019

2.6 TESTING

The cured 38-in. x 62-in. window belt subcomponent and 11-in. x 11-in. element preform assemblies were tested as shown in the test matrix (Fig. 33). These tests evaluated the tension, compression, shear, and normal tension, and related elastic properties of the two textile preform suppliers' test articles. The small elements are representative of the cross-stiffened intersections. Results from the finite-element analysis were used to predict failure and high-strain areas to locate the strain gages.

All testing was accomplished at the NGC Elements and Material Test Facility. An MTS, Inc., servo-hydraulic "mega" machine (1,000,000-lb calibrated capacity) was used to test the subcomponent and an MTS servo-hydraulic, 90,000-lb machine was applied to the smaller test elements.

34

SPECIMEN	TEST	DESCRIPTION
	ELEMENT NORMAL TENSION AMBIENT COND	1.5 X 1.5 3 ARTICLES, FII 3 ARTICLES, ICI/FIBERITE
	ELEMENT AXIAL TENSION LONGITUDINAL AMBIENT COND	7.0 X 7.0 2 ARTICLES, FII 2 ARTICLES, ICI/FIBERITE
	ELEMENT AXIAL COMPRESSION LONGITUDINAL AMBIENT COND	7.0 X 7.0 1 ARTICLE, FII 1 ARTICLE, ICI/FIBERITE
	ELEMENT AXIAL TENSION CIRCUMFERENTIAL AMBIENT COND	7.0 X 7.0 1 ARTICLE, FII 1 ARTICLE, ICI/FIBERITE
	SUBCOMPONENT SHEAR AMBIENT COND	38.0 X 62.0 1 ARTICLE, FII 1 ARTICLE, ICI/FIBERITE

R93-1172-018

Fig. 33 Test Matrix, Cross-stiffened Structure

2.7 ACTUAL & PROJECTED COSTS

A cost comparison was made of the IM7/3501-6 Gr/Ep subcomponent using preforms that are woven and stitched and resin film infused versus the standard tape prepreg with autoclave cure.

Table 6 shows the actual cost for Unit 1 and the projected cost for Unit 100 of the subcomponent fabricated using a woven and stitched preform and RFI. For Unit 1 (actual), the total cost of $42,286 includes a nonrecurring cost for tooling of $253 prorated for 100 units. The recurring costs include the preform (material and labor), the film epoxy used on RFI, and the labor for RFI of the preform and quality assurance. The projected cost for the 100th unit is $7,231.

35

Table 6 Cost of Woven & Stitched RFI/Autoclave-Cured IM7/3501-6 Gr/Ep Subcomponent (38 in. x 62 in.)

	UNITS COST, $	
	#1 (ACTUAL)	#100 (PROJECTED)
PREFORM	30,783	3,500
FILM EPOXY	950	800
LABOR FOR RFI	8,940	1,898
QUALITY ASSURANCE	1,360	780
RECURRENT COST, $	42,033	6,978
TOOLING*	253	253
TOTAL COST, $	42,286	7,231
* TOOLING PRORATED FOR 100 UNITS		
MR93-1172-020		

A similar cost comparison, Table 7, was made for a cross-stiffened subcomponent consisting of crossing blades in one direction and "I's" in the other direction. The nonrecurring tooling cost of $220 has again been prorated for 100 units. The costs for the first unit and the 100th unit were generated using the Composite Fabricating Cost Estimating Technique (FACET) model developed under the *DoD Fabrication Guide, 3rd Edition.* The total cost for the first unit is $38,517; for the 100th unit, it is $11,384.

Table 7 Cost of Standard Tape/Autoclave-Cured IM7/3501-6 Gr/Ep Subcomponent (38 in. x 62 in.)

	UNIT #1	UNIT #100
LABOR	31,292	4,756
MATERIAL	5,905	5,778
QUALITY ASSURANCE	1,100	630
RECURRENT COST, $	38,297	11,164
TOOLING*	220	220
TOTAL COST, $	38,517	11,384
*TOOLING PRORATED FOR 100 UNITS		
MR93-1172-021		

A comparison of the cost of standard tape versus woven and stitched IM7/3501-6 Gr/Ep cross-stiffened subcomponents is shown in Table 8. For Unit 1, the resin-film-infused woven and stitched preform subcomponent is 9.8% higher in cost than the standard tape autoclave cured one. For the 100th unit, however, the projected cost savings of using RFI and woven and stitched preforms over the standard tape and autoclave cure is 36.5%.

Table 8 Comparison of Cost of Standard Tape vs. Woven & Stitched IM7/3501-6 Gr/Ep Cross-stiffened Subcomponent (38 in. x 62 in.)

	STANDARD TAPE & AUTOCLAVE		WOVEN & STITCHED & RFI/AUTOCLAVE	
	UNIT		UNIT	
	#1	#100	#1	#100
COST, $	38,517	11,384	42,286	7,231

MR93-1172-022

3 -- TASK 4: DESIGN GUIDELINES/ANALYSIS OF TEXTILE-REINFORCED COMPOSITES

3.1 VERIFICATION/ANALYSIS

3.1.1 Specimen Fabrication & Test Procedure

The two test specimen configurations are shown in Fig. 34 and Fig. 35, respectively. The specimens were fabricated from dry, AS4 uniweave fabric preforms that were RFI molded with 3501-6 resin. Uniweave fabric consists of unidirectional Hercules AS4 carbon fiber tows woven together with 225-denier glass fibers. The weave fibers made up a small portion (~2%) of the weight of the fabric. Each configuration had both a stitched and an unstitched version.
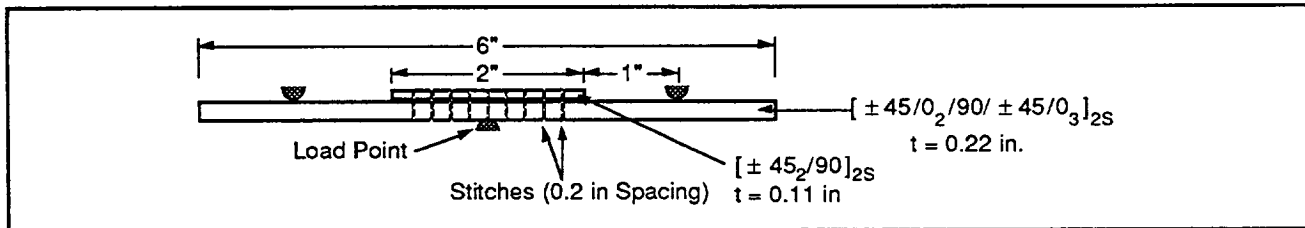
Fig. 34 Three-point Bending Specimen with Stitched, Attached Flange
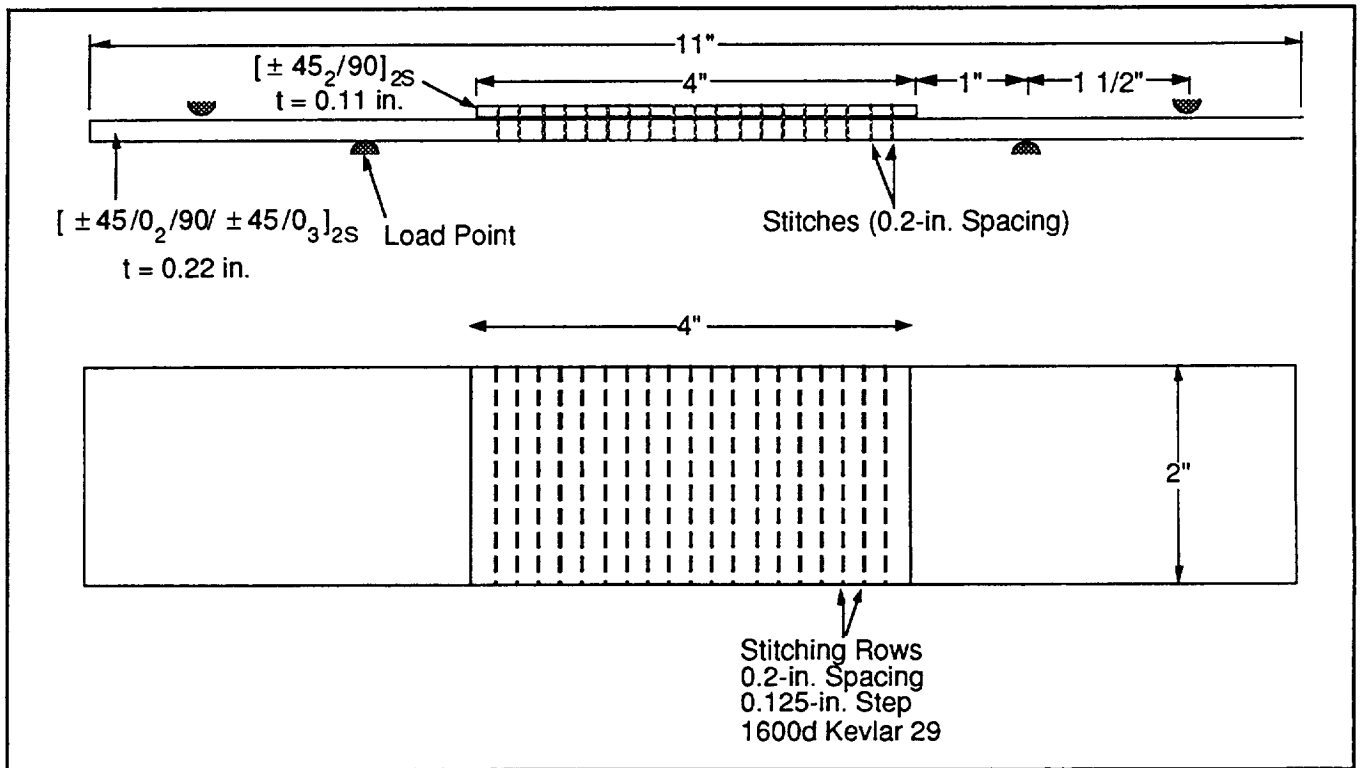
Fig. 35 Four-point Bending Specimen with Stitched, Attached Flange

39

The stitched flanges were attached to the skin before molding by laying up the skin and the flange together and mounting them in a 34-in. x 34-in. sewing frame. Then, 4-in.-wide or 2-in.-wide rows of 1600d Kevlar 29 lock stitching secured the flanges to the skin. The stitch rows were 0.2 in. apart, with a 0.125-in. step. After stitching, the excess flange material was cut away.

During the RFI process, the dry textile preforms were placed on top of a pre-weighed film of degassed 3501-6 epoxy resin lying in the bottom of the metal mold. The mold cover had a cavity in the shape of the flange. Holes vented the excess resin. After closing the mold and sealing it around the edges, the entire mold was placed in a hot press and evacuated at 30 mm Hg. Platens at 285°F heated the preform to reduce the viscosity of the resin, and mechanical pressure (100 psi) from the platens forced the resin into the fabric preform. Raising the platen temperatures to 350°F and holding for 2 hr fully cured the composite panels.

The fiber volume fractions were 58-59%. C-scans of the panels showed very few voids; however, a resin-rich area on one side of the flange and bent or displaced fibers on the other side were visible on some of the unstitched panels. Shifting of the flange after the closing of the mold potentially caused this problem.

A crosshead rate of 0.02 in. per minute loaded the bending specimens, while the load, displacement, and crack growth were monitored. The load cell on the hydraulic load frame measured the load, and a displacement transducer measured the center span displacement. The edges of the specimens were painted with white paint to make the crack clearly visible. A rule with 0.1-in. spacing was drawn on the side of the specimen to record the crack length as a function of the load. The crack length and the load were manually recorded nominally every 0.1 in. of crack length. When the crack reached the center of the specimen, the three-point bend test was stopped. The four-point bend test was stopped after a crack propagated 1 in. The tests did not use any form of starter crack.

3.1.2 Test Results/Analysis

A typical pair of load-displacement curves is shown in Fig. 36 for stitched and unstitched three-point bending specimens. The sudden discontinuities in the curves correspond to sudden extensions of the crack. The curves also show that the stitched specimen is stiffer than the unstitched, beginning with the initial linear portion of the curve. The average stiffness for the stitched three-point specimens was 15% greater than for the unstitched specimens, while the stitched four-point specimens were 9% stiffer than the corresponding unstitched version. Using properties for AS4/3501-6 Uniweave taken from Ref. 1, the stiffness was calculated using both finite elements and SUBLAM. The calculated values were 9% and 7% greater than the experimental values for the three-point and four-point stitched specimens, respectively. The analysis requires the interlaminar shear stiffnesses, G_{13} and G_{23}. These values were not available, and therefore typical Gr/Ep values ($G_{13} = 0.8$ Msi, $G_{23} = 0.5$ Msi) were used in the original analysis. One hypothesis for the discrepancies in stiffness is that the actual transverse shear stiffnesses of this material are less than the assumed values, perhaps due to the uniweave form. Consequently, the values in the analysis were adjusted downward ($G_{13} = 0.4$ Msi, $G_{23} = 0.25$ Msi) to obtain a better correspondence between the test and the analysis.
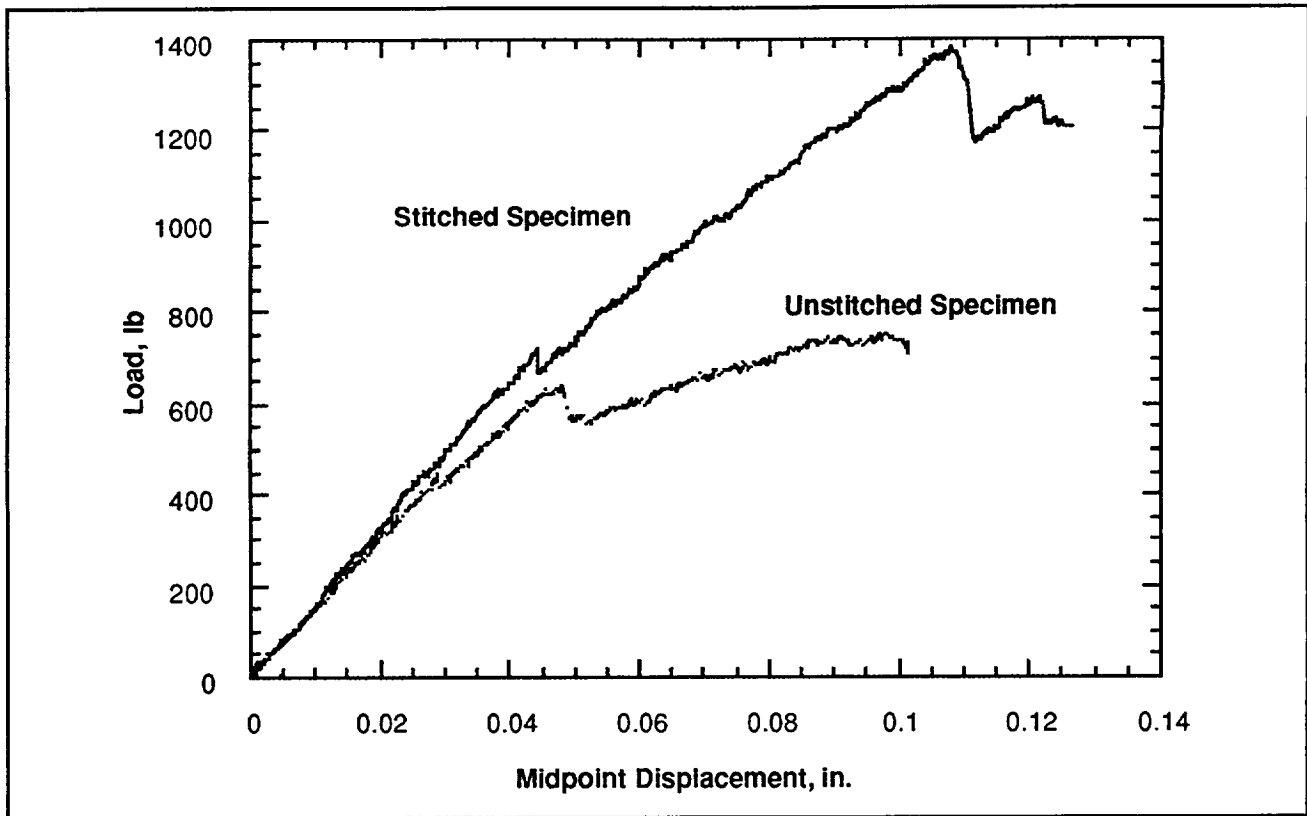
Fig. 36   Typical Force-displacement Curves for Stitched & Unstitched Three-point Bending Specimens

From the load-vs.-crack-length data for the unstitched specimens, the strain-energy-release-rate can be back-calculated. The results of this calculation are shown in Fig. 37 for the mode I and mode II components. In these plots, "a" is the crack length. Ideally, the values obtained from the three-point and the four-point specimens should overlap. However, the results show that the three-point specimens tend to have a lower value of G. The plots also indicate that G increases with crack length. The increase in G with crack length is frequently associated with bridging of fibers. The initial G_I is greater than would normally be expected for 3501-6 resin. This may be due to the lack of a starter crack, or to the uniweave material form. Finally, we note that the four-point specimens, i.e., numbers 4 and 5, appear to be outliers, although there was no obvious difference in these specimens.

The stitching analysis requires both the critical G_I and the critical G_{II} (G_{Icrit} and G_{IIcrit}). The unstitched specimens are mixed-mode, but do not provide sufficient information to determine both values. Based on typical Gr/Ep properties, we assumed that $G_{IIcrit} = 4\ G_{Icrit}$. The following linear mixed mode crack growth criterion also was assumed:

$$\frac{G_I}{G_{Icrit}} + \frac{G_{II}}{G_{IIcrit}} = 1$$

Using these two assumptions, G_{Icrit} was determined so that a good fit to the initial crack extension load for the unstitched specimens was obtained. This yielded a G_{Icrit} of 2.2 in.-lb/in.^{2}.

41
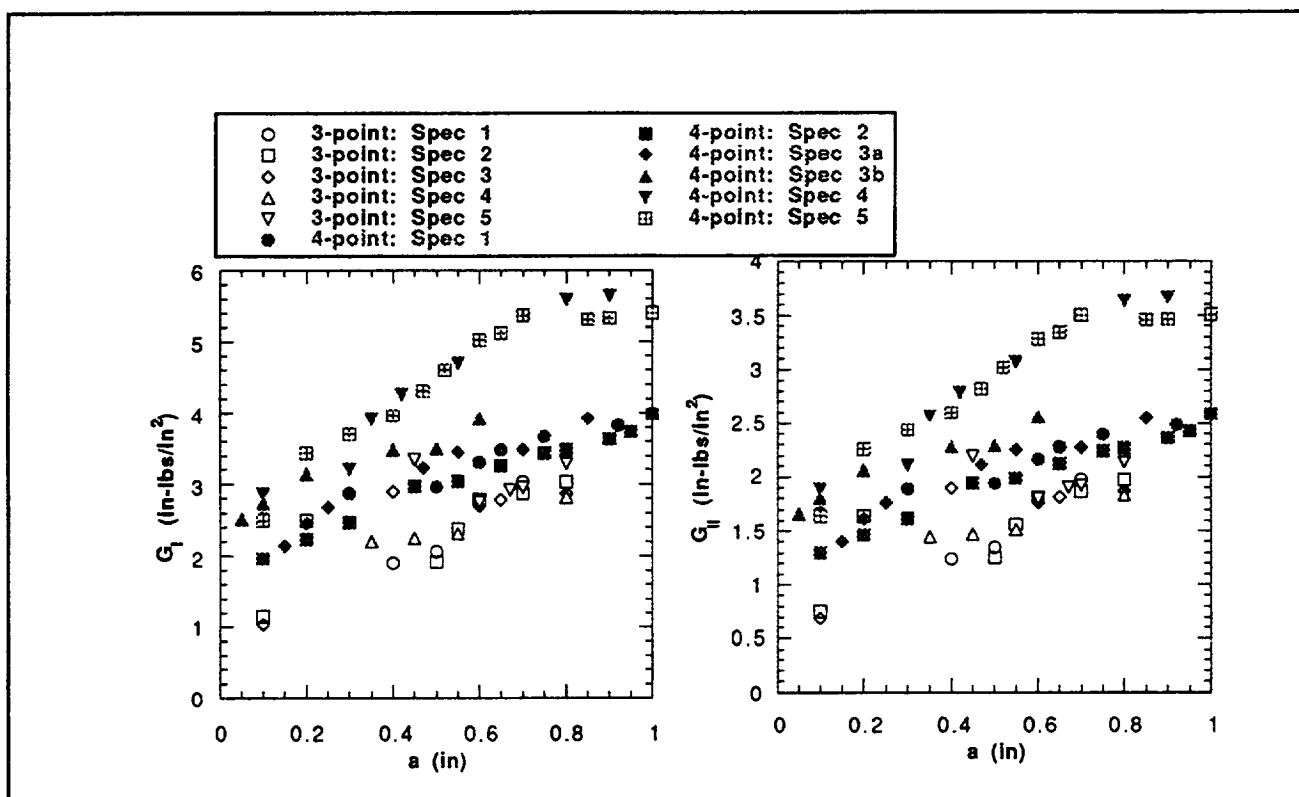
Fig. 37   Experimental Values of G$_I$ & G$_{II}$ vs. Crack Length

The predicted and experimental loads for crack growth are given in Fig. 38 and 39. Two values of the stitched spring stiffness were used. The first, k = 1.2 x 10^5 lb/in.^{2}, assumes that the stitch is fully debonded. The second, k = 4.7 x 10^5 lb/in.^{2}, assumes that the stitch is bonded, but that the matrix behaves as an elastic-plastic material, calculated using the methods given in Ref. 2. Both curves for the stitched cases fall below the experimental data. The change in assumed stitch stiffness affects how rapidly the stitches begin to suppress the crack growth, but has little effect on the maximum load that may be applied. The predictions use the initial values of G, and do not take the observed crack resistance curve into account. Therefore, in Fig. 38, the unstitched predicted load goes down with increasing crack length (unstable growth), while the experimental values increase with crack length.

The failure of the analysis to predict the full effect of the stitches may be related to the simple model in which the stitch resists only through-thickness stretching. In this model, the stitch does nothing to suppress mode II crack growth. In the analysis of the stitched specimens, the stitching was sufficiently stiff to suppress mode I crack growth completely. The results indicate that stitches also reduce mode II growth. Figure 40 shows the sliding displacement that occurs at the stitch locations in the three-point bending specimens. Stitches may resist this sliding motion either by shearing or by local large rotations.

42
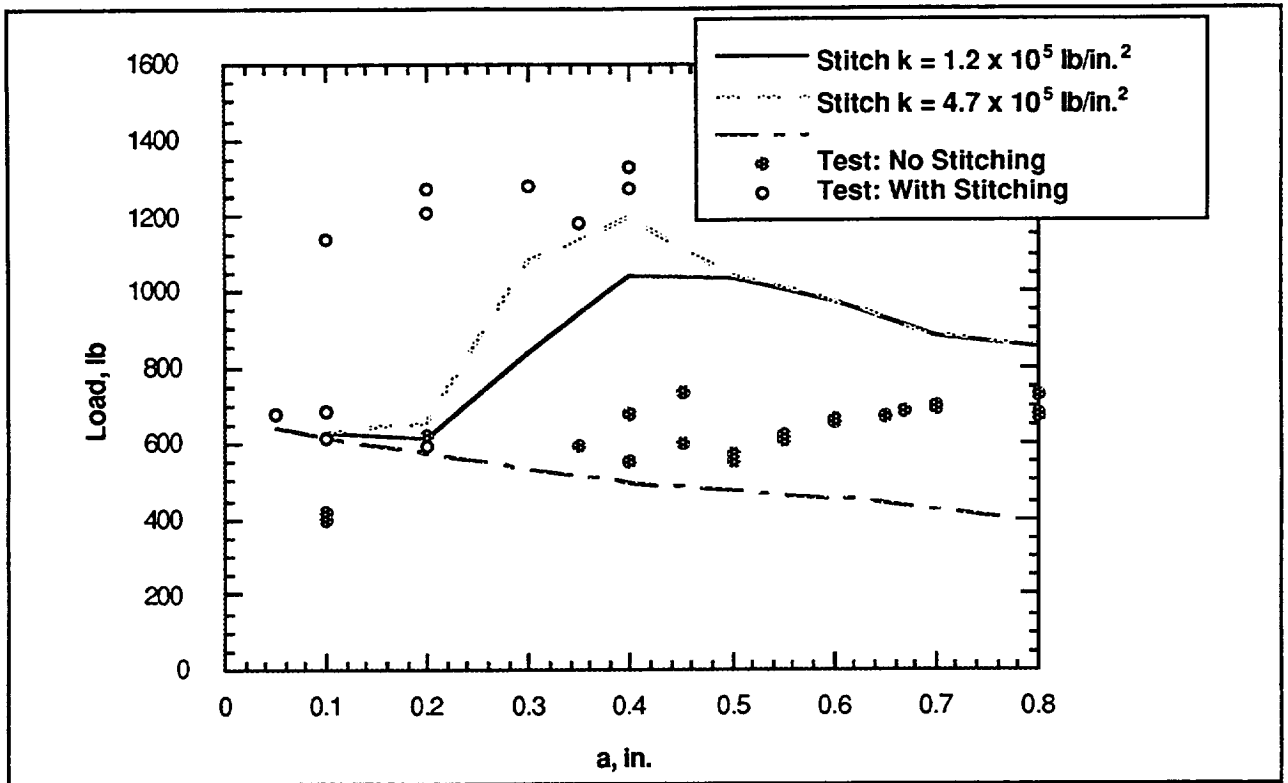
Fig. 38 Predicted & Measured Loads Required for Crack Extension (Three-point Bending Case)
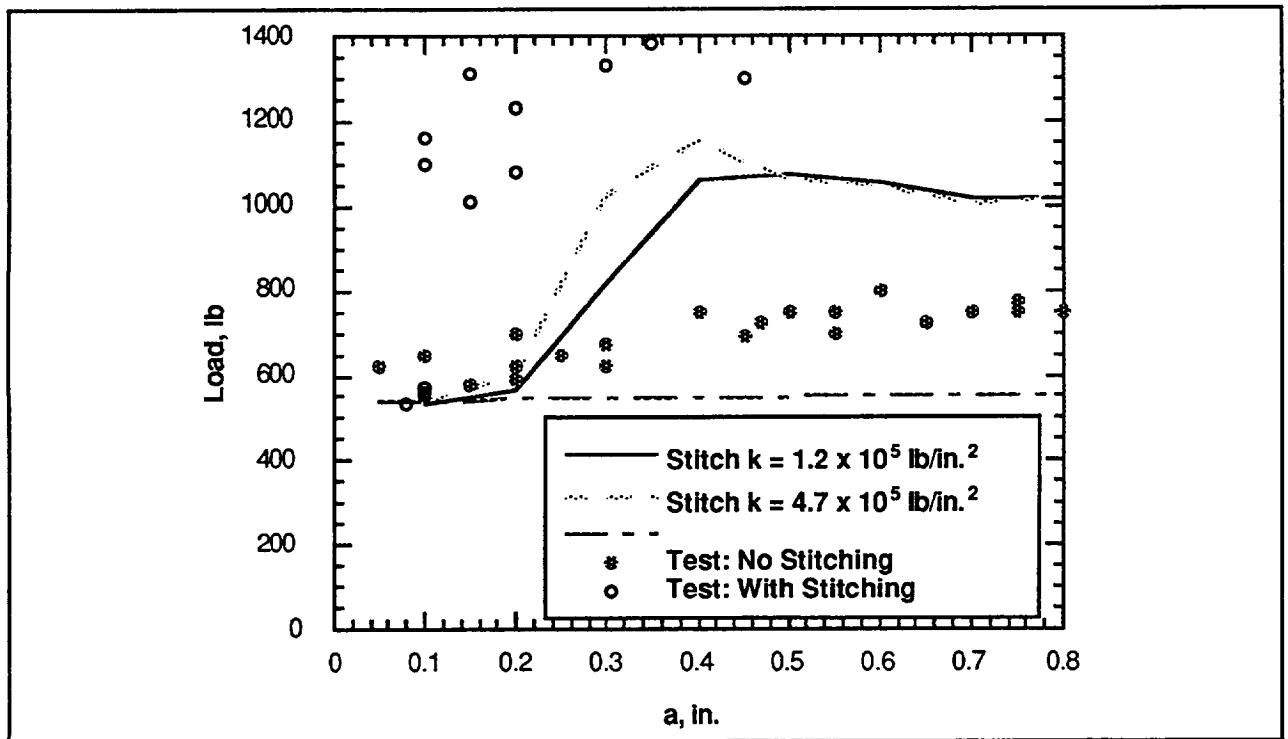
Fig. 39 Predicted & Measured Loads Required for Crack Extension (Four-point Bending Case)

43
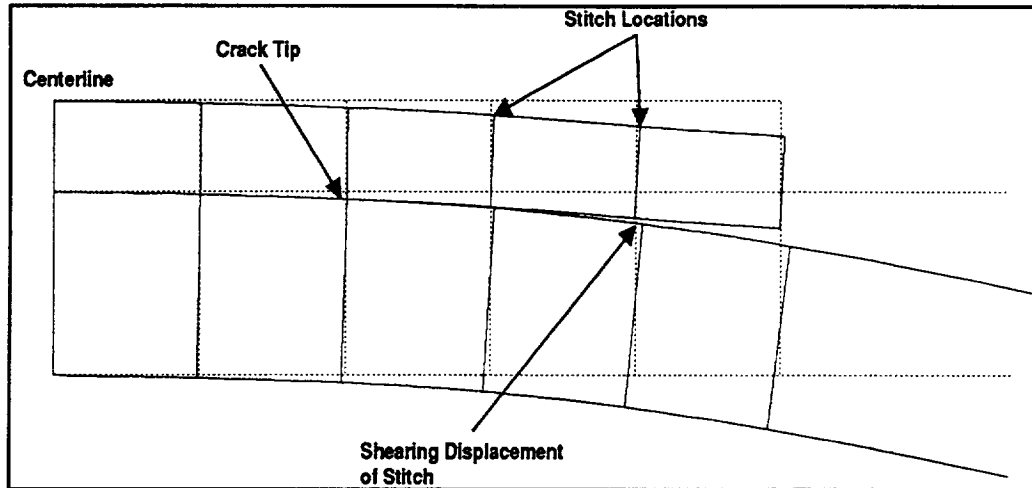
Fig. 40 Deformed Three-point Bending Specimen from SUBLAM Analysis

3.2 PARAMETRIC STUDIES

The inherent design flexibility of composite structures makes it difficult to create generic design graphs. Consequently, design with composite invariably involves computer software. However, some highly idealized configurations can be treated in a parametric manner to give a feel for the mechanics involved, and to give order-of-magnitude estimates for the stitch parameters needed to stop delamination growth. Such idealizations have been examined using the SUBLAM program to create a series of design charts.

A number of simplifications had to be made to create problems that can be nondimensionalized. One simplification is that we treat plates made from a homogeneous, orthotropic material, instead of laminates. This removes stacking sequence considerations from the problem. For the problems studied, we have further assumed that the orthotropic material has the properties of a quasi-isotropic lay-up of graphite/epoxy.

Another simplification involves our treatment of delamination growth. A general analysis would involve tracking the growth of a delamination until either unstable growth occurs or the structure collapses. The simplified approach is to determine the strain-energy-release rate for a delamination of a predetermined size. Furthermore, we assume the delamination size is smaller than the spacing between stitches. Thus, the models include only a single row of stitches. The approach being presented implies that the through-thickness reinforcement should be selected to stop a delamination within a single row of stitches; this is a conservative criterion.

The stiffness of the stitch is an independent parameter in the design charts. Our models assume that the cross section of the structure is constant. Consequently, a row of stitches is actually treated as a two-dimensional sheet. The spring stiffness, k, of such a sheet is defined by the force-displacement relation:

$$k = N/d$$

where d is the displacement, and N is a running load with units lb/in. Therefore, the units of k are $lb/in.^2$, and k can be estimated by the relation:

44

$$k = 6.222 \times 10^{-9} \frac{E \, n \, w}{\rho \, l} \text{ lb/in}^2$$

where E is the modulus of the stitching material (lb/in.^{2}), n is the stitch pitch along the row (penetrations/in.), w is the weight of the stitch in denier, r is the volume density of the stitch material (lb/in.), and l is the effective length of the stitch (in.). The constant represents a unit conversion from denier to lb/in. A lower bound on the stiffness can be determined by assuming that the stitch is fully debonded. In that case, l is the total thickness of the laminate. If the stitch does not fully debond, the effective length is smaller, and the stitch acts as a stiffer spring.

The design charts give running load, f_S (lb/in.), for the row of stitches. This load can be used to estimate the applied load needed to fail the row of stitches. The strength of the row can be estimated from:

$$f_s^{ult} = 6.222 \times 10^{-9} \frac{\sigma_s^{ult} \, n \, w}{\rho} \text{ lb/in.}$$

where σ_s^{ult} is the ultimate strength of the stitching material.

The delamination growth criterion used in our charts is the strain-energy-release-rate (G). The charts give the modes I and II values for G. If G_I and G_{II} are determined for a trial applied load, then, assuming a linear interaction curve, the critical load for delamination growth is given by:

$$R = \left(\frac{G_I}{G_{I \, crit}} + \frac{G_{II}}{G_{II \, crit}} \right)^{-\frac{1}{2}}$$

where $G_{I \, crit}$ and $G_{II \, crit}$ are the critical material values for pure mode I and mode II, and R is a scaling factor that multiples the trial applied load (assuming proportional loading). In the design charts, the values of G are given in nondimensional form. The combination of parameters used for nondimensionalization is given on the individual charts.

The first idealized geometry treats a sudden change in thickness for a cantilevered beam (Fig. 41). This problem could represent the attached flange of a stiffener. We have assumed that the initial delamination length is 1.25 h_1.

Three load cases can be considered: pure moment, pure normal shear at the crack tip, and axial load. The results for the pure moment case are given in Fig. 42-44 for a range of h_2/h_1 values. If one observes the trends with respect to changes in h_2, there appears to be a sudden change in behavior when $h_2 = 0.2 \, h_1$. This jump in the results is being investigated. Note that G_{II} actually increases with increasing stitch stiffness. However, for most brittle composites, the critical mode II toughness for the material is much greater than the mode I value. Therefore, the decrease in G_I is more significant toward suppressing delamination.

To use the charts of this form, it is suggested that the analyst determine the combination of moment, shear, and axial load at the crack tip for a particular case. The values of G can be determined from the charts for each load component independently. The individual G's can then be summed, and the interaction equation given above can be used to determine the load scaling factor (if R is less than 1, then there is a negative margin of safety for crack growth). Flanges with gradual tapers can be analyzed approximately by using the local thickness at the stitch row location.
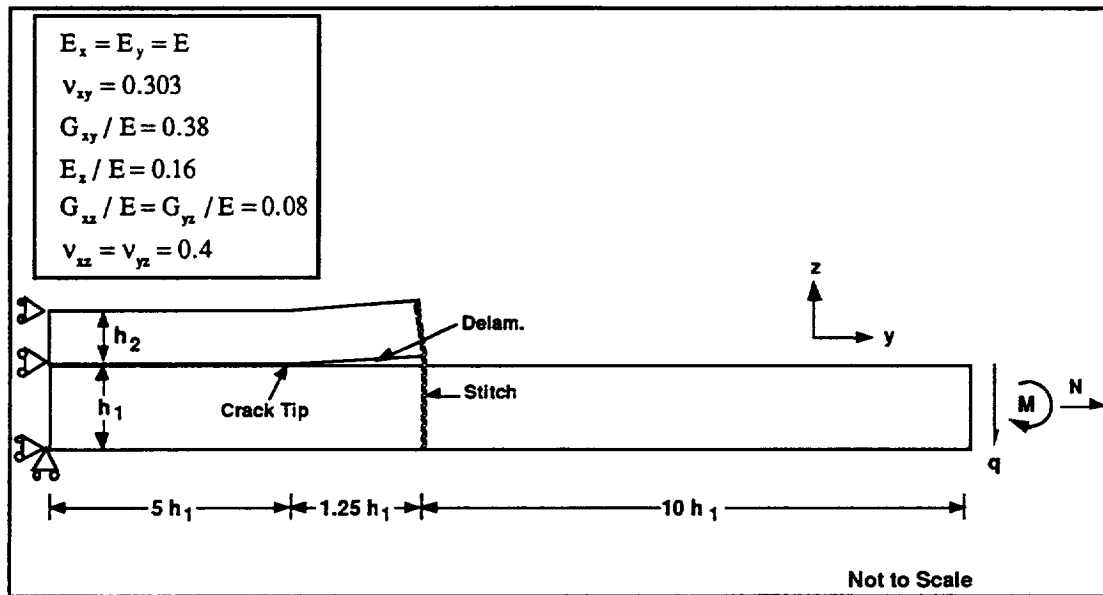
Fig. 41   Idealization of Attached Flange
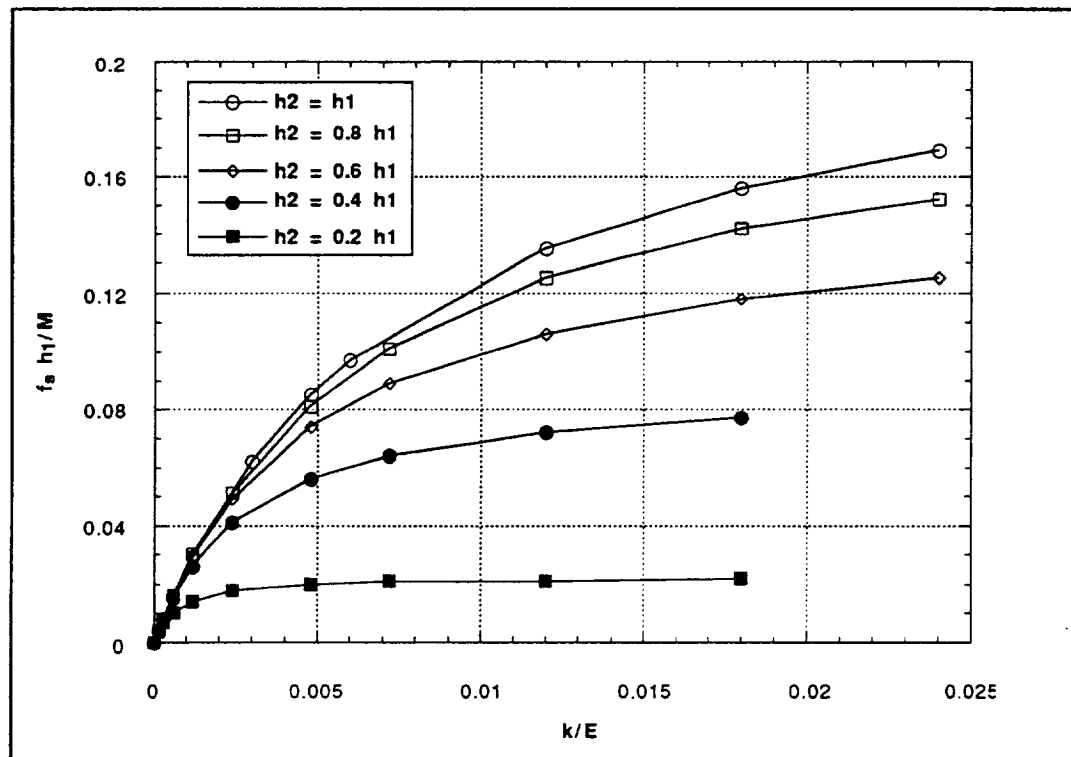
Fig. 42   Normalized Stitch Force for Attached Flange Under Moment Load

46
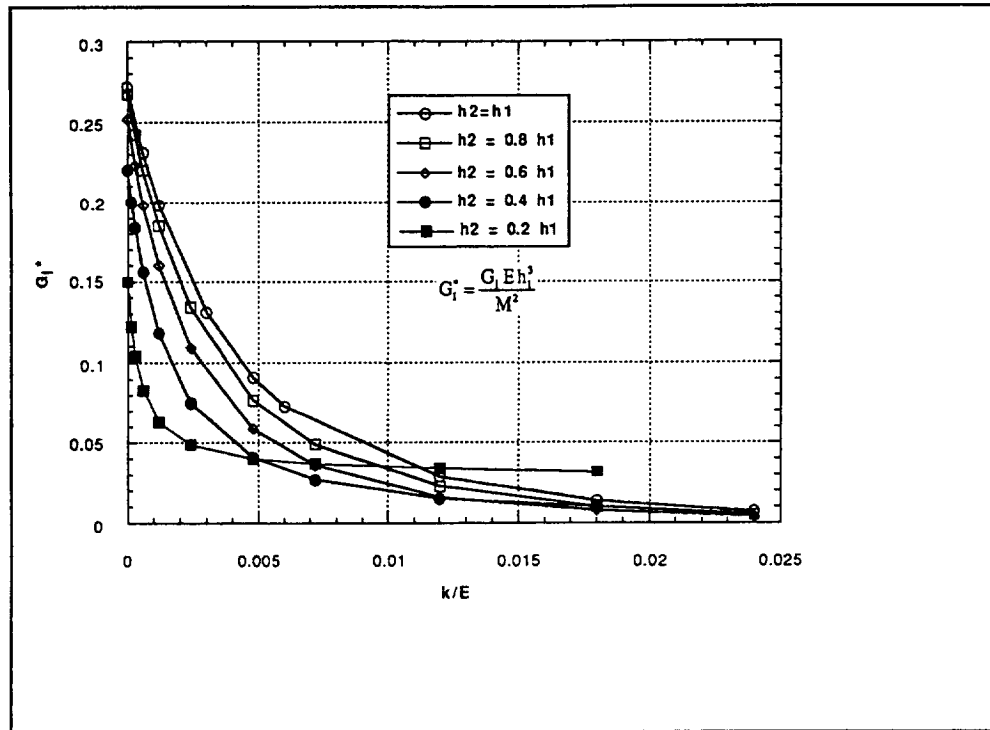
Fig. 43 Normalized G$_I$ for Attached Flange Under Moment Load
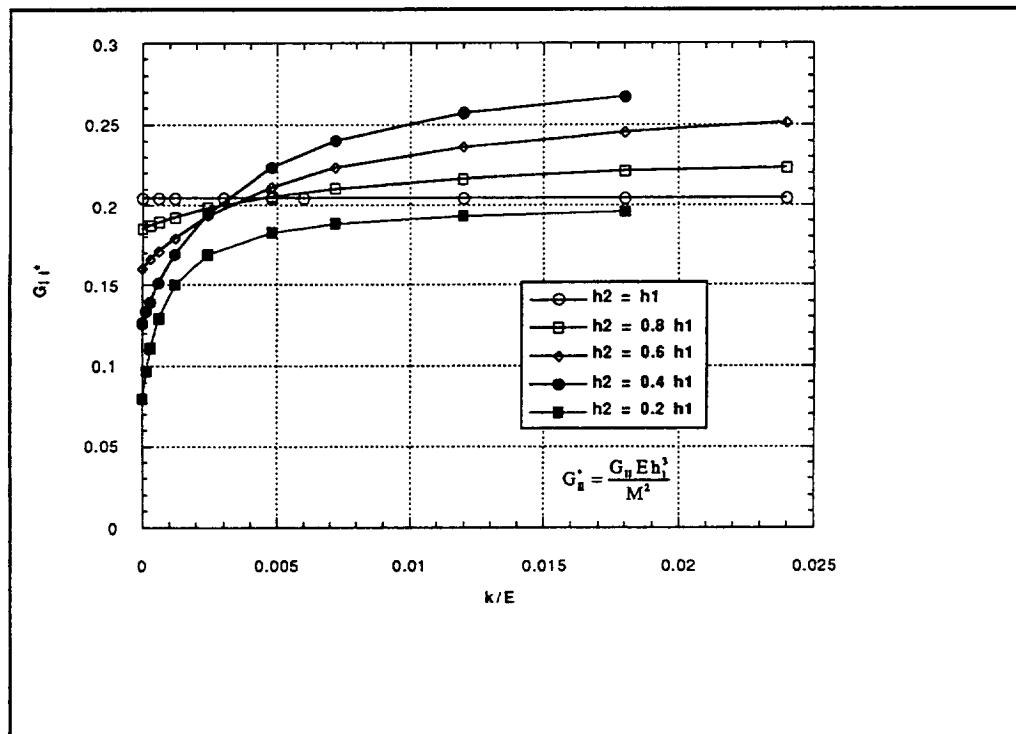
Fig. 44 Normalized G$_{II}$ for Attached Flange Under Moment Load

47

A second, idealized problem represents the stiffener pull-off problem (Fig. 45). In this model, we assume that the filler material has already failed. Because the load condition is symmetric, only half of the geometry is modeled, and symmetry boundary conditions are applied. The stitch row is placed at the dividing line between the flat and the curved parts of the stiffener laminate. Creating a generic series of plots for this problem is more difficult since the structure is not statically determinant. Thus, the loads at the crack tip will be affected by the length of the skin segment and the boundary conditions for the skin. For the idealization, we assume that the skin is clamped at a distance of 50 h_1 from the centerline. The sensitivity of the results to these arbitrary dimensions needs to be investigated. Based on Grumman design practice, the inside radius of the curved laminate is equal to the laminate thickness.
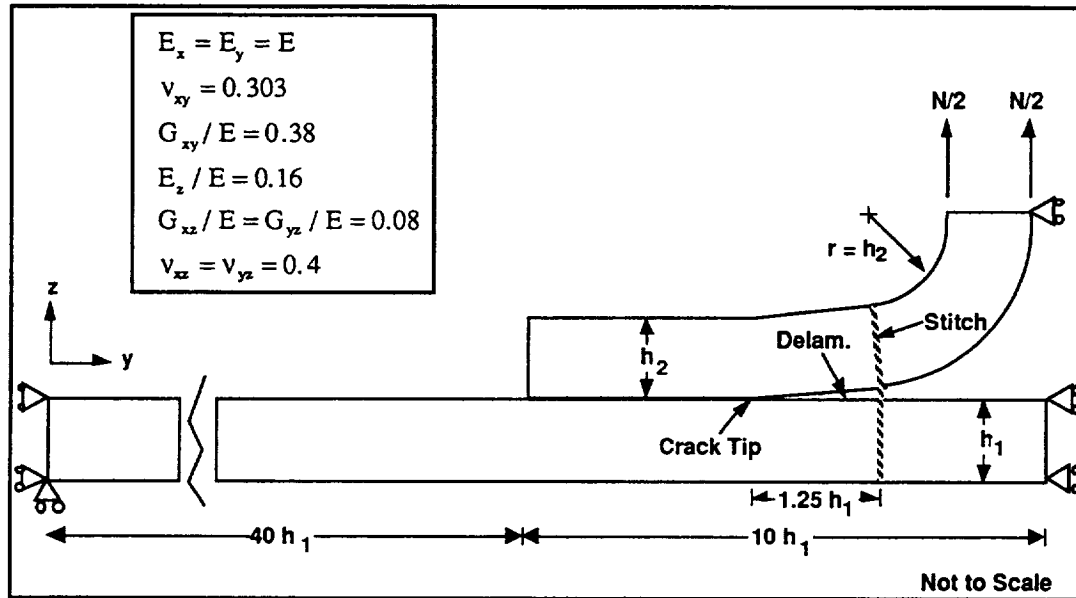
Fig. 45 Idealization for Stiffener Pull-off Problem

The results for the pull-off problem are given in Fig. 46-48. Curves are not given for $h_2 = h_1$ and $h_2 = 0.8\ h_1$ because the crack was closed for these values, making the stitch ineffective. In these cases, the crack could extend in pure mode II. This behavior may be related to the qualitative observation made in Ref. 3, that stitches placed near the heel of a stiffener appeared to be failing in shear. Figure 47 indicates that G_I approaches a constant value even for large values of the stitch stiffness. Thus, for the assumed delamination length, there is a limit to how effectively the stitches can suppress mode I fracture.

48
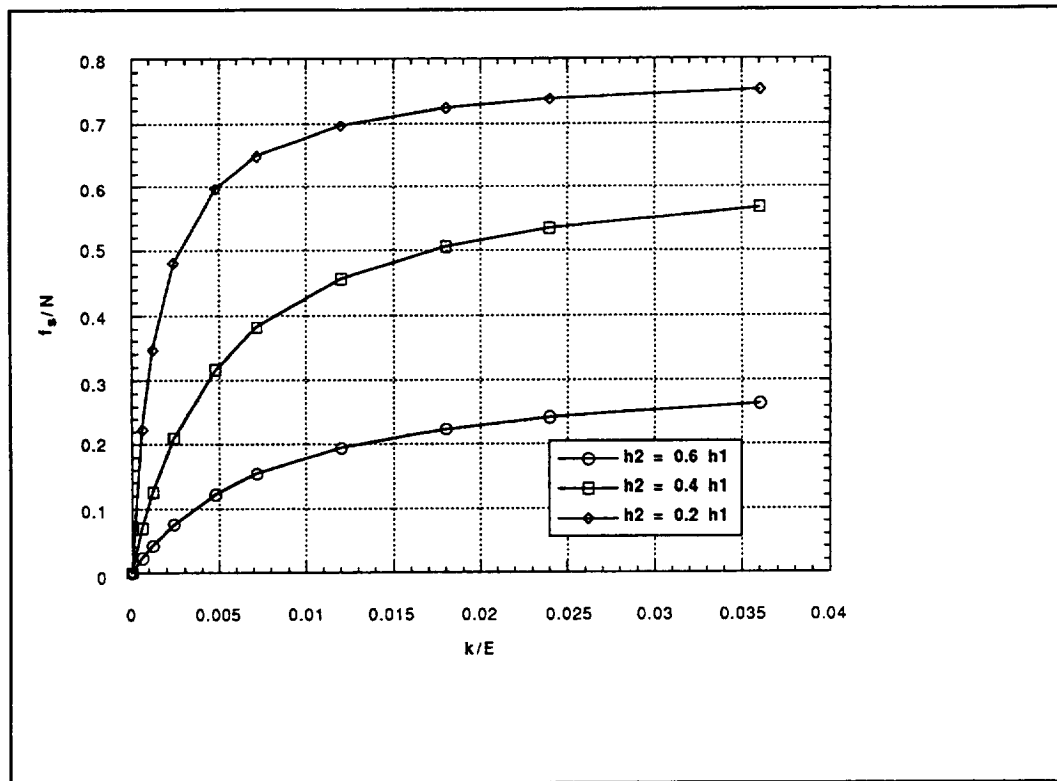
Fig. 46   Normalized Stitch Force for Pull-off Problem

$$G_I^* = \frac{G_I E h}{N^2}$$
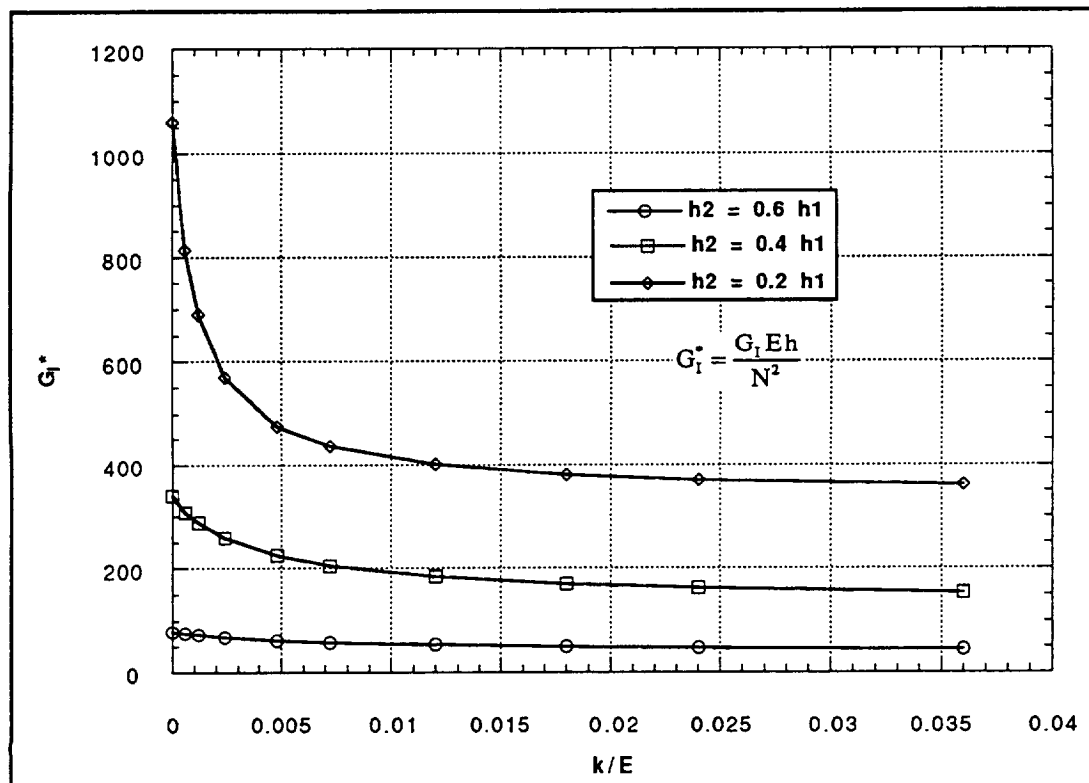
Fig. 47   Normalized G_I for Pull-off Problem
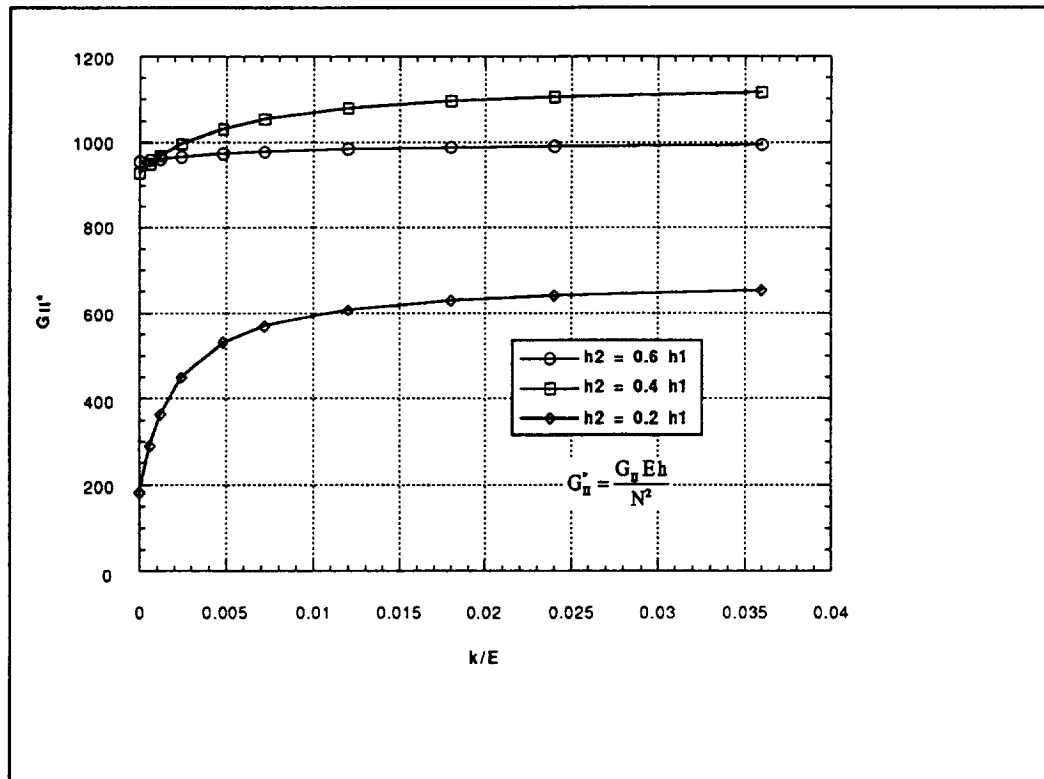
Fig. 48 Normalized G_{II} for Pull-off Problem

3.3 REFERENCES

1. "Innovative Composite Aircraft Primary Structures (ICAPS), February 1992 Technical Progress Report," prepared for NASA/Langley Research Center under contract NAS1-18862, McDonnell Douglas Corp., p. 17.

2. Flanagan, Gerry, "Development of Design Guidelines for Stitching Skins to Substructure," presented at Fourth NASA/DoD Advanced Composites Technology Conference, Salt Lake City, UT, 7-11 June 1993.

3. Cacho-Negrete, Carlos, "Integral Composite Skin and Spar (ICSS) Study Program -- Vol, 1," AFWAL-TR-82-3053, September 1982, p. 269.

50

4 -- TASK 5: INTEGRALLY WOVEN FUSELAGE PANEL

4.1 COMPONENT DESCRIPTION & DESIGN CRITERIA

The design criteria, panel size, load conditions, test parameters, damage scenarios, and multiple load conditions were established at a NASA/industry workshop held in Hampton, Virginia. The panel is representative of the lower side quadrant of a commercial transport aircraft fuselage as shown in Fig. 49 and is 60 in. wide and 90 in. long with a radius of 122 in. Multiple intersecting continuous fiber frames and stringers support the skin. The panel was designed for combined loads of 4500 lb/in. longitudinal compression, 2200 lb/in. hoop tension, and 2000 lb/in. in-plane shear. No buckling was permitted below 30% of design ultimate load, and the minimum skin gage requirement was 0.072 in.
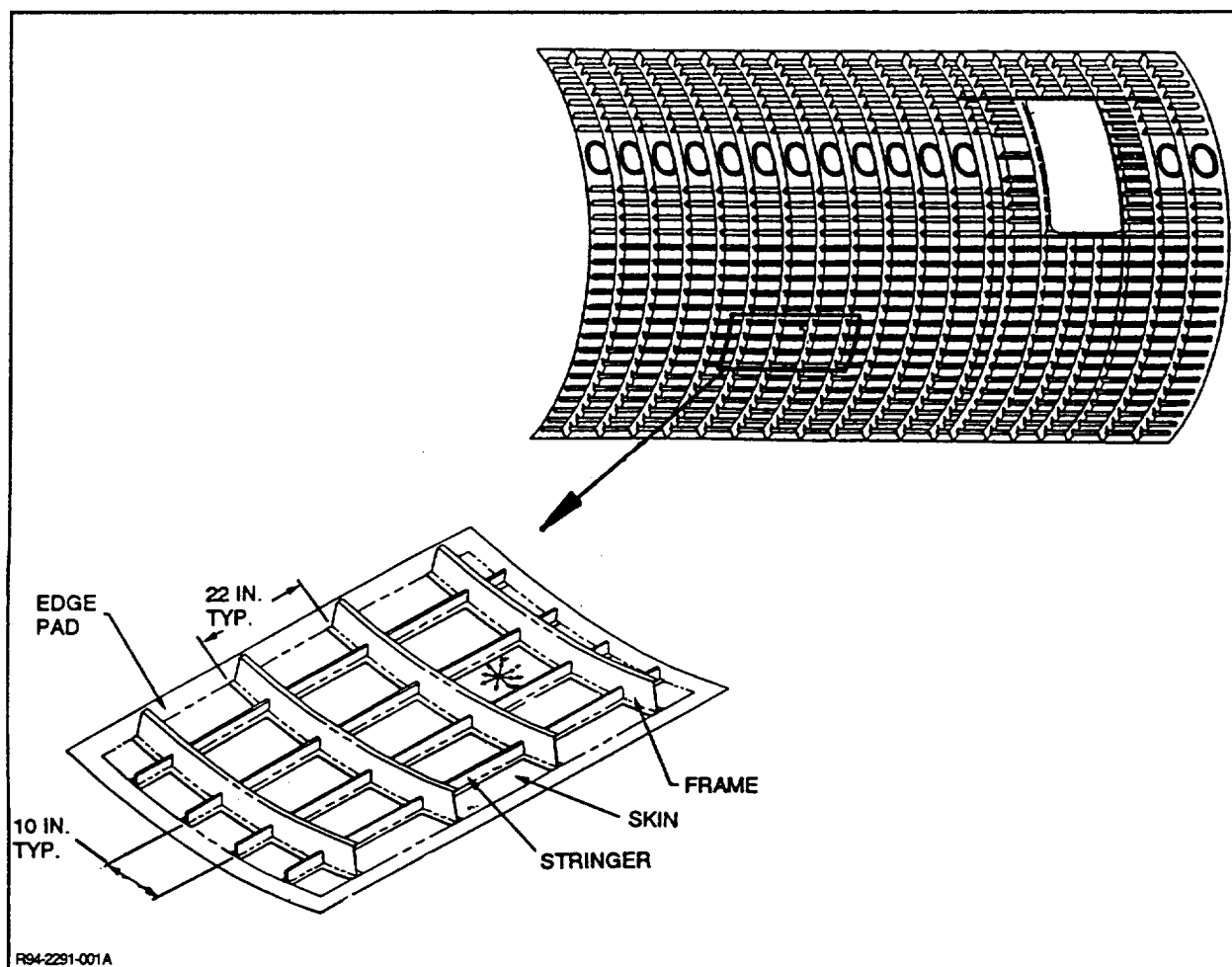
Fig. 49 Lower Side Panel Component

The fail-safe design allowable strain (80% limit) was selected to be 2400×10^{-6} in./in. for this application. This is commensurate with Boeing's fail-safe allowable strain of $2000-3000 \times 10^{-6}$ in./in. The resulting design ultimate strain was 4500×10^{-6} in./in.

The frame spacing of 22 in. was based on an earlier window belt design developed for this program, while the stringer spacing was a design variable that was optimized for weight.

51

4.2 DESIGN & ANALYSIS

4.2.1 Design

The fuselage panel is 60 in. x 90 in. with a radius of 122 in. There are four longitudinal blade stringers, 1.59 in. x 0.306 in.; four J-frames, 5.34 in. x 0.141 in.; and a 0.095-in.-thick skin with 0.191-in.-thick pads under the blade stringers and 0.124-in.-thick pads under the frames. The intersections of the woven stringers and frame preform have continuous fibers through the intersection to provide structural continuity. Integrally woven flanges, 0.10-in.-thick, on the stringers and frames are stitched to the skin with Kevlar 29 thread using 0.25-in. stitch length and a 0.50-in. row pitch. Kevlar 29, 1600-denier thread also is used to stitch the skin plies together on a 0.50-in. row pitch. The stitching provides stability to the dry preform and enhances the damage tolerance of the final article. In addition, the woven preform has a maximum graphite fiber "Z" reinforcement of 6% to lock the warp (0°) and weft (90°) fibers together. Additional plies are added around the edge of the panel for test fixture load introduction fasteners. The entire dry preform is infused with 3501-6 epoxy resin by RFI.

The textile fuselage panel subcomponent drawing defining the composite lay-up is significantly different from that used for unidirectional tape or broadgoods composite design. For typical 2-D composite applications, fiber orientation, number of plies, and stacking sequence can be defined exactly on the engineering drawing and, in turn, fabricated as specified. On the other hand, 3-D woven preform assemblies cannot be as simply defined because of the diversity of weaving/stitching processes, complexity of fiber orientations, choice of tow sizes, and variations of fiber architecture.

To enable preform fabricators to exercise creative solutions and promote freedom in design, and to avoid imposing adverse restrictions on a design, the drawing stipulates fiber volume, final part thicknesses and tolerances, target percentages of 0°, 90°, and ±45° directional yarns, maximum allowable "Z" reinforcement, and stitching requirements. This notation provides the freedom to develop a complex fiber architecture and preform assembly with the techniques and equipment familiar to each potential supplier. However, if not concurrently engineered, this method can compromise the structural capability of the resulting assembly. Figures 50 and 51 show the notation for the blade stringer and the J-frame.
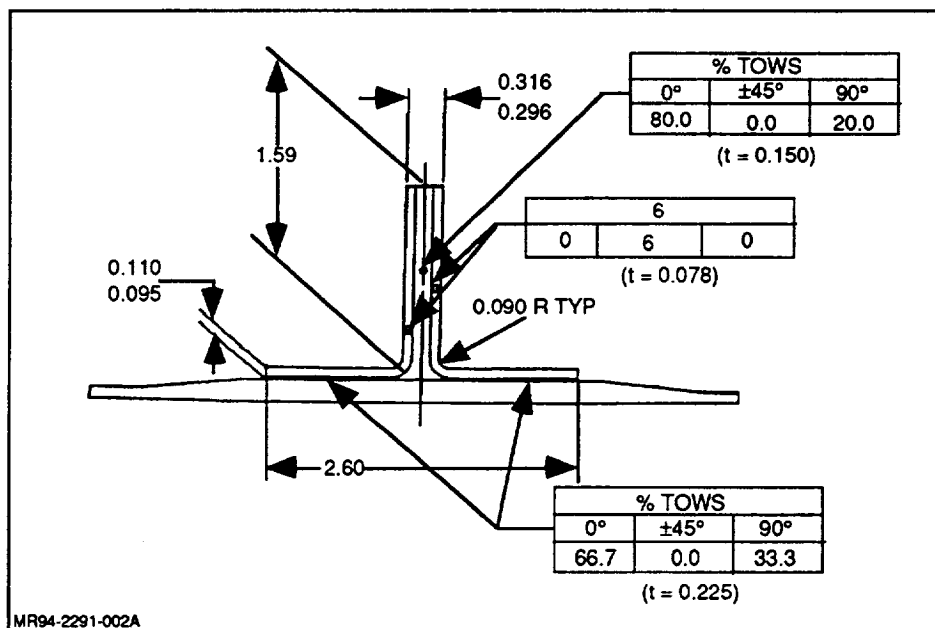
Fig. 50 Textile Architecture Definition for Stringer

52
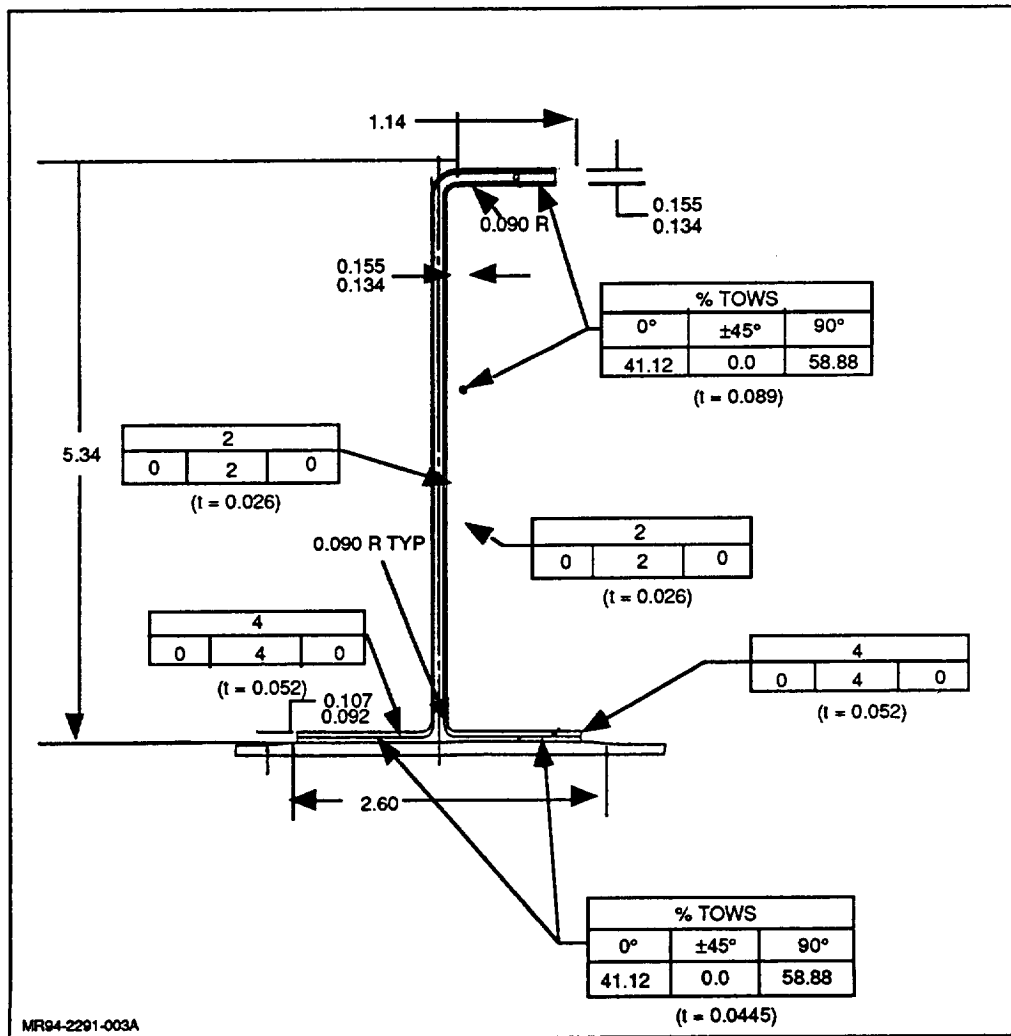
Fig. 51 Textile Architecture Definition for J-frame

4.2.2 Analysis

The fuselage panel was initially sized using composite laminate analysis methods assuming a 60% fiber volume, a $4500 \cdot 10^{-6}$ in./in. ultimate allowable strain, and IM7 graphite properties. Panel stability, stringer stability, and maximum fiber strain were determined.

Several configurations were initially evaluated. Discrete pad skins with blades and J-stringers as well as a spread skin with blades were sized for 10-in. and 12-in. stringer spacings for a total of six configurations. A spread skin with J-stringers was not sized based on the higher weight of the spread skin with blade stringers over the weight of the discrete pad skin with blade stringers. These six configurations were sized for the combined loads of maximum longitudinal compression, hoop tension, and in-plane shear. In addition, the configurations were sized for maximum longitudinal compression and in-plane shear only because the hoop tension has a delaying effect on initial buckling. This was done primarily to identify any differences in the relative weights of the configurations. Tables 9 and 10 are a summary of the twelve sizings.

53

Table 9 Summary of Configurations for 10-in. Stringer Spacing

	$N_x = -4500$ lb/in. $N_{xy} = 2000$ lb/in.					
	$N_y = 2200$ lb/in.			$N_y = 0$		
	BLADE		J	BLADE		J
	SPREAD SKIN	DISCRETE PAD	DISCRETE PAD	SPREAD SKIN	DISCRETE PAD	DISCRETE PAD
t (SKIN)	0.075 15/50/35 %	0.075 15/50/35 %	0.075 15/50/35 %	0.140 10/80/10 %	0.140 10/80/10 %	0.140 10/80/10 %
t (PAD)	——————	0.065	0.065	——————	0.060	0.060
w (PAD)	——————	3.00	3.00	——————	2.00	2.00
HEIGHT	2.11	1.44	1.27	1.86	1.48	1.22
t (WEB)	0.46 40/50/10 %	0.34 40/50/10 %	0.23 50/40/10 %	0.42 40/50/10 %	0.34 40/50/10 %	0.24 50/40/10 %
w (FLANGE)	——————	——————	0.553	——————	——————	0.577
t (BAR)	0.1776	0.1572	0.1498	0.2295	0.2163	0.2093

NOTES: t = THICKNESS
w = WIDTH

MR94-2291-004A

Table 10 Summary of Configurations for 12-in. Stringer Spacing

	$N_x = -4500$ lb/in. $N_{xy} = 2000$ lb/in.					
	$N_y = 2200$ lb/in.			$N_y = 0$		
	BLADE		J	BLADE		J
	SPREAD SKIN	DISCRETE PAD	DISCRETE PAD	SPREAD SKIN	DISCRETE PAD	DISCRETE PAD
t (SKIN)	0.085 20/50/30 %	0.085 20/50/30 %	0.085 20/50/30 %	0.160 10/80/10 %	0.160 10/80/10 %	0.160 10/80/10 %
t (PAD)	——————	0.085	0.085	——————	0.080	0.080
w (PAD)	——————	2.00	2.15	——————	2.00	2.00
HEIGHT	2.20	1.50	1.40	1.98	1.37	1.25
t (WEB)	0.50 40/50/10 %	0.40 40/50/10 %	0.25 50/40/10 %	0.45 40/50/10 %	0.36 40/50/10 %	0.23 50/40/10 %
w (FLANGE)	——————	——————	0.601	——————	——————	0.553
t (BAR)	0.1820	0.1634	0.1562	0.2451	0.2310	0.2244

NOTES: t = THICKNESS
w = WIDTH

MR94-2291-005A

The discrete pad skin with blade stringers on a 10-in. spacing was chosen as the configuration to be developed further. This decision was based on the weight advantage of a discrete pad skin over a spread skin. Blades were chosen over J-stringers because the weight differences were not significant and the complexities of trying to weave two intersecting elements with flanges did not justify the small weight benefit. A 10-in. spacing was chosen so that four stringers could be placed on the panel without the outer two stringers being too close to the edge of the panel and the test fixture.

For the detailed design and analysis of the lower fuselage panel, the IM7 fiber was changed to AS4 in the interest of affordability. The nominal fiber volume also was reduced to 56%, based on our experience with the manufacture of woven Y-spars and cross-stiffened window belt panels by the RFI process. Discussions were held with the selected preform fabricator, ICI/Fiberite, to ensure that the design concurred with their method of fabrication. The skin was made by stitching layers of bidirectional and unidirectional fabric together. The bidirectional fabric was a 50/50 weave and had a per ply cured thickness of 0.013 in., while the unidirectional fabric had a 95/5 weave with a 0.007 in. per ply thickness. The woven preform for the blade stringer was configured to have 80% warp yarns and 20% weft yarns with a nominal thickness of 0.150 in. Preform flanges were designed to have 66.65% warp and 33.35% weft yarns for a thickness of 0.0225 in. Both warp yarn percentages include a maximum of 6% graphite fiber "Z" reinforcement. Similarly, a woven angle interlock laminate for the J-frame also was designed to be compatible with typical fuselage frames found in large commercial airliners.

In addition, bidirectional fabric was stitched to the sides of the J-frame and stringer webs and flanges to provide ±45° fiber reinforcement. These changes resulted in the revised design shown in Table 11, which buckles at 54.5% of design ultimate load and has a smeared thickness of 0.1999 in.

Table 11 Blade/Discrete Pad Configuration: AS4/350-6Gr/Ep (56% FV)

ELEMENT	THICKNESS	% 0°	% ±45°	% 90°
SKIN	0.093	8.50	55.90	35.60
PAD	0.191	52.88	27.23	19.89
BLADE WEB	0.306		50.98	9.80
BLADE FLANGE	0.101	39.22	77.61	7.69
FRAME WEB	0.141	14.9	36.88	37.16
FRAME FLANGE	0.097	1	53.89	27.15

MR2291-006A

55

A 3-D NASTRAN finite-element model of the lower fuselage panel was constructed (please see Fig. 52). The model contains 14,700 nodes; 86,800 degrees of freedom; and 14,500 elements. Individual load cases were run for longitudinal compression, internal pressure, and in-plane shear. The boundary conditions for each case were chosen to represent the panel as part of a continuous fuselage. The individual load cases were then combined into a final load case. Figures 53-57 show membrane strains for the lower quarter of the panel for the individual load cases and for the combined load case. The longitudinal compression-only case and the in-plane shear only case were run for unit displacements, and the results were factored to the proper load before incorporation into the combined load case.
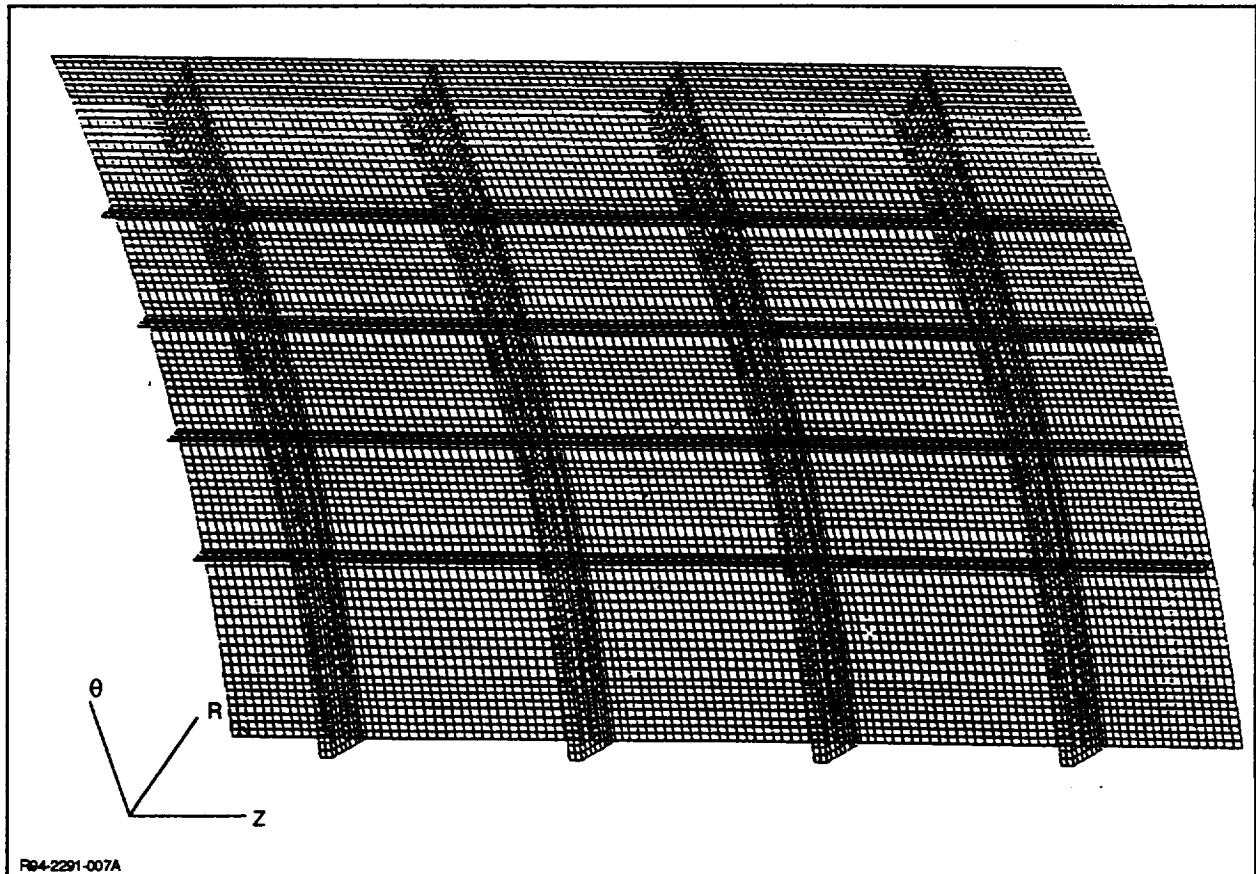
Fig. 52 NASTRAN Finite-Element Model

Preliminary buckling and postbuckling analyses of the lower fuselage panel were performed using the PANDA2 code (Ref. 1). PANDA2 is a preliminary design tool for the rapid optimization of stiffened, composite, flat, or cylindrically curved panels or complete shells. PANDA2 was selected for the analyses because it is very fast and because it provides valuable information about the basic postbuckling behavior of the fuselage panel. Furthermore, results obtained from PANDA2 will furnish a basis for setting up the finite element model for the subsequent detailed QSTAGS analysis of the panel. For example, postbuckling wavelengths obtained from PANDA2 will help in the selection of the number of elements in the QSTAGS model.

56
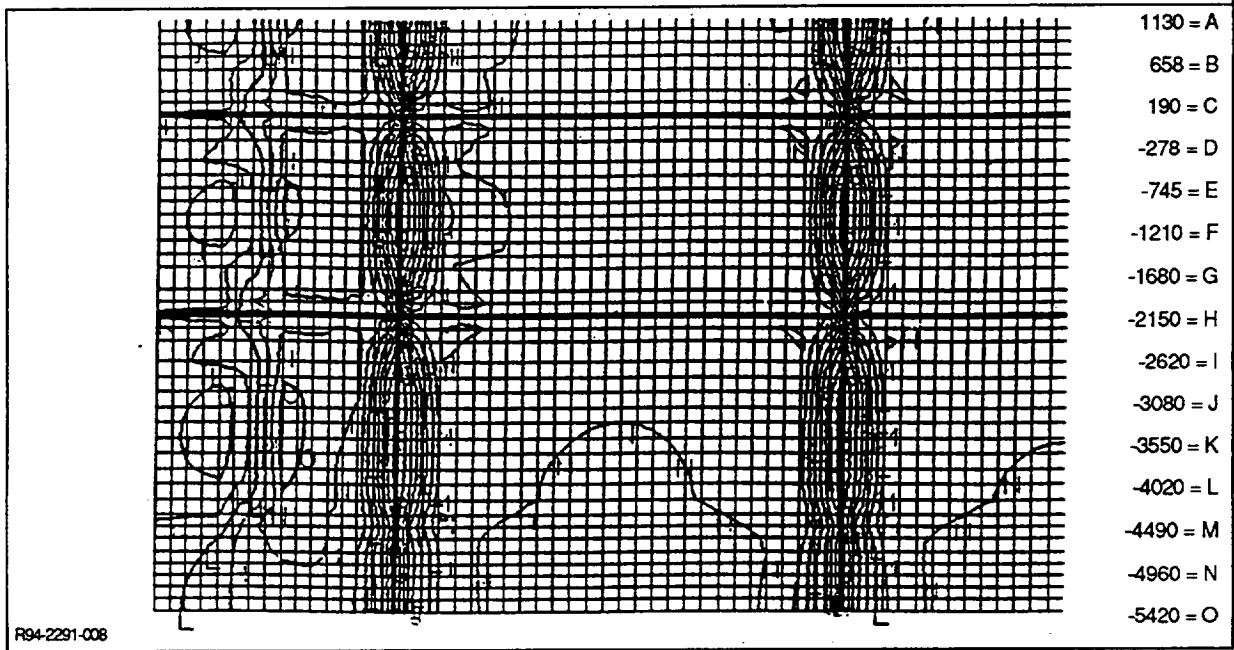
Fig. 53 Longitudinal Strain (10^{-6} in./in.) due to Longitudinal Compression Only

Legend for Fig. 53:
1130 = A
658 = B
190 = C
-278 = D
-745 = E
-1210 = F
-1680 = G
-2150 = H
-2620 = I
-3080 = J
-3550 = K
-4020 = L
-4490 = M
-4960 = N
-5420 = O

R94-2291-008
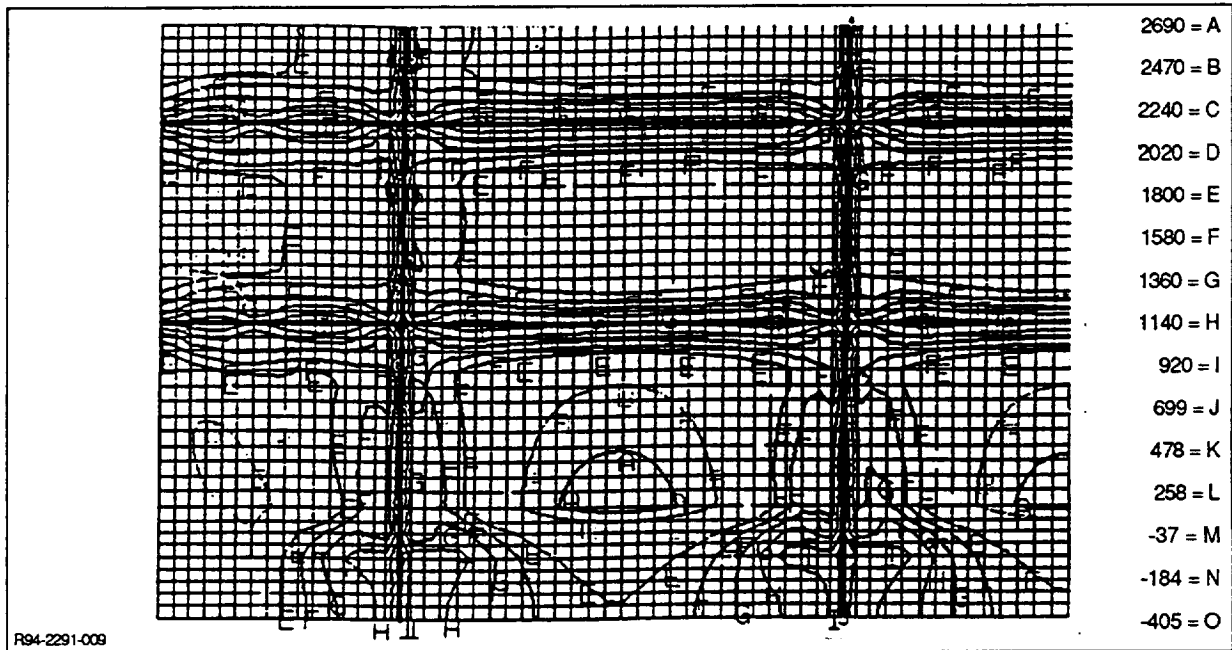
Fig. 54 Hoop Strain (10^{-6} in./in.) due to Internal Pressure Only

Legend for Fig. 54:
2690 = A
2470 = B
2240 = C
2020 = D
1800 = E
1580 = F
1360 = G
1140 = H
920 = I
699 = J
478 = K
258 = L
-37 = M
-184 = N
-405 = O

R94-2291-009

57

3180 = A
2960 = B
2740 = C
2520 = D
2300 = E
2080 = F
1860 = G
1640 = H
1420 = I
1200 = J
986 = K
766 = L
547 = M
328 = N
108 = O

R94-2291-010A
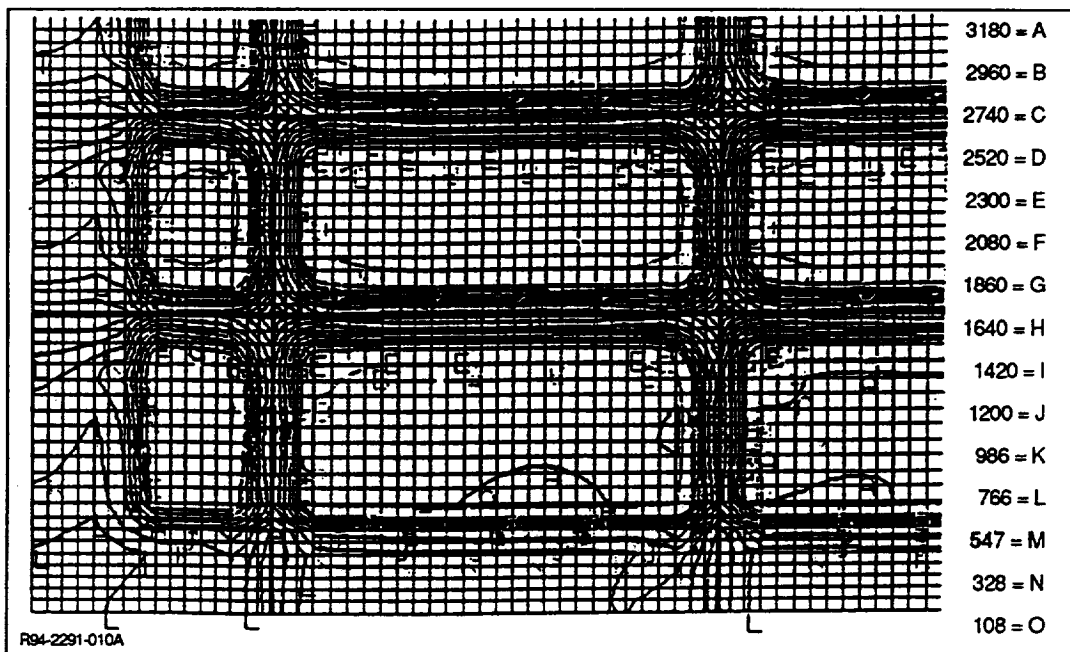
Fig. 55 Principal Tensile Strain (10^{-6} in./in.) due to In-plane Shear Only

2340 = A
1740 = B
1130 = C
521 = D
-87 = E
-695 = F
-1300 = G
-1910 = H
-2520 = I
-3130 = J
-3730 = K
-4340 = L
-4950 = M
-5560 = N
-6170 = O

R94-2291-011A
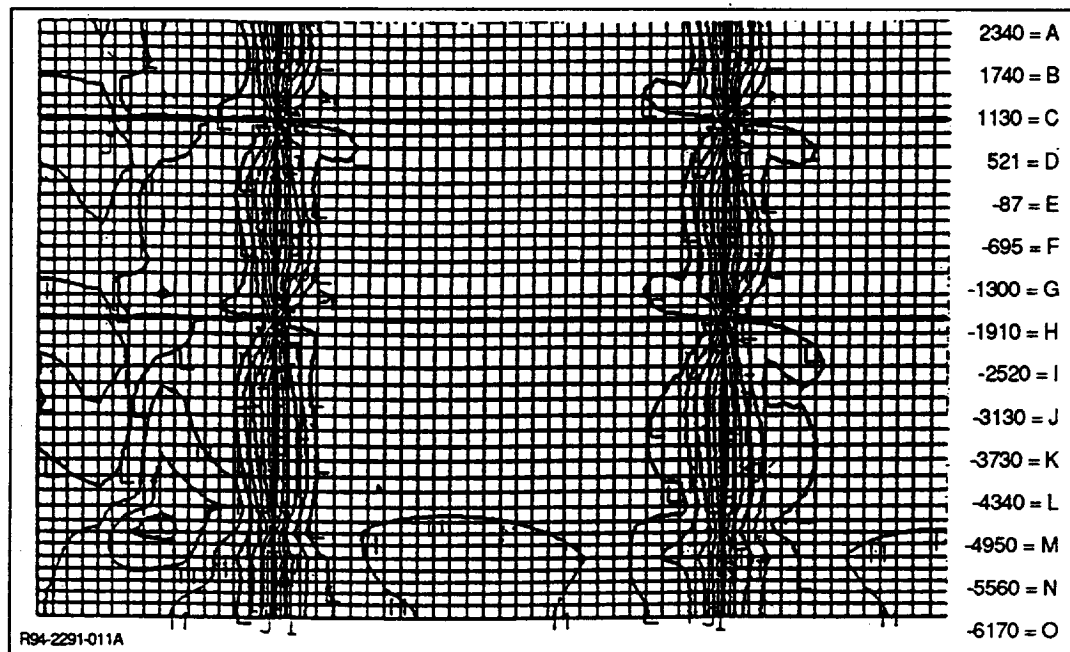
Fig. 56 Longitudinal Strain (10^{-6} in./in.) due to Combined Loads

58
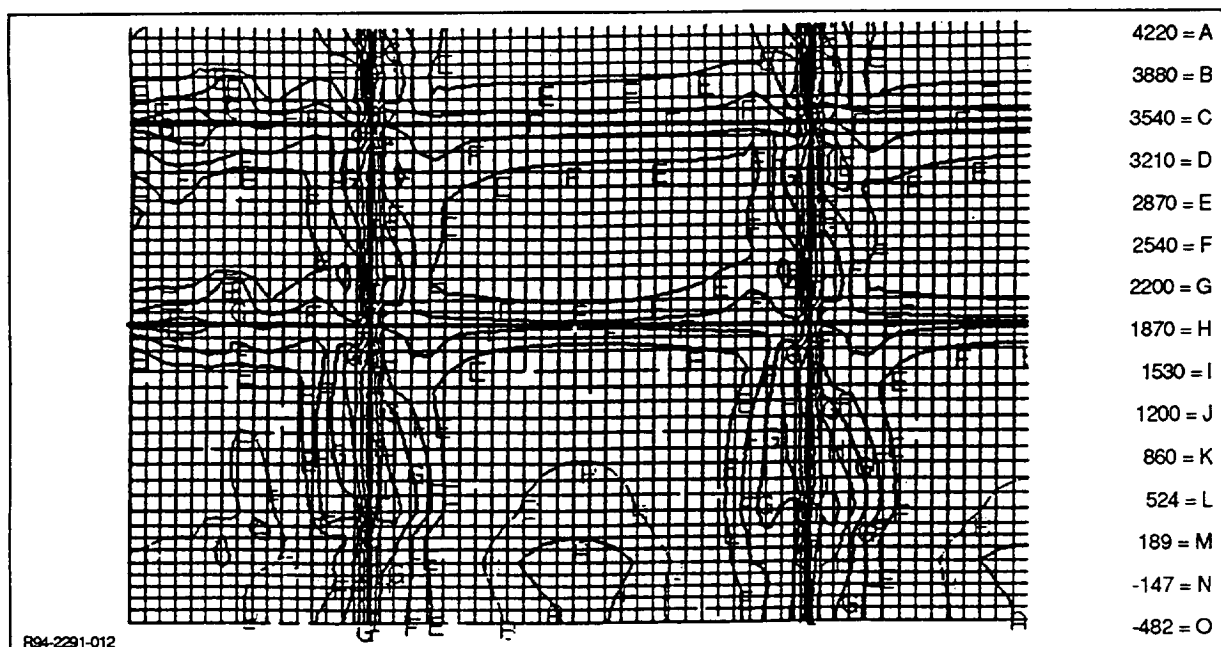
Fig. 57 Hoop Strain (10^{-6} in./in.) due to Combined Loads

PANDA2 Method – For this initial PANDA2 analysis, smeared properties were used to represent the skin, stringer, and frame laminates, and the panel was assumed to be perfect. In subsequent PANDA2 analyses, we plan to specify the lay-up for each laminate and to account for the effects of initial imperfections. The buckling and postbuckling analyses were performed for the combined loading condition consisting of: (1) axial compression N_x and in-plane shear N_{xy}, both of which were increased proportionally in the nonlinear analysis, and (2) internal pressure p and corresponding hoop tension N_y, both of which were kept constant in the analysis.

PANDA2's "test simulation" mode of analysis (Ref. 1) was used to perform the nonlinear analysis for each of 20 load steps until the specified maximum design load level was reached. The lowest buckling load was found to occur at 53% of the design load and corresponds to a local mode with seven axial halfwaves between adjacent rings.

In determining local buckling and postbuckling behavior, PANDA2 uses a single-panel module, shown in Fig. 58. The module consists of one stringer, including the stringer base, and the panel skin whose width equals the stringer spacing, b. The cross section of the panel module is discretized in the hoop direction. Variations of responses in the axial direction are represented by trigonometric functions. Figure 58 gives a view of the deformed panel module cross section for a number of load levels. Each deformed shape corresponds to the axial station for which the post-local-buckling, out-of-plane displacement, w, is a maximum. It is seen from the figure that w is larger in the panel skin on the left side of the stringer than on the right side. This is because local deformations from the internal pressure and from local buckles reinforce each other on the left side, whereas these deformations tend to offset each other somewhat on the right side, and because of the skewed deformation pattern caused by the shear loading.

59

O   UNDEFORMED PANEL MODULE. DEFLECTION SCALE FACTOR=10.72
Δ   PANEL MODULE DEFORMED BY LOADS IN STEP NO. 11 (BUCKLING)
+   PANEL MODULE DEFORMED BY LOADS IN STEP NO. 12
X   PANEL MODULE DEFORMED BY LOADS IN STEP NO. 13
◇   PANEL MODULE DEFORMED BY LOADS IN STEP NO. 14
▽   PANEL MODULE DEFORMED BY LOADS IN STEP NO. 16
⊠   PANEL MODULE DEFORMED BY LOADS IN STEP NO. 18
✕   PANEL MODULE DEFORMED BY LOADS IN STEP NO. 20 (DESIGN LOAD)

Fig. 58 PANDA2 Prediction of Deformation of Locally Postbuckled Panel Module as Loading is Increased

Figure 59 depicts a 3-D view of a portion of the panel module that corresponds to one full axial wave of the local postbuckling pattern at the design load. According to PANDA2, there are seven axial halfwaves along the 22-in. length of the panel between frames. Hence, the plot in the figure covers about one-third of this length. The inclined lines in Fig. 59 represent slopes of nodal lines of the local buckling pattern in the far-postbuckling regime. This figure and the preceding one reveal that the extra thickness provided by the stringer base (pad and attached flange) diminishes the rotation of the stringer about its axis.

4.3 FABRICATION OF FUSELAGE PANEL

The design and manufacture of the lower fuselage panel preform consisted of an innovative way of using the strengths of different preform technologies and combining them to produce a structurally sound component. The technologies that were used in the manufacture of this preform were: 3-D angle interlock weaving, 2-D bias weaving, tackifying, and stitching.

60
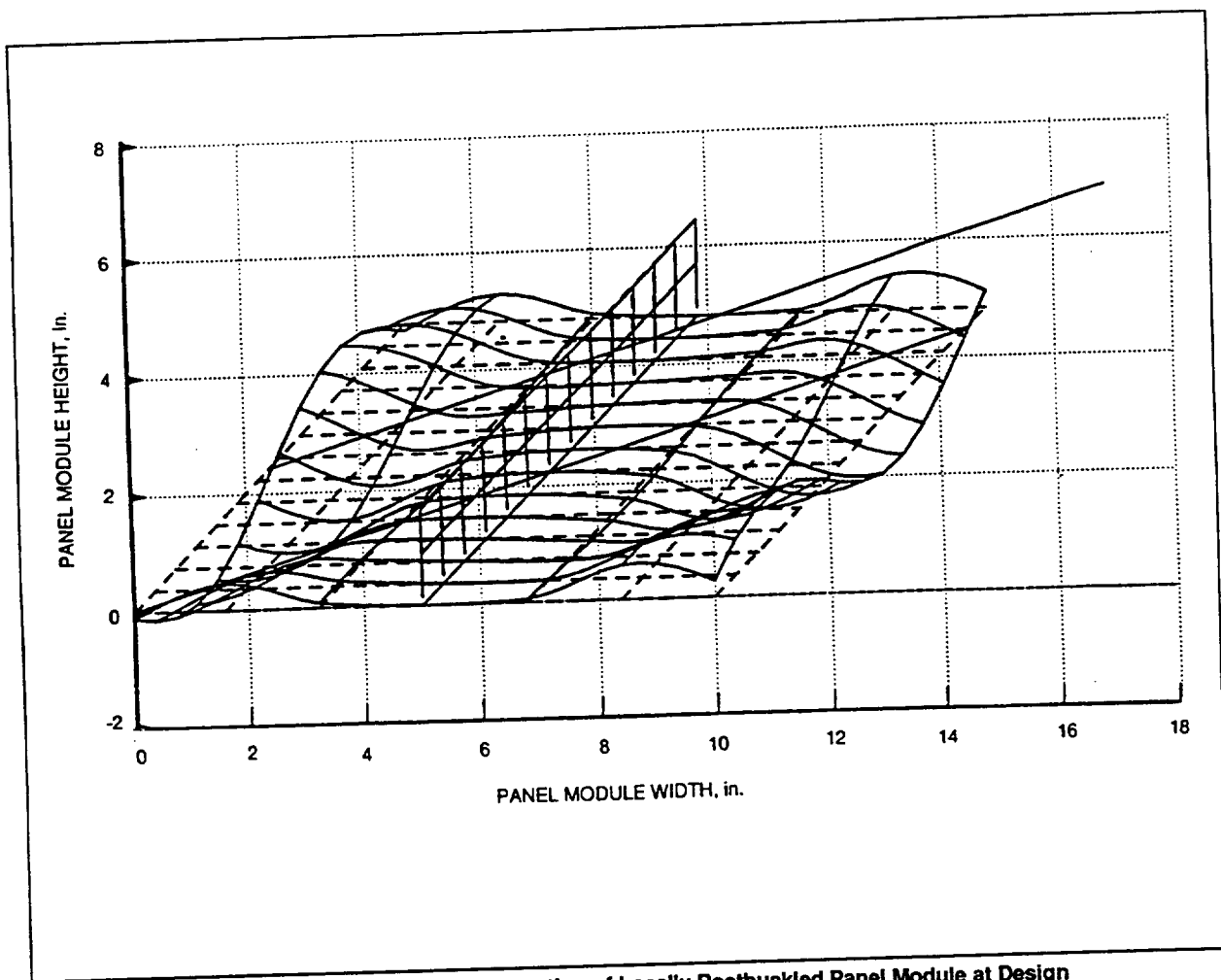
Fig. 59 PANDA2 Prediction of Deformation of Locally Postbuckled Panel Module at Design Load. *One full axial wavelength of deformation pattern is shown. The inclined lines represent slopes of local buckling pattern in far-postbuckling regime.*

Three-dimensional weaving was used in the manufacture of the stringer and frame preform core. This component is the one that carries the continuous longitudinal fibers through the intersections and carries the transverse fibers of the substructure elements. Two-dimensional bias weaving was used in the stringers, the frames, and the skin plies. In the stringers and the frames, the use of 2-D bias weaving was necessary to introduce the bias reinforcement that 3-D weaving could not provide. Tackifying was used in the manufacture of the stringers and the skin. The use of a tackifier was crucial for debulking the preform to near-net shape dimensions. Stitching was used in the manufacture of the stringers and the skin plies in order to mechanically integrate the bias plies to the 3-D woven core.

The design of the lower fuselage panel preform was broken down into five steps: (1) design of the 0.306-in. blade stringer, (2) design of the 0.141-in. J-frame, (3) design of the 3-D angle interlock woven core that would include the stringers and the J-frames, (4) design of the skin of the fuselage panel, and (5) design of the stringer and J-frame pad buildups in the skin.

61

There are four stringers in the lower fuselage panel with the 0.306-in. thickness. These four stringers consist of a 3-D angle interlock woven core sandwiched between ±45° fabric ply lay-ups. The preliminary requirements for the stringers called for a 0.306-in. thickness with 39.22% of the fibers in the 0° direction, 50.98% in the ±45° direction, and 9.8% in the 90° direction. The actual design of the preform contains 30.94% of the fibers in the 0° direction, 4.61% in the "Z" direction, 51.56% in the ±45° direction, and 12.89% in the 90° direction. The ±45° fiber reinforcement was introduced in the form of bias fabric ply lay-ups. The fabric plies consisted of a bias fabric with AS4 material and a fiber areal weight of 351.2 g/m². There were six plies of bias fabric laid up on each side of the 3-D core. Table 12 outlines the stringer fiber architecture.

Table 12 Preform Fiber Orientation Percentages: Blade Stringer Thickness = 0.306 in.

	LAYER	ORIENTATION	TOW YIELD, g/m	TOW DENSITY, g/cm³	TOWS/in.²	Z ANGLE	FAW, g/m²	PLY THICKNESS, in.
2-D FABRIC	1	±45	0.446	1.78	20	0	351.2	0.0132
	2	±45	0.446	1.78	20	0	351.2	0.0132
	3	±45	0.446	1.78	20	0	351.2	0.0132
	4	±45	0.446	1.78	20	0	351.2	0.0132
	5	±45	0.446	1.78	20	0	351.2	0.0132
	6	±45	0.446	1.78	20	0	351.2	0.0132
3-D WEAVE	7	90	0.892	1.78	10	0	351.2	0.0132
	8	0	2.676	1.78	12	0	1264.2	0.0470
	9	90	0.892	1.78	10	0	351.2	0.0132
	10	0	2.676	1.78	12	0	1264.2	0.0470
	11	90	0.892	1.78	10	0	351.2	0.0132
	A	Z	0.446	1.78	12	56	376.8	0.0140
2-D FABRIC	12	±45	0.446	1.78	20	0	351.2	0.0132
	13	±45	0.446	1.78	20	0	351.2	0.0132
	14	±45	0.446	1.78	20	0	351.2	0.0132
	15	±45	0.446	1.78	20	0	351.2	0.0132
	16	±45	0.446	1.78	20	0	351.2	0.0132
	17	±45	0.446	1.78	20	0	351.2	0.0132

A GOES THROUGH THE THICKNESS OF THE 3-D WEAVE

| | | TOTAL THICKNESS | 0.306 |

EST RESULTS:
Vf	59.00%	
%0°	30.94%	
%90°	12.89%	
%±45°	51.56%	
%Z	4.61%	

MR94-2291-015B

There are four J-frames in the lower fuselage panel with the 0.141-in. thickness. These four J-frames consist of a 3-D angle interlock woven core sandwiched between fabric ply lay-ups. The preliminary requirements for the J-frames called for a 0.141-in. thickness with 25.96% of the fibers in the 0° direction, 36.88% in the ±45° direction, and 37.16% in the 90° direction. The actual design of the preform contains 23.52% of the fibers in the 0° direction, 7.87% in the "Z" direction, 39.21% in the ±45° direction, and 29.40% in the 90° direction. The ±45° fiber reinforcement was introduced in the form of bias fabric ply lay-ups. The fabric plies consisted of a bias fabric with AS4 material and a fiber areal weight of 351.2 g/m². There were two plies of bias fabric laid up on each side of the 3-D core. Table 13 outlines the J-frame fiber architecture.

Table 13 Preform Fiber Orientation Percentages: J-frame Thickness = 0.141 in.

	LAYER	ORIENTATION	TOW YIELD, g/m	TOW DENSITY, g/cm^3	TOWS/in.^{2}	Z ANGLE	FAW, g/m^2	PLY THICKNESS, in.
2-D FABRIC	1	±45	0.446	1.78	20	0	351.2	0.0138
	2	±45	0.446	1.78	20	0	351.2	0.0138
3-D WEAVE	3	90	0.892	1.78	10	0	351.2	0.0138
	4	0	0.892	1.78	12	0	421.4	0.0166
	5	90	0.892	1.78	10	0	351.2	0.0138
	6	0	0.892	1.78	12	0	421.4	0.0166
	7	90	0.892	1.78	10	0	351.2	0.0138
	A	Z	0.446	1.78	12	41.6	281.8	0.0112
2-D FABRIC	8	±45	0.446	1.78	20	0	351.2	0.0138
	9	±45	0.446	1.78	20	0	351.2	0.0138

A GOES THROUGH THE THICKNESS OF THE 3-D WEAVE	TOTAL THICKNESS	0.141

EST RESULTS:	Vf	56.20%
	%0°	23.52%
	%90°	29.40%
	%±45°	39.21%
	%Z	7.87%

MR94-2291-0168

The flanges consist of weaving yarns in the "Z" direction and 90° yarns that are continuous from the web of the frame. The preliminary requirements for the flanges called for a 0.101-in. thickness with 14.7% of the fibers in the 0° direction, 77.61% in the ±45° direction, and 7.69% in the 90° direction. The actual design of the preform contains 0.00% of the fibers in the 0° direction, 11.26% in the "Z" direction, 76.06% in the ±45° direction, and 12.68% in the 90° direction. The thickness was increased to 0.104 in. to yield a fiber volume of 59% in the flange. Differences like these are to be expected when working with small thicknesses and the available yarns in the web. The ±45° fiber reinforcement was introduced in the form of bias fabric ply lay-ups. The fabric plies consisted of a bias fabric with AS4 material and a fiber areal weight of 351.2 g/m^2. There were six plies of bias fabric laid up on top of the 3-D core. Table 14 outlines the fiber architecture for the stiffener flanges.

Table 14 Preform Fiber Orientation Percentages: Stringer Flange Thickness = 0.104 in.

	LAYER	ORIENTATION	TOW YIELD, g/m	TOW DENSITY, g/cm^3	TOWS/in.^{2}	Z ANGLE	FAW, g/m^2	PLY THICKNESS, in.
2-D FABRIC	1	±45	0.446	1.78	20	0	351.2	0.0132
	2	±45	0.446	1.78	20	0	351.2	0.0132
	3	±45	0.446	1.78	20	0	351.2	0.0132
	4	±45	0.446	1.78	20	0	351.2	0.0132
	5	±45	0.446	1.78	20	0	351.2	0.0132
	6	±45	0.446	1.78	20	0	351.2	0.0132
3-D WEAVE	7	90	0.892	1.78	10	0	351.2	0.0132
	A	Z	0.646	1.78	12	12	312.0	0.0116

A GOES THROUGH THE THICKNESS OF THE 3-D WEAVE	TOTAL THICKNESS	0.104

EST RESULTS:	Vf	59.00%
	%0°	0.00%
	%90°	12.68%
	%±45°	76.06%
	%Z	11.26%

MR94-2291-0178

The flanges consist of weaving yarns in the "Z" direction and 90° yarns that are continuous from the web of the frame. The preliminary requirements for the flanges called for a 0.0965-in. thickness with 18.96% of the fibers in the 0° direction, 53.89% in the ±45° direction, and 27.15% in the 90° direction. The actual final design of the preform contains 0.00% of the fibers in the 0° direction, 11.26% in the "Z" direction, 76.06% in the ±45° direction, and 12.68% in the 90° direction. Initially, the preform for the flange had fewer fibers in the ±45° direction in conformance with the preliminary requirements, but this resulted in a fiber volume of 47.85% for a thickness of 0.0965 in. due to the smaller thickness of the woven portion of the flange. This low fiber volume was determined to be undesirable, and two additional layers of ±45° bias fabric were added between the flange and the cover. The thickness increased to 0.104 in. and the fiber volume to 59%. The ±45° fiber reinforcement was introduced in the form of bias fabric ply lay-ups. The fabric plies consisted of a bias fabric with AS4 material and a fiber areal weight of 351.2 g/m^2. Four plies of bias fabric were laid up on top of the 3-D core and two plies were laid up below it, as described earlier. Table 15 outlines the fiber architecture for the frame flanges.

Table 15 Preform Fiber Orientation Percentages: J-frame Flange Thickness = 0.104 in.

	LAYER	ORIENTATION	TOW YIELD, g/m	TOW DENSITY, g/cm^3	TOWS/in.^{2}	Z ANGLE	FAW, g/m^2	PLY THICKNESS, in.
2-D FABRIC	1	±45	0.446	1.78	20	0	351.2	0.0132
	2	±45	0.446	1.78	20	0	351.2	0.0132
	3	±45	0.446	1.78	20	0	351.2	0.0132
	4	±45	0.446	1.78	20	0	351.2	0.0132
3-D WEAVE	5	90	0.892	1.78	10	0	351.2	0.0132
	A	Z	0.646	1.78	12	12	312.0	0.0116
2-D FABRIC	6	±45	0.446	1.78	20	0	351.2	0.0132
	7	±45	0.446	1.78	20	0	351.2	0.0132

A GOES THROUGH THE THICKNESS OF THE 3-D WEAVE	TOTAL THICKNESS	0.104

EST RESULTS:	Vf	59.00%
	%0°	0.00%
	%90°	12.68%
	%±45°	76.06%
	%Z	11.26%

MR94-2291-0188

The design of the 3-D woven core consisted of integrating the four 0.306-in. stringers with the four 0.141-in. J-frames and their flanges in a cross-stiffened arrangement. This task was carried out using ICI/Fiberite's proprietary CADET weaving program. With this software, all the tows that were part of the design of each individual stiffener were traced along their corresponding path. Figure 60 illustrates the yarn paths for two stringers and one J-frame of the preform as well as for the flanges of these sections. The program then turned this graphical representation of the yarn paths into weaving motions for use on the electronic jacquard weaving loom. The 3-D core was designed to be woven as a "collapsed egg crate," as shown in Fig. 61, for the earlier window belt preform. After weaving, the cross-stiffened preform was unfolded to the lower fuselage panel configuration.
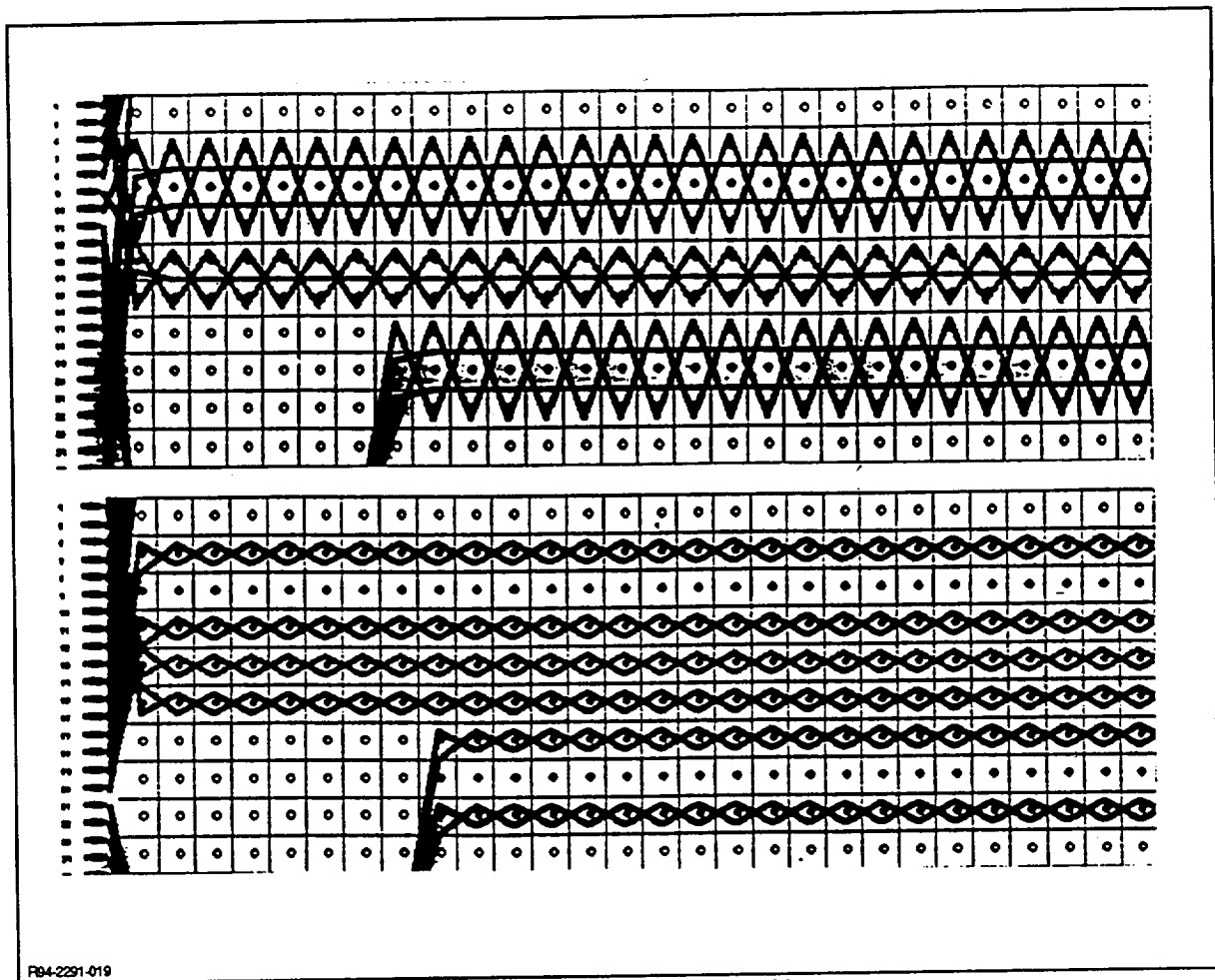
Fig. 60 Three-dimensional Angle Interlock Core Architecture

The basic skin consists of a stitched fabric lay-up and does not contain a 3-D angle interlock woven core. There is one layer of 0°/90° fabric interleaved with four layers of unidirectional fabric in the transverse or 90° direction and four layers of bias fabric in the ±45° direction. The preliminary requirements called for a 0.095-in. thickness with 8.5% of the fibers in the 0° direction, 55.9% in the ±45° direction, and 35.6% in the 90° direction. The actual final design of the skin preform contains 14.71% of the fibers in the 0° direction, 58.82% in the ±45° direction, and 26.47% in the 90° direction. Pads under the stringers were built up by interleaving 14 layers of unidirectional fabric into the basic skin parallel to the stringer, while pads under the J-frames were built up by interleaving four layers of unidirectional fabric into the basic skin parallel to the J-frames. The fiber areal weight of the unidirectional fabric was 158.0 g/m² and the areal weight of the bias fabric was 351.2 g/m². Tables 16, 17, and 18 outline the fiber architecture for the basic skin, the stringer pads, and the J-frame pads.

65
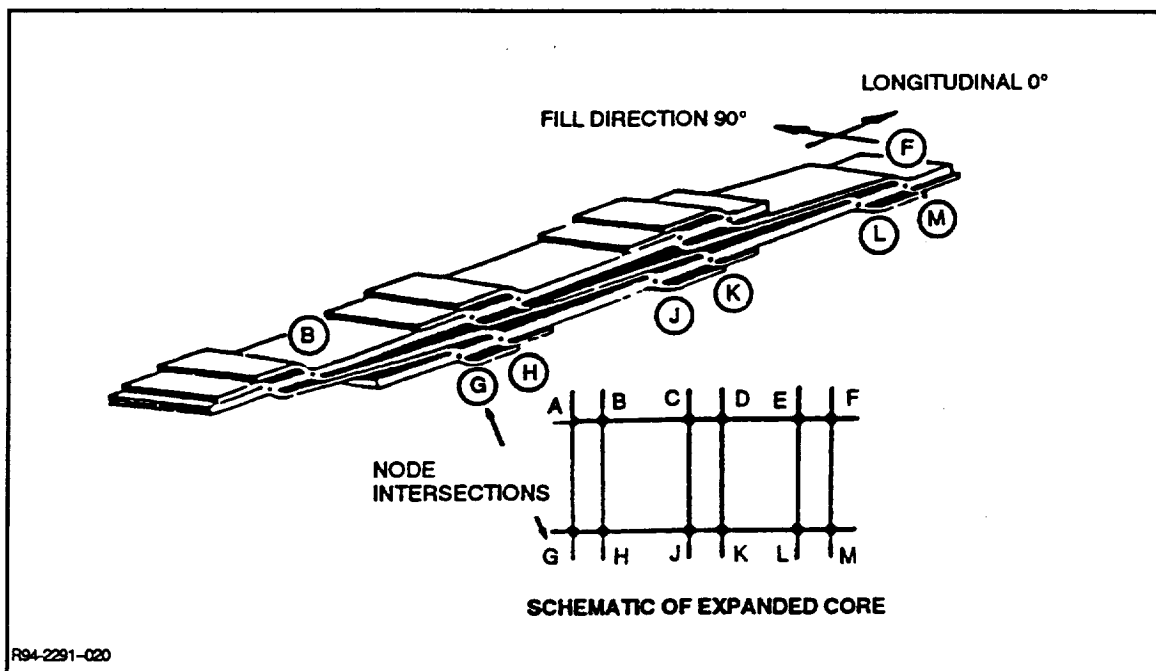
Fig. 61 "Collapsed Egg Crate" Woven Configuration

Table 16 Preform Fiber Orientation Percentages: Basic Skin Thickness = 0.095 in.

	LAYER	ORIENTATION	TOW YIELD, g/m	TOW DENSITY, g/cm^3	TOWS/In.^{2}	Z ANGLE	FAW, g/m^2	PLY THICKNESS, in.
2-D FABRIC	1	±45	0.446	1.78	20	0	351.2	0.0140
	2	90	0.223	1.78	18	0	158.0	0.0063
	3	90	0.223	1.78	18	0	158.0	0.0063
	4	±45	0.446	1.78	20	0	351.2	0.0140
	5	0/90	0.446	1.78	20	0	351.2	0.0140
	6	±45	0.446	1.78	20	0	351.2	0.0140
	7	90	0.223	1.78	18	0	158.0	0.0063
	8	90	0.223	1.78	18	0	158.0	0.0063
	9	±45	0.446	1.78	20	0	351.2	0.0140
						TOTAL THICKNESS		0.095

EST RESULTS:	Vf	55.50%
	%0°	14.71%
	%90°	26.47%
	%±45°	58.82%
	%Z	0.00%

66

Table 17 Preform Fiber Orientation Percentages: Stringer Pad Thickness = 0.190 in.

	LAYER	ORIENTATION	TOW YIELD, g/m	TOW DENSITY, g/cm^3	TOWS/in.^{2}	Z ANGLE	FAW, g/m^2	PLY THICKNESS, in.
2-D FABRIC	1	±45	0.446	1.78	20	0	351.2	0.0152
	2	90	0.223	1.78	18	0	158.0	0.0068
	3	90	0.223	1.78	18	0	158.0	0.0068
	4	0	0.223	1.78	18	0	158.0	0.0068
	5	0	0.223	1.78	18	0	158.0	0.0068
	6	0	0.223	1.78	18	0	158.0	0.0068
	7	0	0.223	1.78	18	0	158.0	0.0068
	8	0	0.223	1.78	18	0	158.0	0.0068
	9	±45	0.446	1.78	20	0	351.2	0.0152
	10	0	0.223	1.78	18	0	158.0	0.0068
	11	0	0.223	1.78	18	0	158.0	0.0068
	12	0/90	0.223	1.78	18	0	158.0	0.0068
	13	0	0.223	1.78	18	0	158.0	0.0068
	14	0	0.223	1.78	18	0	158.0	0.0068
	15	±45	0.446	1.78	20	0	351.0	0.0152
	16	0	0.223	1.78	18	0	158.0	0.0068
	17	0	0.223	1.78	18	0	158.0	0.0068
	18	0	0.223	1.78	18	0	158.0	0.0068
	19	0	0.223	1.78	18	0	158.0	0.0068
	20	0	0.223	1.78	18	0	158.0	0.0068
	21	90	0.223	1.78	18	0	158.0	0.0068
	22	90	0.223	1.78	18	0	158.0	0.0068
	23	±45	0.446	1.78	20	0	351.2	0.0152

EST RESULTS:	Vf	51.00%				TOTAL THICKNESS		0.190
	%0°	54.22%						
	%90°	13.65%						
	%±45°	32.13%						
MR94-2291-022B	%Z	0.00%						

Table 18 Preform Fiber Orientation Percentages: J-frame Pad Thickness = 0.124 in.

	LAYER	ORIENTATION	TOW YIELD, g/m	TOW DENSITY, g/cm^3	TOWS/in.^{2}	Z ANGLE	FAW, g/m^2	PLY THICKNESS, in.
2-D FABRIC	1	±45	0.446	1.78	20	0	351.2	0.0144
	2	90	0.223	1.78	18	0	158.0	0.0065
	3	90	0.223	1.78	18	0	158.0	0.0065
	4	90	0.223	1.78	18	0	158.0	0.0065
	5	90	0.223	1.78	18	0	158.0	0.0065
	6	±45	0.446	1.78	20	0	351.2	0.0144
	7	0/90	0.446	1.78	20	0	351.2	0.0144
	8	±45	0.446	1.78	20	0	351.2	0.0144
	9	90	0.223	1.78	18	0	158.0	0.0065
	10	90	0.223	1.78	18	0	158.0	0.0065
	11	90	0.223	1.78	18	0	158.0	0.0065
	12	90	0.223	1.78	18	0	158.0	0.0065
	13	±45	0.446	1.78	20	0	351.2	0.0144

EST RESULTS:	Vf	54.00%				TOTAL THICKNESS		0.124
	%0°	11.63%						
	%90°	41.86%						
	%±45°	46.51%						
MR94-2291-023B	%Z	0.00%						

The manufacture of the preform consisted of five main tasks:

1. Weaving bias fabric for the stringers, the J-frames, and the basic skin
2. Weaving unidirectional fabric for the stringer pads, the J-frame pads, and the basic skin
3. Weaving the 3-D angle interlock core
4. Assembly of the preform
5. Stitching.

Weaving of the bias plies was done by using ICI/Fiberite's PX weaving equipment. This weaving machine is capable of weaving a continuous-length material with fiber orientations at ±45°. Once the bias fabric was woven, it was sprayed with a tackifier. Ten percent by volume of tackifier was deposited on the plies of fabric. The tackifier consisted of an uncatalyzed epoxy resin (a mixture of Shell Epon 836 and Epon 1001F). This tackifier was chosen because it would dissolve in the resin system during infiltration of the preform. The main role of the tackifier was to allow debulking during lay-up.

Weaving and tackifying of the unidirectional fabric were done in a manner similar to that for the bias fabric.

Weaving the lower fuselage panel core in a collapsed configuration presented the greatest challenge during fabrication of the preform. Because all of the intersections were continuous, it was necessary to carry very close tolerances during the weaving operation to ensure that the intersections occurred at the right place. Every weaving motion had to be carried out with extreme care so that no level of bulk was woven into the part. The use of tracer threads became an essential part of the control operation; the stringer and the J-frame were woven with a glass tracer every linear inch. As each inch was woven, careful measurements of each element were made and this information was fed back to the weaving program to validate the take-up rate or to modify it accordingly.

The assembly of the preform, as shown in Fig. 62, was accomplished with the aid of a preforming tool that consisted of aluminum blocks to position the elements of the core in their desired location. The use of the tackifier became a crucial element in aiding the debulking of the preform while working with the forming tools. The application of heat was necessary to soften the tackifier. The rectangular tools were then pressed into location, forcing the preform into the desired location. When the preform cooled down, the preforming tools were removed and the preform was set up for stitching.

Stitching was carried out immediately after the preform was removed from the preforming tool in order to minimize the bulking back of the preform. Kevlar 29 1,600-denier sewing thread was used for stitching the preform. Stitching was done with a 0.50-in. row spacing and a 0.25-in. stitch length for the skin, stringer, J-frames, and flanges. Stitching was crucial in integrating the laid-up plies with the woven core. Once stitching was completed, the preform was a self-supporting piece that could withstand further handling during infiltration. Figure 63 shows the completed preform.
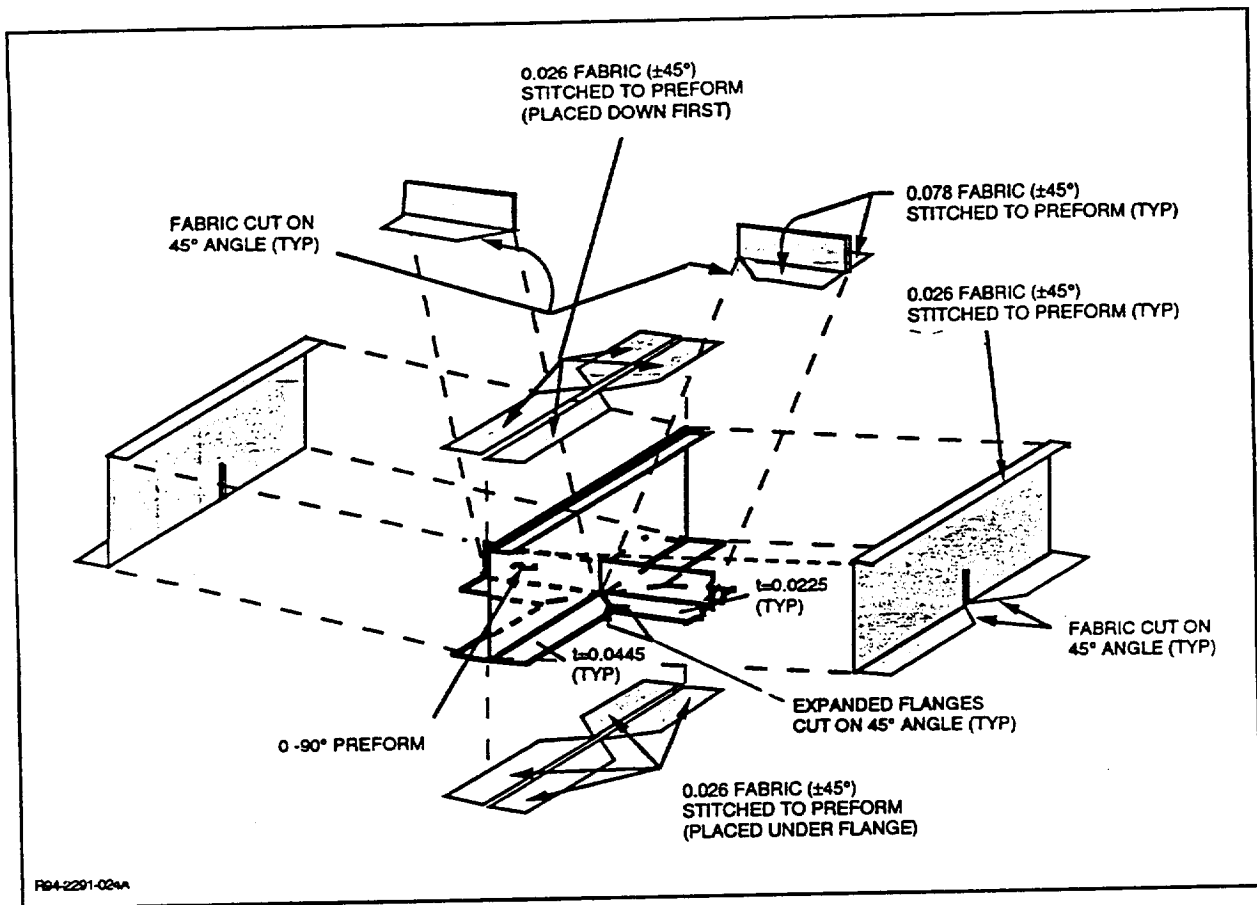
0.026 FABRIC (±45°)
STITCHED TO PREFORM
(PLACED DOWN FIRST)

FABRIC CUT ON
45° ANGLE (TYP)

0.078 FABRIC (±45°)
STITCHED TO PREFORM (TYP)

0.026 FABRIC (±45°)
STITCHED TO PREFORM (TYP)

t=0.0225
(TYP)

t=0.0445
(TYP)

FABRIC CUT ON
45° ANGLE (TYP)

EXPANDED FLANGES
CUT ON 45° ANGLE (TYP)

0 -90° PREFORM

0.026 FABRIC (±45°)
STITCHED TO PREFORM
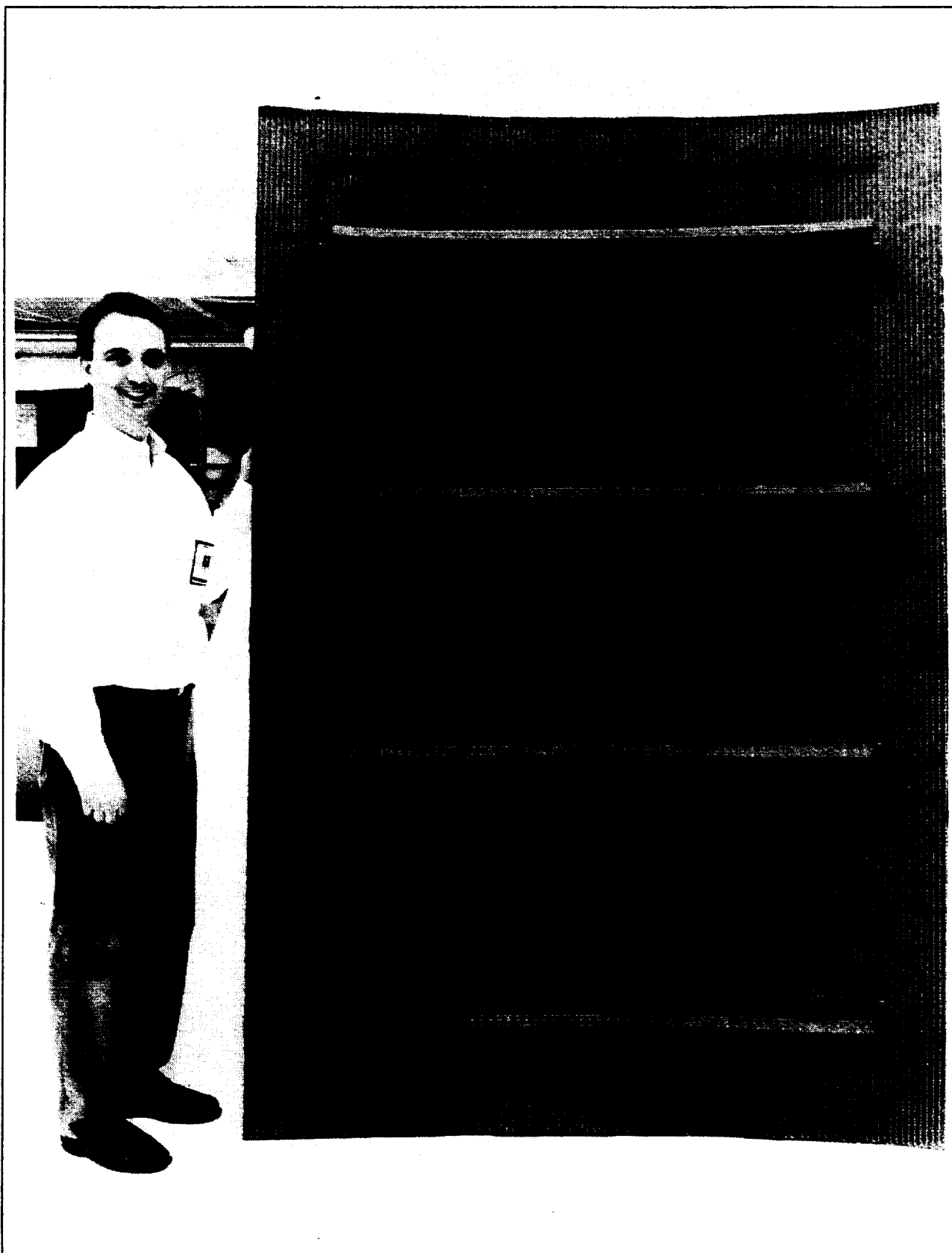(PLACED UNDER FLANGE)

R94-2291-024A

Fig. 62 Assembly of Lower Fuselage Panel Cross-stiffened Preform

69

Fig. 63 60-in. x 90-in. Woven AS4 Graphite Fuselage Preform #3

2291-025

The lower fuselage panel infusion and cure tooling features a 0.50-in.-thick, roll-formed steel base (66 in. x 96 in.) with welded bulkheads for support (Fig. 64). Molded graphite/epoxy tooling used for the infusion and cure of the back side of the J-frames is attached to the steel base to act as rigid hard details. Aluminum plates tool the inside face of the skin and blade stringers. The tooling is tied together using a composite grid over the top of the panel for dimensional control during cure. Figures 65 and 66 show the tooling for the J-frames and for the stringers, respectively.
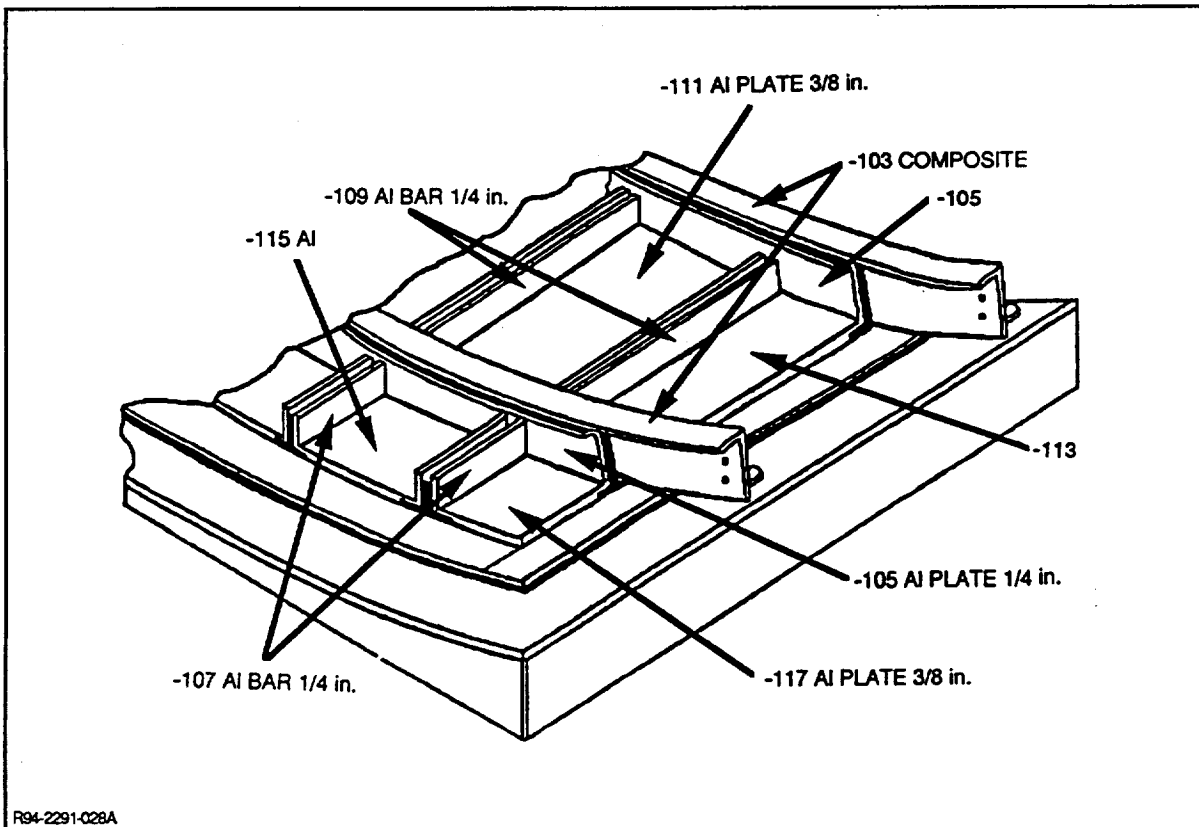

Fig. 64 Sketch of Cure Fixture for Woven AS4/3501-6 Gr/Ep Lower Fuselage Panel

The preforms were vacuum-bag infused with 3501-6 epoxy resin film. The first preform used to prove out the tooling underwent five compactions. The second preform went through only three compaction steps: one for the initial infusion, a second to add resin (both under 30-50 psi), and a third for high pressure (100 psi) to compact and reduce part thickness. All debulks were at 180°F for an hour. The bagging scheme was one layer of TFP under and on top of the panel. One layer of pin prick was placed on top of the TFP, and the entire part was completely covered with breather cloth. When the resin started to bleed through, the part was cooled back to room temperature and inspected for weight, thickness, and degree of wet out. If the part was not acceptable, infusion or bleeding was continued as necessary or more resin was added and infused. Figure 67 shows the lower fuselage panel preform after infusion with 3501-6 epoxy resin.
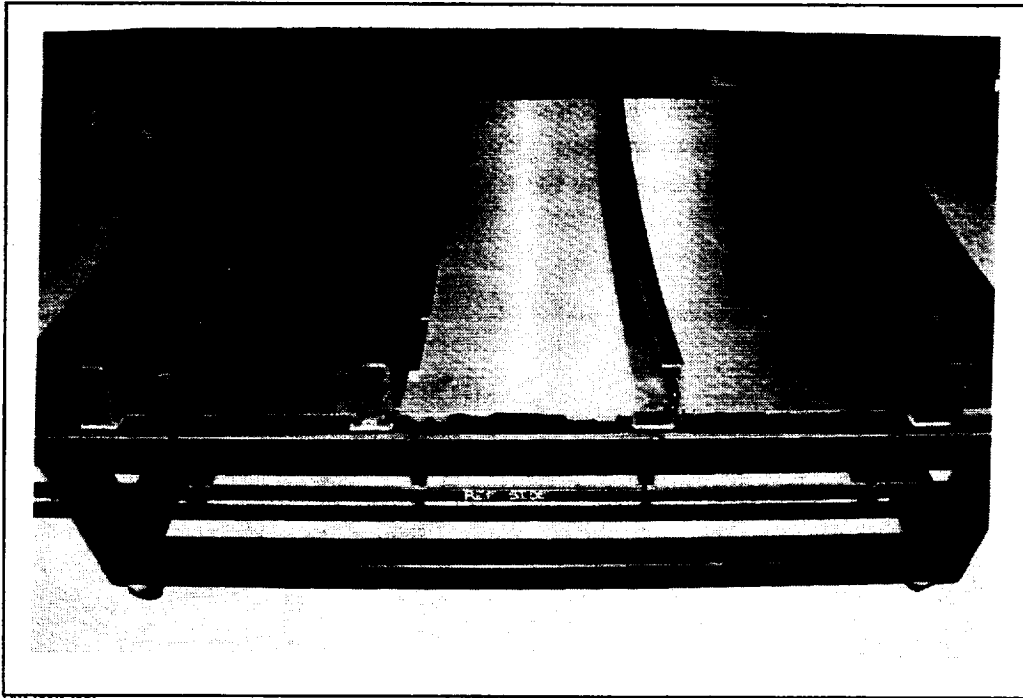
71

Fig. 65 Lower Fuselage Panel Cure Tooling, Including Graphite J-frames

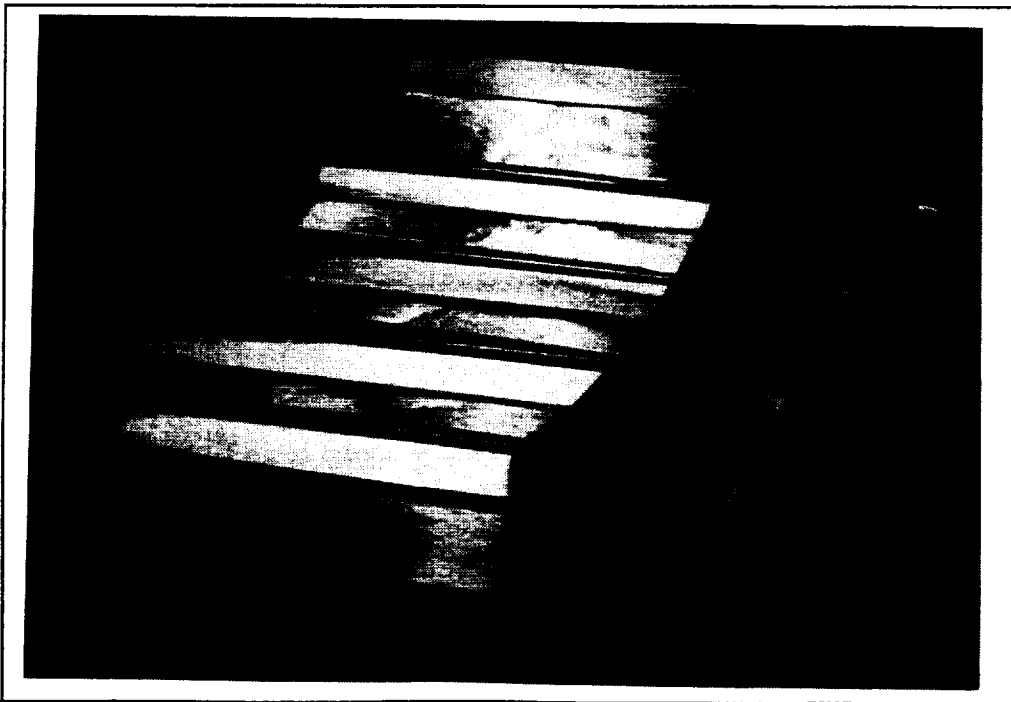Fig. 66 Lower Fuselage Preform Ready for Infusion, Showing Tooling Details
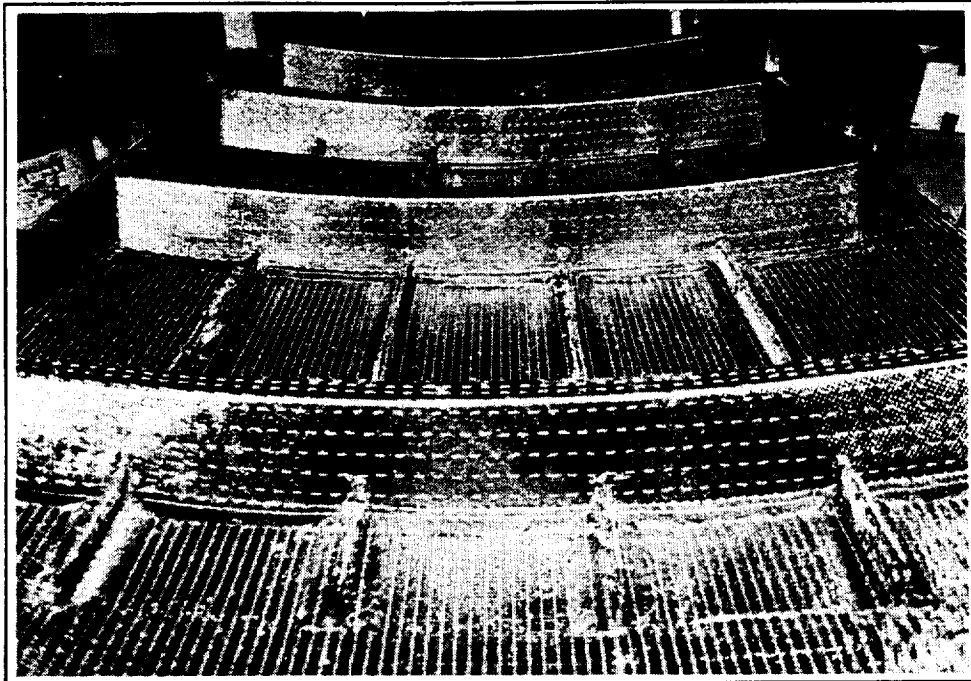
Fig. 67 Lower Fuselage Preform After Infusion with 3501-6 Epoxy Resin

The preform was placed in the curing fixture. Teflon-wrapped rubber blocks were used in all corners and spaces to prevent bridging of the bag. When the tooling was in place, the part was bagged and pressurized to 30 psi to check the bag's integrity; then heat was applied at 2-5°F/min. to 225°F. At 225°F, the part was held for 60 min. to allow the resin to begin gelling. Then the vacuum was vented and the pressure increased to 100 psi. Heating continued at 2-5°F/min. to 350°F and held for 120 min. The part was then cooled to 140°F before releasing the pressure and removing the part.

4.4 DIMENSIONAL INSPECTION

Dimensionally, the cured part was within tolerance; visually, the stringers and the frames were straight and the intersections square. Table 19 shows a comparison of dimensions and weights for dry-to-cured for the panel. A 59% fiber volume was achieved for the cured panel. Preliminary findings indicate less than 2% voids by volume.

Table 19 Comparison of Average Dimensions from Dry to Cured, for Lower Fuselage Panel

	DRY	AFTER CURE
0.306-in. STRINGER	0.425	0.327
0.141-in. J-FRAME	0.205	0.133
0.095-in. SKIN	0.140	0.111
WEIGHT, lb	54.0	75.5
% RESIN BY WEIGHT	—	33.0

MR94-2291-034A

73

4.5 TESTING

Element testing was done during the design of the cross-stiffened window belt panel. The results provided guidance in the design of the lower fuselage panel. Tension and compression tests done on the stringer cross sections verified the ability of the woven intersection to achieve failure strains of 7500×10^{-6} in./in., exceeding the ultimate strain allowable of 4500×10^{-6} in./in.

The cured 60-in. x 90-in. lower fuselage panel will be tested at NASA/Langley in a combined loads test machine (D-box) that will simultaneously apply longitudinal compression loads, internal pressure loads, and in-plane shear loads.

4.6 ACTUAL & PROJECTED COSTS

A cost comparison was made of the AS4/3601-6 Gr/Ep lower fuselage panel using preforms that are woven, stitched, and Resin Film Infusion (RFI) processed versus the standard tape prepreg with autoclave cure.

Table 20 shows the actual cost for Unit 1 and the projected cost for Unit 100 of the lower fuselage panel fabricated using a woven and stitched preform and RFI. For Unit 1 (actual), the total cost of $52,363 includes a nonrecurring cost for tooling of $445 prorated for 100 units. The recurring costs include the preform (material and labor), the film epoxy used on RFI, and the labor for RFI of the preform, and quality assurance. The projected cost for the 100th unit is $19,798.

Table 20 Cost of Woven & Stitched RFI/Autoclave-cured AS4/3501-6 Gr/Ep Lower Fuselage Panel

	UNIT COST, $	
	#1 (ACTUAL)	#100 (PROJECTED)
PREFORM	33,334	14,000
FILM EPOXY	2,800	1,487
LABOR FOR RFI	13,700	2,671
QUALITY ASSURANCE	2,084	1,195
RECURRING COST, $	51,918	19,353
TOOLING*	445	445
TOTAL COST, $	52,363	19,798
*TOOLING PRORATED FOR 100 UNITS		
MR94-2291-035		

A similar cost comparison, Table 21, was made for a cocured lower fuselage panel consisting of longitudinal blade stringers in one direction and curved precured "zee" frames with mouse-holes in the other direction. The nonrecurring tooling cost of $387 has again been prorated for 100 units. The costs for the first unit and the 100th unit were generated using the Composite Fabricating Cost Estimating Technique (FACET) model developed under the *DoD Fabrication Guide, 3rd Ed.* The total cost for the first unit is $57,550, and for the 100th unit it is $25,188.

74

Table 21 Cost of Standard Tape/Autoclave-cured AS4/3501-6 Gr/Ep Lower Fuselage Panel

	UNIT COST, $	
	#1	#100
LABOR MATERIAL QUALITY ASSURANCE	40,123 15,440 1,600	8,720 15,121 960
RECURRING COST, $ TOOLING*	57,163 387	24,801 387
TOTAL COST, $	57,550	25,188
*TOOLING PRORATED FOR 100 UNITS		

MR94-2291-036

A comparison of the cost of standard tape versus woven and stitched AS4/3501-6 Gr/Ep cross-stiffened curved fuselage panels is shown in Table 22. For Unit 1, the RFI woven and stitched preform fuselage panel is 9.0% lower in cost than the standard tape autoclave cured one. For the 100th unit, the projected cost savings of using RFI and woven and stitched preforms over the standard tape and autoclave cure is 21.4%.

Table 22 Comparison of Costs of Standard Tape vs. Woven & Stitched AS4/3501-6 Gr/Ep Lower Fuselage Panel

	STANDARD TAPE & AUTOCLAVE		WOVEN & STITCHED & RFI/AUTOCLAVE	
	UNIT		UNIT	
	#1	#100	#1	#100
COST, $	57,550	25,188	52,363	19,798

MR94-2291-037A

4.7 REFERENCES

1. Bushnell, D., "Optimization of Composite, Stiffened, Imperfect Panels Under Combined Loads for Service in the Postbuckling Regime," *Computer Methods in Applied Mechanics and Engineering*, Vol. 103, 1993, pp. 43-114.

5 – CONCLUSIONS

5.1 TEXTILE PREFORM TECHNOLOGY FOR AIRFRAME STRUCTURES

Results of this investigation have led to the following conclusions:
- Through-the-intersection, continuous fiber, cross-stiffened, woven preform assemblies that offer scale-up potential are feasible
- Textile preforms offer unique composite material solutions to all cross-stiffened structures such as bulkheads, frames, keels, beams, skin panels, and doors
- Resin Film Infusion (RFI) is a suitable processing method for textile preforms
- Significant production acquisition cost savings on the order of 21% are possible with textile preforms over conventional tape prepreg lay-up
- The focus should be expanded to develop a solid data base and preform definition.

Designers who employ textile preform technology for airframe structures need significant insight into the processing methodology to adequately define the part, design the tooling, and be confident in the end-product performance. Based on the two preform methods presented in this report, there is a significant difference in approach and final product. The differences in material, tow and yarn sizes, weaving architecture, utilization of binders (tackifiers), stitching, and loft will interact and are expected to result in different end-product performance. There is much that must be further developed and standardized, or at least controlled, to ensure repeatability and structural integrity from one textile supplier to another.

The engineering drawing presentation utilizing percentages of fiber orientations provided freedom to define the preform but resulted in diverse approaches that will have an impact on the end-product performance. Drawing improvements and standards must be defined that will more capably control the end-result. There is much to be learned in providing engineering definition to woven preform assemblies. At present, this type of design freedom would not be permitted for production hardware since geometry and structural integrity are essential for product performance.

The test base for recurring weaving architectural patterns must be expanded in order to assess the impact on structural properties. The knockdowns associated with the "Z" weaver locking yarns and stitching must be determined.

The analytical methodologies must be further developed to allow accurate prediction of structural capability, considering the variations of architecture, varying yarn sizes, fiber volume, and defects.

The application of the uncatalyzed epoxy binders and tackifiers used to enable debulking of the preform must be thoroughly evaluated to assure that there is no deleterious effect on the processed article. These assessments should consider the effects of percentage of resin content, the effects of nonuniform mixture with the structural resin, the necessity to purge, and compatibility with both RFI and RTM processing methods.

The preform net final dimensions must be closely controlled to enable effective tooling to be designed. Lofts of 100-200% are unacceptable for pocketed, cross-stiffened preforms. It would be desirable to provide debulked preforms to 10% of net.

5.2 DESIGN GUIDELINES/ANALYSIS OF TEXTILE-REINFORCED COMPOSITES

A methodology has been developed that can be used to select appropriate through-thickness reinforcements. Verification tests of the analysis were somewhat ambiguous because the pure mode I and mode II fracture toughnesses for the material were not available. The analysis gives conservative results for the amount of additional load a stitched flange can take without delaminating. This conservatism seems to be related to the ability of stitching to suppress mode II fracture, in addition to the mode I behavior included in the model.

The analysis gives us the ability to create nondimensional curves that help in designing cocured structures with through-thickness reinforcements. Despite the shortcomings revealed in the testing, the analysis provides a conservative method of design, while minimizing the amount of element testing that must be performed.

REPORT DOCUMENTATION PAGE

1. AGENCY USE ONLY (Leave blank)	2. REPORT DATE Sept. 1996	3. REPORT TYPE AND DATES COVERED Contractor Report

4. TITLE AND SUBTITLE

Novel Composites for Wing and Fuselage Applications
Textile Reinforced Composites and Design Guidelines

6. AUTHOR(S)

J. A. Suarez, C. Buttitta, et al.

5. FUNDING NUMBERS

C NAS1-18784
TA 3, 4, 5

WU 538-10-11-02

7. PERFORMING ORGANIZATION NAME(S) AND ADDRESS(ES)

Northrop Grumman Corp.
Advanced Technology & Development Center
Bethpage, New York 11714-3595

8. PERFORMING ORGANIZATION REPORT NUMBER

9. SPONSORING/MONITORING AGENCY NAME(S) AND ADDRESS(ES)

NASA Langley Research Center
Hampton, VA 23681-0001

10. SPONSORING/MONITORING AGENCY REPORT NUMBER

NASA CR-201612

11. SUPPLEMENTARY NOTES

Langley Technical Monitor: H. Benson Dexter
Final Report

12a. DISTRIBUTION/AVAILABILITY STATEMENT

Unclassified–Unlimited
Subject Category 24
Availability: NASA CASI (301) 621-0390

12b. DISTRIBUTION CODE

13. ABSTRACT (Maximum 200 words)

Design development was successfully completed for textile preforms with continuous cross-stiffened epoxy panels with cut-outs. The preforms developed included 3-D angle interlock weaving of graphite structural fibers impregnated by resin film infiltration (RFI) and shown to be structurally suitable under conditions requiring minimum acquisition costs. Design guidelines/analysis methodology for such textile structures are given. The development was expanded to a fuselage side-panel component of a subsonic commercial airframe and found to be readily scalable. The successfully manufactured panel was delivered to NASA/Langley for biaxial testing. This report covers the work performed under Task 3 -- Cross-Stiffened Subcomponent; Task 4 -- Design Guidelines/Analysis of Textile-Reinforced Composites; and Task 5 -- Integrally Woven Fuselage Panel.

14. SUBJECT TERMS

3-D Woven Textile Preforms. Fuselage Side Panel. Textile Design and Guidelines. Resin Transfer Molding. Resin Film Infusion. Cost/Weight Comparison.

15. NUMBER OF PAGES
86

16. PRICE CODE
A05

17. SECURITY CLASSIFICATION OF REPORT Unclassified	18. SECURITY CLASSIFICATION OF THIS PAGE Unclassified	19. SECURITY CLASSIFICATION OF ABSTRACT Unclassified	20. LIMITATION OF ABSTRACT